19780004170
NASA-RP-1009
78N12113

An introduction to orbit dynamics and its application to satellite-based earth monitoring systems

NASA Reference Publication 1009

An Introduction to Orbit Dynamics and Its Application to Satellite-Based Earth Monitoring Missions

David R. Brooks
Langley Research Center
Hampton, Virginia

National Aeronautics
and Space Administration

**Scientific and Technical
Information Office**

1977

PREFACE

This report provides, by analysis and example, an appreciation of the long-term behavior of orbiting satellites at a level of complexity suitable for the initial phases of planning Earth monitoring missions. The basic orbit dynamics of satellite motion are covered in detail. Of particular interest are orbit plane precession, Sun-synchronous orbits, and establishment of conditions for repetitive surface coverage. Orbit plane precession relative to the Sun is shown to be the driving factor in observed patterns of surface illumination, on which are superimposed effects of the seasonal motion of the Sun relative to the equator. Considerable attention is given to the special geometry of Sun-synchronous orbits, orbits whose precession rate matches the average apparent precession rate of the Sun. The solar and orbital plane motions take place within an inertial framework, and these motions are related to the longitude-latitude coordinates of the satellite ground track through appropriate spatial and temporal coordinate systems. It is shown how orbit parameters can be chosen to give repetitive coverage of the same set of longitude-latitude values on a daily or longer basis. Several potential Earth monitoring missions which illustrate representative applications of the orbit dynamics are described. The interactions between orbital properties and the resulting coverage and illumination patterns over specific sites on the Earth's surface are shown to be at the heart of satellite mission planning. A requirement for global surface coverage is seen to be a potentially severe constraint on satellite systems, depending on the mission objectives. In some contexts, this requirement strongly suggests multiple-satellite systems, whereas in less restrictive situations, "global coverage" can be redefined such that a single satellite can provide adequate data. The approach taken in the examples stresses the need for considering mission output as a whole, treating the entire data base as an entity rather than a series of separate measurements. This is consistent with use of this type of data as input to large-scale, long-term activities which can best justify the use of satellite systems.

CONTENTS

I. INTRODUCTION

Since the beginning of the space age, satellites have been employed to examine our own planet. There is currently an abundance of missions - speculative, planned, and operational - to exploit the capabilities of a variety of space-based sensing systems in order to understand, monitor, control, and utilize the Earth and its atmosphere. One of the initial steps in designing such missions is, invariably, to gain an understanding of how a satellite orbit can best be matched to the requirements for meeting one or more objectives. This matching involves not just selecting the best initial or instantaneous orbit parameters but also attempting to maximize the useful return of data over the desired range of conditions for the entire life of the mission. The purpose of this report is to provide, by analysis and example, an appreciation of the long-term behavior of orbiting satellites at a level of complexity suitable for the initial phases of planning Earth monitoring missions.

Section II of the report, "Dynamics of Earth-Orbiting Satellites," deals with the basic orbit dynamics required to depict the motion of satellites in their orbits. The time scale of interest for Earth observation ranges typically from a few months to a few years. This means that the major effects of the Earth's nonsymmetrical gravitational field must be accounted for but some less significant orbital perturbations can be ignored at this stage of analysis. With these limits in mind, it is possible to achieve a sufficiently representative and self-consistent picture of satellite motion which allows an analyst to study and compare various orbit options while avoiding the complexities and loose ends of higher order orbit dynamics. A subsection of Section II deals with Sun-synchronous orbits, which have important implications because of their special geometrical relationship to the Sun's apparent motion about the Earth.

Section III, "Establishing Patterns of Surface Coverage From a Satellite," deals with viewing the Earth's surface and the ways in which orbits can be modified to produce particular patterns of coverage. The problems of keeping track of the Sun's apparent motion with respect to a satellite are examined in detail. This involves such requirements as looking at (or not looking at) the Sun for measurements or calibration as well as accounting for variations in lighting conditions beneath the path of a satellite during the entire course of a mission.

Section IV, "Some Examples of Geographical Coverage and Solar Illumination Patterns for Long-Duration Earth Monitoring Missions," presents some typical applications of the orbit analyses of the previous sections. Several different types of missions are considered, each with its own sampling and coverage requirements. The limitations of a single satellite in satisfying some global coverage requirements are illustrated, and the alternative of multiple-satellite systems is briefly discussed.

The general aim of the analytic sections of this report is to present a tutorial approach to orbit dynamics around which a mission analyst, starting

with no previous knowledge of orbital mechanics, can construct a set of self-contained and self-consistent computing tools. The requirements for the exact form of such tools will vary with circumstance, so that no attempt has been made here to formulate specific computer programs, although some BASIC language algorithms have been given in appendix A for a few standard calculations. In the applications section (Section IV) the aim has been not to exhaust the possibilities of analysis for each topic of interest, but to provide, through typical situations, a feeling for the potential and limitations of space-based Earth monitoring missions. In particular, Section IV is intended to provide some insight into several types of coverage patterns and how they develop over seasonal and yearly time periods.

II. DYNAMICS OF EARTH-ORBITING SATELLITES

In this section, the equations required to propagate a satellite along its orbit are considered. First, the necessary coordinate systems are derived for locating a satellite in time and space relative to the Earth and Sun. Then, first-order perturbations are introduced to take into account the well-known oblateness of the Earth, the result of which is that orbital paths are not fixed in inertial space but precess about the Earth.

Coordinate Systems in Space

As outlined in the Introduction, analysis for Earth observations involves locations on the Earth's surface (the satellite ground track, for example) and also the Sun's position relative to a satellite in space or its viewing point on the Earth's surface or elsewhere. Thus, it is natural to assume that two basic coordinate systems for locating points will be required. One is a system of locating points on the Earth's surface - longitudes and latitudes - and the other describes the apparent motion of the Sun through space relative to the Earth.

The longitude-latitude L-λ system is described in figure 1. The equator forms the x-y plane, and the x-axis is arbitrarily defined by a vector in the

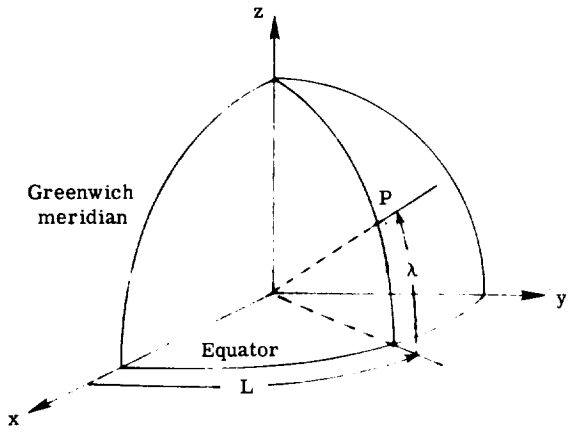

Figure 1.- Definition of a longitude-latitude coordinate system.

equatorial plane which passes through the same meridian that passes through Greenwich, England. This meridian has a longitude of 0° by definition. The latitude of a point P is defined as the angle between the equator and P, measured along the meridian passing through P. Longitude is defined as the angle between the Greenwich meridian and the meridian passing through P. Latitude is usually defined as having values between 90° (North Pole) and -90° (South Pole). Longitude usually takes positive values between 0° and 180° for points east of Greenwich and between 0° and -180° for points west of Greenwich, although it is often convenient in computer applications to define longitude between 0° and 360° measured east from Greenwich.

The Earth-Sun geometry is illustrated in figure 2. The ecliptic plane is defined by the Earth's motion around the Sun. The x-axis of an Earth-centered

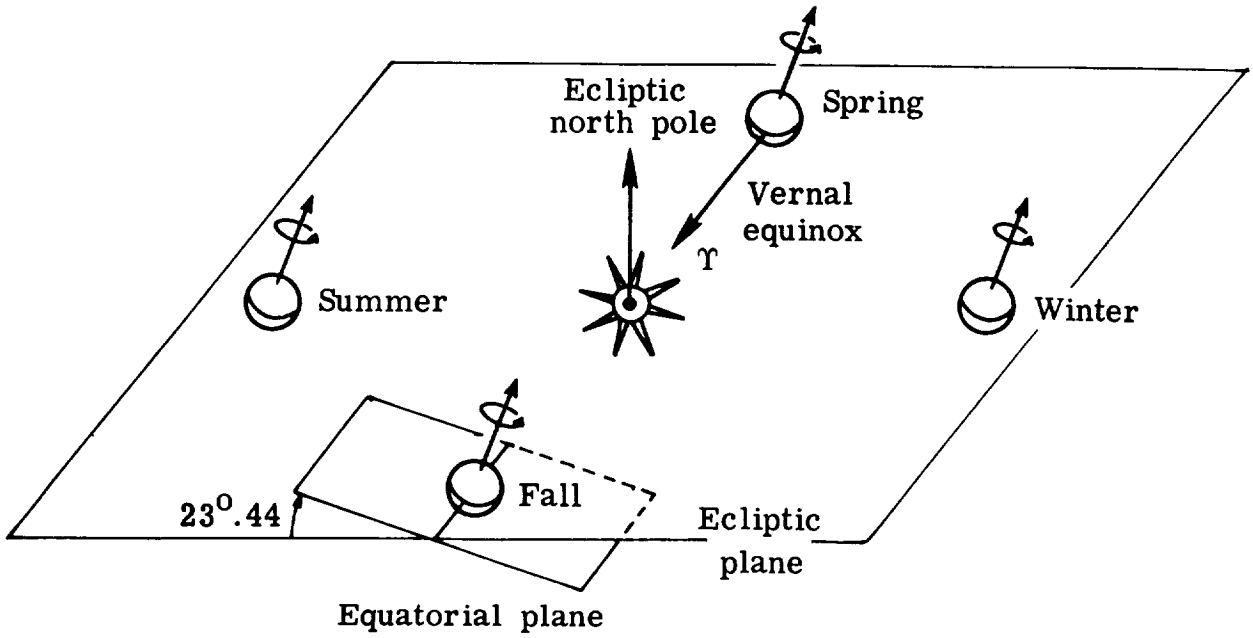

Figure 2.- Earth's motion around the Sun.

Cartesian coordinate system is defined by the vector pointing from the Earth to the Sun at the instant of the vernal equinox, that is, the instant at which the subsolar point crosses the equator moving from south to north. This Earth-centered geometry is shown in figure 3. The celestial sphere is a fictitious globe of apparently infinite radius which contains the "fixed"[1] stars against which the Sun, the planets, and the satellite appear to move as viewed from the Earth. The projection of the Earth's equator onto the celestial sphere is called the equinoctial and the ecliptic is defined by the Sun's trace as it

[1]As used herein, "fixed "means that the motion of stars against the celestial sphere is too small to be noticed on the time scales of importance in this analysis.

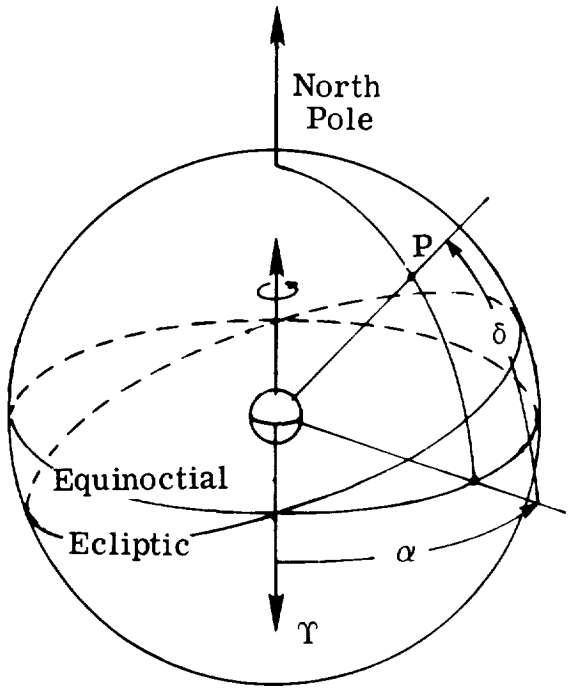

Figure 3.- Celestial sphere and right-ascension—declination coordinate system.

appears to move among the stars. The vernal equinox represents a particular location on the celestial sphere, determined by the intersection of the equinoctial and the ecliptic, as the Sun moves from south to north. From the signs of the zodiac, this intersection is called the first point of Aries and is represented by the symbol for the ram's head Υ. This definite point in the heavens is now located about 15° west of the constellation Pleiades. (The directions east and west on the celestial sphere are defined in the same way as an observer would identify these directions on a globe model of the Earth.)

The reference planes and directions thus established depend on the motion of the Earth about the Sun and about its own axis. The Earth can be thought of as an orbiting gyroscope which maintains the reference systems and their interrelationships. For many purposes, this is a sufficiently accurate mental picture, but in fact the gyroscope analogy suffers from some irregularities. Chiefly because of the small unsymmetrical forces of the Sun and the Moon on the Earth's equatorial bulge and secondarily because of the perturbing effects of the other planets, the Earth's axis precesses in space at the rate of about 50.25 seconds of arc in a year, advancing the time of the vernal equinox by about 20 minutes per year. This results in a slow but steady westward motion in the location of the first point of Aries, with a period of about 25 725 years. An additional secondary effect is the variation of the obliquity (inclination) of the Earth's equator to the ecliptic plane. The obliquity is currently about 23°.44 and is decreasing at a rate of about 47 seconds of arc per century. Detailed discussions of these effects are given in reference 1.

It is easy to see from figure 3 that the position of a point P on the celestial sphere can be defined by two angles relative to the vernal equinox vector and the equinoctial. The right ascension α is measured along the equinoctial positive to the east from Υ, and the declination δ is measured north from the equinoctial. The dizzying change in perspective from figure 2 to figure 3 is actually simply accomplished by vector transformations. Starting with an Earth ephemeris (a table of or an analytic expression for Earth positions relative to the Sun as a function of time), the negative of the Earth's position vector in heliocentric space is the Sun's position in a geocentric ecliptic system. Since the ecliptic and equatorial systems share the same x-axis (that is, Υ), the transformation into the equatorial (equinoctial) system involves only a vector rotation about Υ. Note now that the L-λ and α-δ coordinate systems both have the equatorial plane as their basis, with only the difference in x-axis to distinguish them. Note too, that values of right ascension and declination, although defined against the celestial sphere, are as suitable for defining points on the Earth's surface as are longitudes and latitudes. For this analysis, declination and latitude are, in fact, equivalent and can be used interchangeably. Finally, note that the right ascension-declination system is an inertial coordinate system in space as perceived by an observer having the vantage point implied by figure 2. That is, although the origin of the coordinate system rotates around the Sun with the Earth, the directions of the three axes remain fixed in space. From the vantage point of an observer on Earth, an inertial system is one whose axes are pointed at fixed positions on the celestial sphere. The discussion of the previous paragraph shows that this inertial framework is only an approximation, as could eventually be determined (and has been) by patient observation of the Earth-Sun system as shown in figure 2. However, for present purposes, the inertial framework is a useful and very good approximation for analysis and will henceforth be accepted as valid. The relationship between the inertial (right-ascension—declination) and rotating (longitude-latitude) systems depends on the location of the Greenwich meridian relative to Υ, the specification of which requires definition of a coordinate system for time. This problem is dealt with in the next section, which digresses long enough to present the necessary background information and ends with the equations which allow transformation back and forth between longitude and right ascension.

Coordinate Systems for Time and the Relationship Between Longitude and Right Ascension

The definition of a time-measuring system requires an agreed-upon starting point and a set of periodic events which can be used to measure intervals of time. Fundamental to an understanding of the physical sciences is an acceptance of the existence of a uniform time which corresponds to the time variable in dynamical equations. However, in practice, it is necessary to admit that measures of time exist only as matters of definition, that these definitions are imperfect ones applied to particular situations, and that discrepancies will *always* exist at some level of application.

If the Earth-Sun-celestial sphere system is used as the means of defining a time system, there are two conventional ways to proceed - sidereal time and

solar time. Sidereal time is governed by the rotation of the Earth relative to the stars. If the instant of passage of a particular star over a meridian is noted, the star will cross the same meridian again in exactly one sidereal day, by definition. This definition is complicated by the motion of the vernal equinox, but for most purposes the problems are not worth considering.

Solar time is governed by the rotation of the Earth relative to the Sun. If the instant of passage of the Sun over a meridian is noted, the Sun will cross the same meridian again in exactly one solar day, by definition. This observable solar day is the basis of what is called apparent solar time. It is not hard to see the difficulties in applying this definition to practical measurements. It is complicated by the slightly elliptical motion of the Earth around the Sun and by the fact that the Sun does not move in the equatorial plane, with the result that the observed length of solar days is only approximately constant. To circumvent this problem, "mean solar time" is defined relative to a fictitious "mean sun" which moves along the equinoctial (the projection of the equator on the celestial sphere) at a constant rate equal to the average apparent rate of motion of the real Sun. Although the mean solar time system is the basis of all civil time measurements - the time by which people set their watches - it is still full of inconsistencies because of the variable rotation rate of the Earth, the fact that the fictitious mean sun cannot be observed, and the fact that the accepted description of the fictitious mean sun is based on another time system (ephemeris time), which depends on the internal consistency of the gravitational theories describing the entire solar system. However, at some point it is necessary to cease worrying about discrepancies and accept mean solar time as a precise and uniform method of relating nonsimultaneous events. Hereinafter, "time" means mean solar time unless stated otherwise. A "day" is 86 400 mean solar seconds, by definition, and a "second" is always a mean solar second.

The meaning of a "year" is complicated by the variety of choices available. Thus, a sidereal year is based on the motion of the Earth relative to the stars - the cycle time for astronomical observation. A year defined relative to the Sun is based on the passage of the Earth from one vernal (or autumnal) equinox to the next. This interval of time is called a tropical year - the cycle time for Earth seasons. It is nearly constant, but not quite, because of the interaction of the planets in the solar system. It is slowly decreasing linearly with time at a rate of 0.53 sec/century (ref. 1); a current approximate length, good for the pertinent time frame, is 365.24220 days. This discussion makes clear that calendar systems are bound to be complicated, as they seek to maintain seasonal relationships by using units (days) which are not exact subdivisions of the tropical (seasonal) year.

Within the framework of mean solar days, there are two time systems of interest in the bookkeeping sense. The first is universal time (UT), a unit of which is, for all practical purposes, equal to the corresponding unit of mean solar time. Universal time is the practical basis of civil time. It is expressed in hours, minutes, and seconds or in fractions of a mean solar day. The zero reference for a universal time day is Greenwich midnight, at the start of a calendar day. Hence, Jan. 1.0 is the start of calendar day Jan. 1, at Greenwich midnight.

The other system of interest, and an important one for analysis, is the Julian date (J.D.) system, which is a method of counting mean solar days consecutively. Its origin was set long enough ago that all recorded astronomical events can, in principle, be assigned an unambiguous Julian date. Since the system was devised by astronomers for their own purposes, the Julian day starts at Greenwich noon so that all astronomical observations during a night of viewing activity have the same Julian date. One standard reference epoch for Julian date tables is Jan. 0.5, 1900 (UT). This is Greenwich noon on calendar day Dec. 31, 1899, or Julian date 241 5020.0. Julian dates are used extensively for keeping track of days in preference to the more cumbersome calendar system. A Julian year is exactly 365.25 days, the average length of the calendar year according to the Julian calendar, and, advantageously, is an exact decimal fraction. A Julian century is 36 525 days. Table 1, from reference 1, lists Julian dates for the first day of each month in the last half of the 20th century. Note that the calendar day starts at a Julian date of XXX XXXX.5, so that Jan. 1.0, 1950, is J.D. 243 3282.5.

Returning now to the relationship between right ascension and longitude, it can be expressed in terms of a constant related to a particular epoch, the Earth's rotational rate, and some measure of time. Reference 1 gives the following equation for the right ascension of the Greenwich meridian at 12 midnight (0 hours UT):

$$\alpha_{g,o} = 99^{o}.6909833 + 36000^{o}.7689T + 0^{o}.00038708T^{2} \qquad (1)$$

where T is the time in Julian centuries from Jan. 0.5, 1900:

$$T = \frac{\text{J.D.} - 241\ 5020.0}{36\ 525} \qquad (2)$$

The appearance of a second-order term in T is due to the accumulated effects of small secular and periodic variations in the Earth's rotational rate and cannot be accounted for in terms of the previous discussion; this part of equation (1) *must* just be accepted as fact. Note that although equation (1) appears to give $\alpha_{g,o}$ as a continuous function of T, it does not actually do so. The value of T must correspond to a time of 0^{h} UT, that is, to Julian dates of the form XXX XXXX.5. A detailed discussion of equation (1) and its relationship to the mean solar time system may be found in reference 1.

At this point, it is useful to reconsider the concept of sidereal time, that is, time relative to a "fixed" x-axis - the vernal equinox. In this sense, the angular position of any meridian is equivalent to some fraction of a sidereal day, with 360^{o} = 24 sidereal hours. Thus, sidereal time and right ascension are equivalent measurements of angular position. To determine the sidereal time (right ascension) of any meridian at any time, it is only necessary to know the rotational rate of the Earth $\dot{\theta}$. Then

$$\alpha = \alpha_{g,o} + (t - t_{o})\dot{\theta} + L_{m} \equiv \alpha_{g} + L_{m} \qquad (3)$$

where $t - t_{o}$ is the universal time of interest and L_{m} is the longitude of the meridian. The Sun's apparent sidereal rate is 360^{o} in 365.2422 mean solar days, so that the Earth must rotate 360 + 360/365.2422 = 360.9856473 degrees

per mean solar day or 0.25068447 degree per mean solar minute. An example (from ref. 2) will make clear the necessary computations: What is the local sidereal time (right ascension α) of a point at 298°.2213 east longitude, at $10^h15^m30^s$ UT on Oct. 12, 1962? (The superscripts show the conventional notations for hours, minutes, and seconds.)

Convert to Julian days:

243 7938.0	J.D., Oct. 0.5, 1962 (from table 1)
+0.5	Add 0.5 day to obtain J.D., Oct. 1.0, 1962
+11.0	Add 11 days to obtain J.D., Oct. 12.0, 1962
243 7949.5	J.D., 0^h UT, Oct. 12, 1962

From equations (1) and (2),

$$T = \frac{243\ 7949.5 - 241\ 5020.0}{36\ 525} = 0.62777549 \text{ Julian century}$$

$$\alpha_{g,o} = 99^\circ.69098 + 280^\circ.40033 + 0^\circ.0001525 = 20^\circ.0915$$

$$10^h15^m30^s = 615.5 \text{ min}$$

And from equation (3),

$$\alpha_g = 20^\circ.0915 + (615.5 - 0)(0^\circ.25068447) = 174^\circ.3878$$

Thus,

$$\alpha = 174^\circ.3878 + 298^\circ.2213 = 112^\circ.6091$$

Note the convention of expressing sidereal "time" in terms of an angle. It could be expressed as $112^\circ.6091 = (24)(112.6091/360)$ hours $= 7^h30^m26^s$, but the time units are not the same as mean solar time units! Therefore, to avoid confusion, the angular notation is used.

A final topic of practical interest in a discussion of time systems is the matter of converting back and forth between the Julian date system and a calendar-clock system. This is a somewhat tedious procedure for hand calculations but is easily taken care of in computerized orbit analysis with the aid of transformation subroutines. It is necessary only to keep in mind that clock times derived from Julian dates are Greenwich times, so that the local clock hour, if that is desired, depends on the time zone of the point of interest. There are 24 such zones, 15° wide, one of which is centered about the Greenwich meridian, ±7.5°. For the purposes of analysis, all time zones are considered to follow meridians, so that local geographical and "daylight savings" fluctuations, such as are common over populated areas of the Earth, are ignored. For example, eastern standard time is 5 hours behind Greenwich mean time, being in the time zone centered at -75°. Therefore, local noon EST occurs at J.D. XXX XXXX.0 + 5/24 = XXX XXXX.208333.

Equations for the Propagation of Satellite Orbits

In an unperturbed spherically symmetric gravitational field, orbiting objects follow the classical laws of Keplerian dynamics. The position of a satellite in a Cartesian coordinate system can be specified completely either by a set of six orbit elements or by six vector components - a position vector plus a velocity vector. (For a basic review of elliptic orbital motion, see ref. 3.) Figure 4 shows the orientation of an orbit in the right ascension-

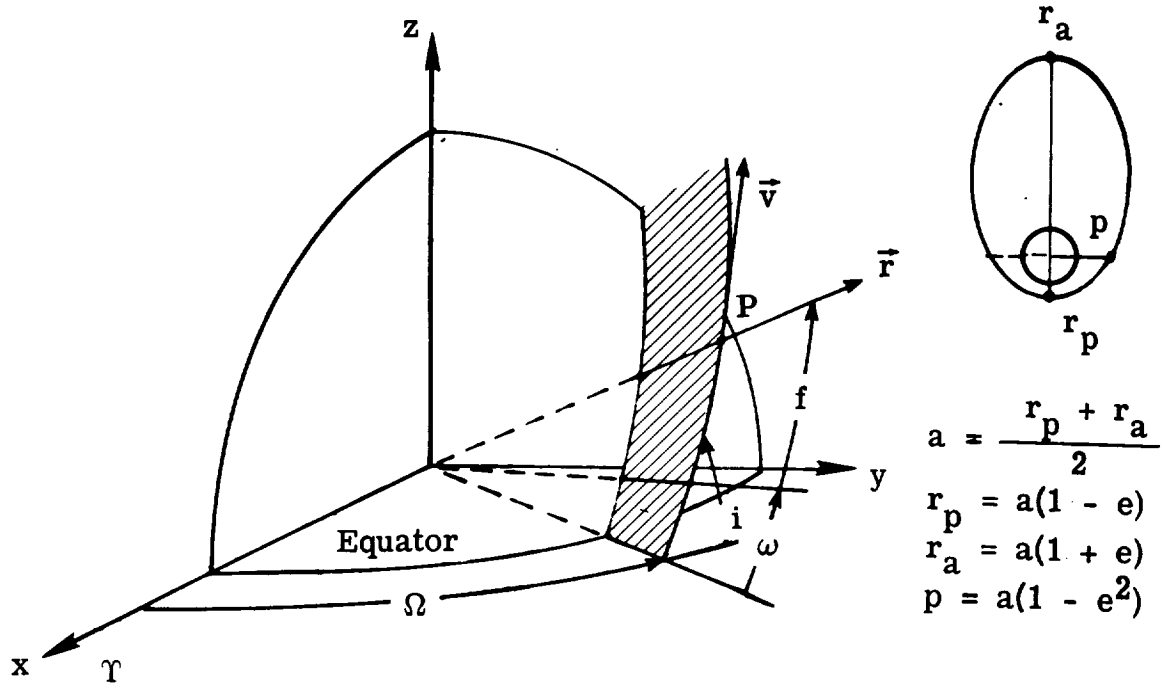

Figure 4.- Defining the position and velocity of a satellite in orbit around the Earth.

declination system previously discussed in detail. Two of the orbit elements, right ascension of the ascending node Ω and inclination i, position the orbital plane in space. The remaining angular elements, argument of perigee ω and true anomaly f, specify the angular position of a satellite at point P along its orbital path relative to the x-y (equatorial) plane. The size and shape of the orbital path are determined by the semimajor axis a and eccentricity e. (Many orbits of interest for Earth monitoring have semimajor axes between about 6600 and 8000 km and are circular, or nearly so, with eccentricities in the range 0.0 to 0.1.) The semimajor axis a is the average of the perigee and apogee r_p and r_a (minimum and maximum radii relative to the source of the gravitational field), as shown in figure 4. The eccentricity e can be thought of as a dimensionless measure of the departure from a circular orbit of radius a, relating a to r_p and r_a as shown. The semilatus rectum p is a derived quantity which will be used in the following analysis; it is measured through the gravitational center along a line perpendicular to a line from perigee to apogee and is equal to the semimajor axis for a circular orbit. Knowledge of all six Keplerian elements - a, e, i, Ω, ω, and f - is equivalent

to knowing the satellite's state vector (position and velocity), which may be obtained in terms of orbit elements as follows (ref. 3):

$$r_x = \left[\cos f(\cos \omega \cos \Omega - \cos i \sin \Omega \sin \omega) + \sin f(-\sin \omega \cos \Omega - \cos i \sin \Omega \cos \omega)\right] \frac{p}{1 + e \cos f} \tag{4a}$$

$$r_y = \left[\cos f(\cos \omega \sin \Omega + \cos i \cos \Omega \sin \omega) + \sin f(-\sin \omega \sin \Omega + \cos i \cos \Omega \cos \omega)\right] \frac{p}{1 + e \cos f} \tag{4b}$$

$$r_z = \left[\cos f \sin i \sin \omega + \sin f \sin i \cos \omega\right] \frac{p}{1 + e \cos f} \tag{4c}$$

$$\dot{r}_x = \sqrt{\frac{\mu}{p}}\left[(\cos f + e)(-\sin \omega \cos \Omega - \cos i \sin \Omega \cos \omega) - \sin f(\cos \omega \cos \Omega - \cos i \sin \Omega \sin \omega)\right] \tag{4d}$$

$$\dot{r}_y = \sqrt{\frac{\mu}{p}}\left[(\cos f + e)(-\sin \omega \cos \Omega + \cos i \cos \Omega \cos \omega) - \sin f\ (\cos \omega \sin \Omega + \cos i \cos \Omega \sin \omega)\right] \tag{4e}$$

$$\dot{r}_z = \sqrt{\frac{\mu}{p}}\left[(\cos f + e)(\sin i \cos \omega - \sin f \sin i \sin \omega)\right] \tag{4f}$$

The gravitational constant μ is equal to 398 601.2 km^3/sec^2 for the Earth; it is this quantity which takes into account the mass associated with a gravitational source and, hence, determines the magnitude of the velocities associated with orbits around a particular body. The inverse of the transformation in equations (4), from state vector to orbit elements, and many other relationships referring to Keplerian orbits and their elements are summarized in reference 3.

Because of the Earth's oblateness, not all the Keplerian elements are constant for Earth satellites. In particular, the orientation of the orbital plane Ω and the argument (location) of the perigee ω precess as a result of the effects of the bulge around the Earth's equator. These precessions, which can be understood in terms of gyroscopic analogies, were thoroughly discussed in the late 1950's. Reference 3 contains an extensive bibliography. The perturbations in Ω and ω are significant, amounting to several degrees per day, and therefore must be accounted for.

The usual treatment of gravitational potential involves expansion of the potential in a series. The following discussion utilizes the first-order theory of Kozai (ref. 4), involving the so-called J_2 term in the gravitational representation. In this formulation

$$\dot{\omega} = \frac{3}{2} J_2 \frac{r_\oplus^2}{p^2} \dot{M}(2 - 2.5 \sin^2 i) \tag{5a}$$

$$\dot{\Omega} = -\frac{3}{2} J_2 \frac{r_\oplus^2}{p^2} \dot{M} \cos i \tag{5b}$$

where

$\frac{3}{2} J_2 = 1.6238235 \times 10^{-3}$ (a dimensionless constant)

$r_\oplus$ Earth's mean equatorial radius, 6378.145 km

$\dot{M}$ perturbed mean motion of the satellite in its orbit, rad/sec

The perturbed mean motion $\dot{M}$ (in radians per second) is based on a modification of the unperturbed (Keplerian) value, which is

$$\dot{M}_o = \frac{2\pi}{\tau_o} \tag{6}$$

where

$$\tau_o = 2\pi a \sqrt{a/\mu} \tag{7}$$

Then, according to Kozai,

$$\dot{M} = \dot{M}_o \left[1 + \frac{3}{2} J_2 \frac{r_\oplus^2}{p^2} \sqrt{1 - e^2} \left(1 - \frac{3}{2} \sin^2 i \right) \right] \tag{8}$$

The mean anomaly at any time is, by definition, just the constant value of $\dot{M}$ multiplied by the time interval from perigee. It is equal to the true anomaly f only for circular orbits, since according to Kepler's laws of orbital motion, the time derivative of true anomaly $\dot{f}$ is a function of position in an orbit when $e \neq 0$, being larger (faster) at perigee than at apogee. (If this were not so, orbiting objects in elliptical orbits could not sweep out equal areas in equal time, as required by Kepler's laws.) By definition, the time required for the mean anomaly to proceed from 0 to 2π rad (0^o to 360^o), that is, from perigee to perigee, is called the anomalistic period τ_A:

$$\tau_A = \frac{2\pi}{\dot{M}} \tag{9}$$

There is another equally valid definition of period brought about by the motion of the perigee - the nodal period τ_N. Figure 5 illustrates the geometry. According to this figure,

$$\tau_N = \frac{2\pi}{\dot{M} + \dot{\omega}} \tag{10}$$

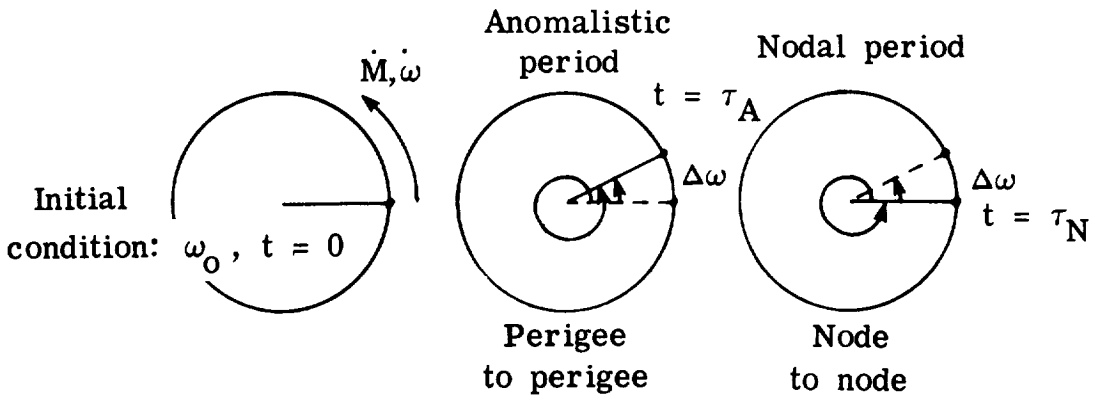

Figure 5.- Anomalistic and nodal orbit periods.

For perigee precession in the direction shown, the anomalistic period is a little longer than the nodal period. Note that the nodal period is the one by which equator crossings of an object in a circular orbit would be counted. That is, if a satellite started at its ascending node on the equator, it would cross again after one nodal period. Note, too, that τ_N as defined only describes the observable behavior of objects in circular orbits, or the mean motion for elliptical orbits. That is, the nodal crossing times of an object in an elliptical orbit - what might be called the observed nodal periods - are not constant but vary with the location of the perigee. Such an object does not cross a given latitude after a length of time τ_N. Therefore, a distinction must in general be made between the actual position (true anomaly) and the "average" position described by the preceding equations for the mean anomaly. The relation between the two involves the solution of a transcendental equation, Kepler's equation, a discussion of which can be found in any textbook on orbital mechanics. Briefly,

$$M = E - e \sin E \tag{11}$$

where M and E must be expressed in radians and E is called the eccentric anomaly; E can be directly related to true anomaly in a number of ways (ref. 3). For example,

$$f = \cos^{-1}\left(\frac{\cos E - e}{1 - e \cos E}\right) \tag{12}$$

There are many ways to solve equation (11) iteratively for E. For example, an easily programed "graphical" solution is given in reference 5. In many cases, a series expansion to the required accuracy can be done without iteration to get directly from M to f. (See ref. 3.)

Equations (5) can be used to propagate Earth orbit elements in the absence of additional perturbations. Of course, a consideration of atmospheric drag would introduce such perturbations - specifically, a secular (nonperiodic) change in semimajor axis. There are other sources which could be considered too, in addition to those due to the neglected higher order gravitational terms.

One example would be the effects of solar radiation, which are known to cause substantial orbit perturbations on hollow balloon satellites. These effects will be ignored for analysis of Earth observation mission, as they will add little to understanding patterns of surface coverage and other pertinent relationships.

At any time t after some initial orbit configuration,

$$\omega = \omega_o + \dot{\omega} t \tag{13a}$$

$$\Omega = \Omega_o + \dot{\Omega} t \tag{13b}$$

A useful formulation gives the changes $\Delta\omega$ and $\Delta\Omega$ corresponding to a mean-anomaly step ΔM:

$$\Delta\omega = \frac{(1.6238235 \times 10^{-3}) r_\oplus^2 \cdot (2 - 2.5 \sin^2 i)}{p^2} \Delta M \tag{14a}$$

$$\Delta\Omega = \frac{(-1.6238235 \times 10^{-3}) r_\oplus^2 \cdot \cos i}{p^2} \Delta M \tag{14b}$$

Expressing ΔM in degrees gives $\Delta\omega$ and $\Delta\Omega$ units of degrees. The time required for a step ΔM is

$$t = \tau_A \frac{\Delta M}{360} \tag{15}$$

Note that for $\Delta M = 360^o$, the time required for a step will be one anomalistic period. Often it is desirable to use nodal periods to generate conditions at successive crossings of a particular latitude. Then ΔM should be modified:

$$\Delta M_N = \Delta M \frac{\tau_N}{\tau_A} \tag{16}$$

Thus, in a computer program for generating orbits, $\Delta M = 360^o$ could be input to produce one orbit revolution, and if desired, it could be modified in the program by an input flag to generate nodal instead of anomalistic revolutions. Of course, any fraction or multiple of either anomalistic or nodal revolutions can be generated with equations (14) to (16) by the appropriate choice of ΔM.

As a final comment on the generation and propagation of orbits with the first-order equations, note that the concept of a perigee must be retained even for circular orbits. It must be assigned an initial value and its motion must be accounted for with equation (14a). This follows from figure 5, which shows that from the point of view of an observer on the Earth, the precession of the perigee in a circular orbit is part of, and cannot be distinguished from, the motion of the satellite around its orbit. Thus, if an observer timed successive *equator crossings* of a satellite in a circular orbit, he would measure the nodal period, which can only be related to the orbit dynamics through both the mean motion and the perigee precession. The distinction would become clear to the observer only if the satellite were in an eccentric orbit, in which case he

would note that the altitude at each crossing and the time between crossings undergo a periodic cycle with a period equal to the time for the perigee to precess 360°.

In order to illustrate the magnitude of first-order effects on typical Earth orbits, table 2 lists Keplerian (unperturbed) and perturbed periods for a range of satellite altitudes h and inclinations i, and table 3 lists precession rates $\dot{\omega}$ and $\dot{\Omega}$ as a function of inclination over the same range of altitudes. For the usually small values of e associated with Earth observation studies, the restriction of tables 2 and 3 to circular orbits does not prevent the values from being representative, as can be seen by examining the contribution of e (through p) in equations (5). The information in tables 2 and 3 is also plotted in figures 6 and 7, respectively.

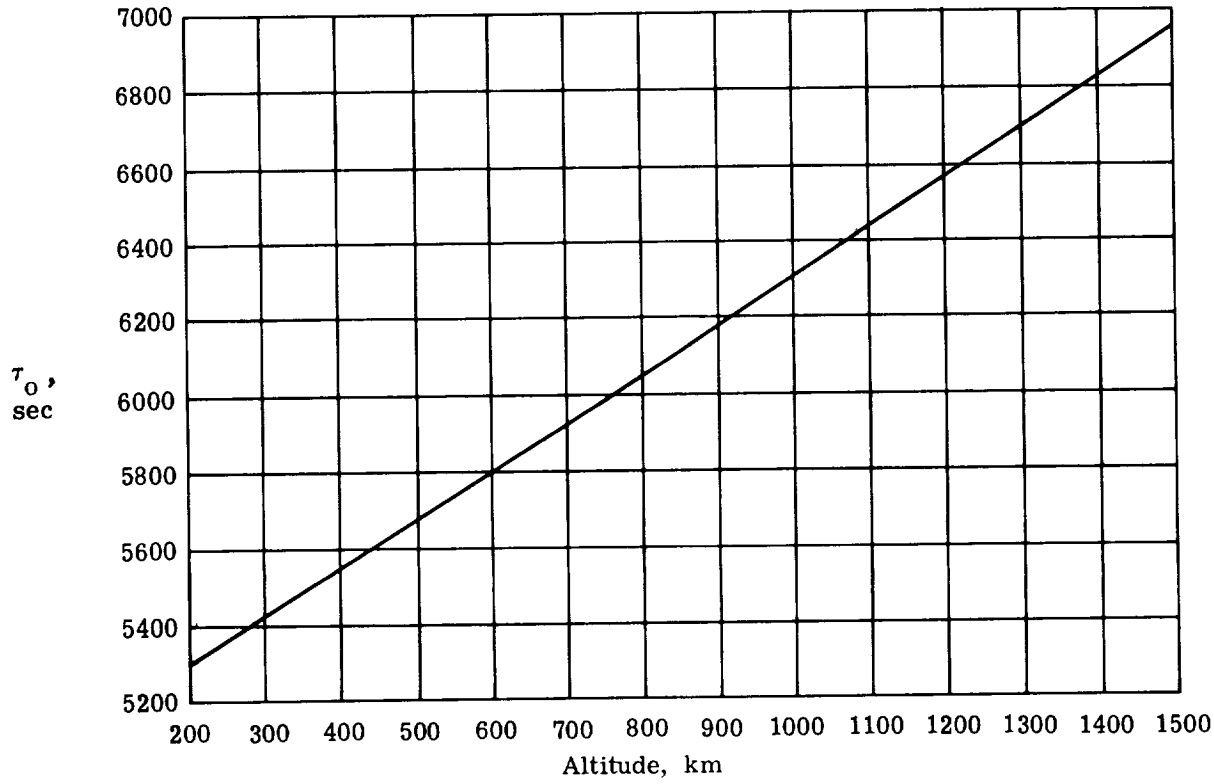

(a) Keplerian period.

Figure 6.- Keplerian period and deviations from the Keplerian period τ_o as a function of orbit altitude and inclination.

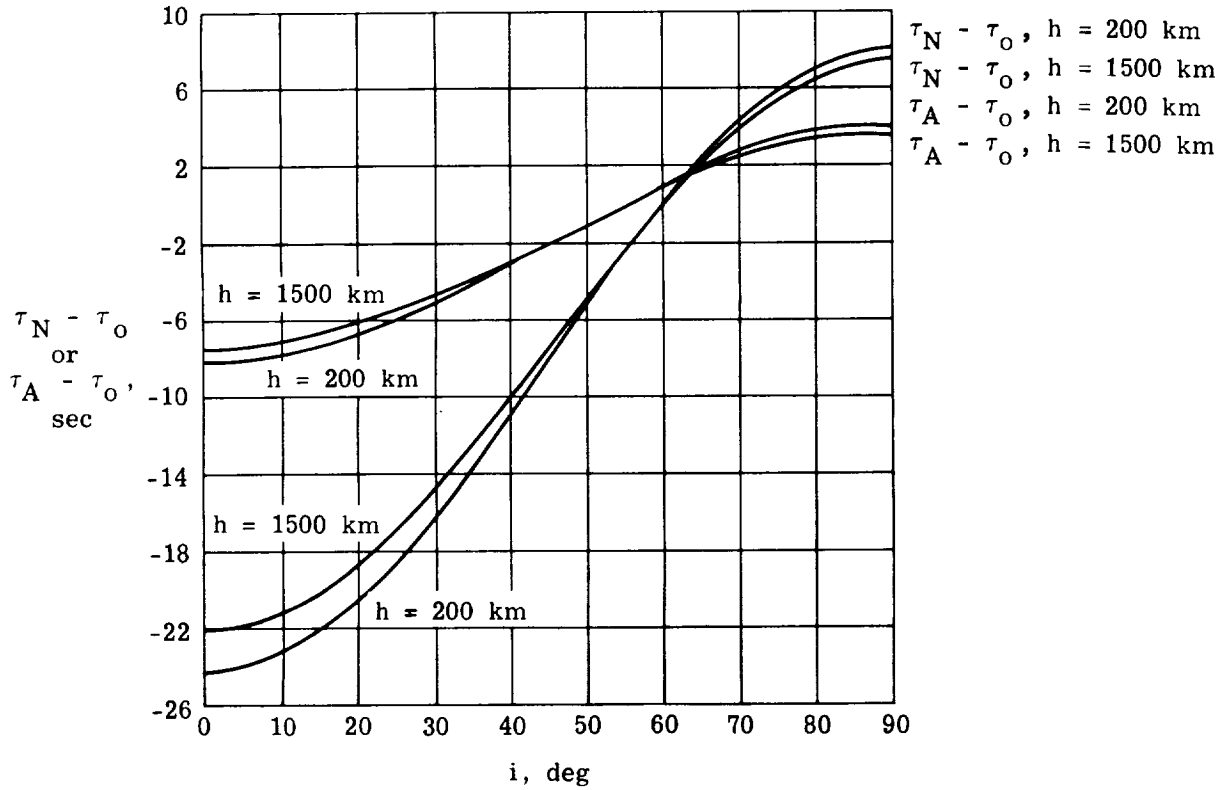

(b) Deviations from a Keplerian period.

Figure 6.- Concluded.

Sun-Synchronous Orbits

For many types of Earth observation it would be desirable to view the same surface regions repeatedly under constant lighting conditions. If it were possible to establish an orbit whose nodal precession matched the solar precession, then the Sun-orbit plane geometry would be fixed, with the lighting conditions at a particular latitude dependent only on the north-south movement of the Sun with the seasons. The best available way to accomplish this is to set the orbital precession rate equal to the average solar precession rate. Recall that the Sun precesses 360° in 1 tropical year of 365.2422 days. Therefore, from equation (5b), the orbital precession rate, in degrees per day, is

$$\frac{360}{365.2422} = 0.9856473 = \dot{\Omega} = \frac{\left(-1.6238235 \times 10^{-3}\right) r_{\oplus}^{2} \dot{M} \cos i}{p^2}$$

Substituting for $\dot{M}$ from equation (8) and converting the units of $\dot{M}$ from radians per second to degrees per day yields:

$$0.9856473 = \frac{-2.0645874 \times 10^{14} \cos i}{a^{3.5}(1 - e^2)^2}\left[1 + \frac{6.605833 \times 10^{4}}{a^2(1 - e^2)^{3/2}}(1 - 1.5 \sin^2 i)\right] \qquad (17)$$

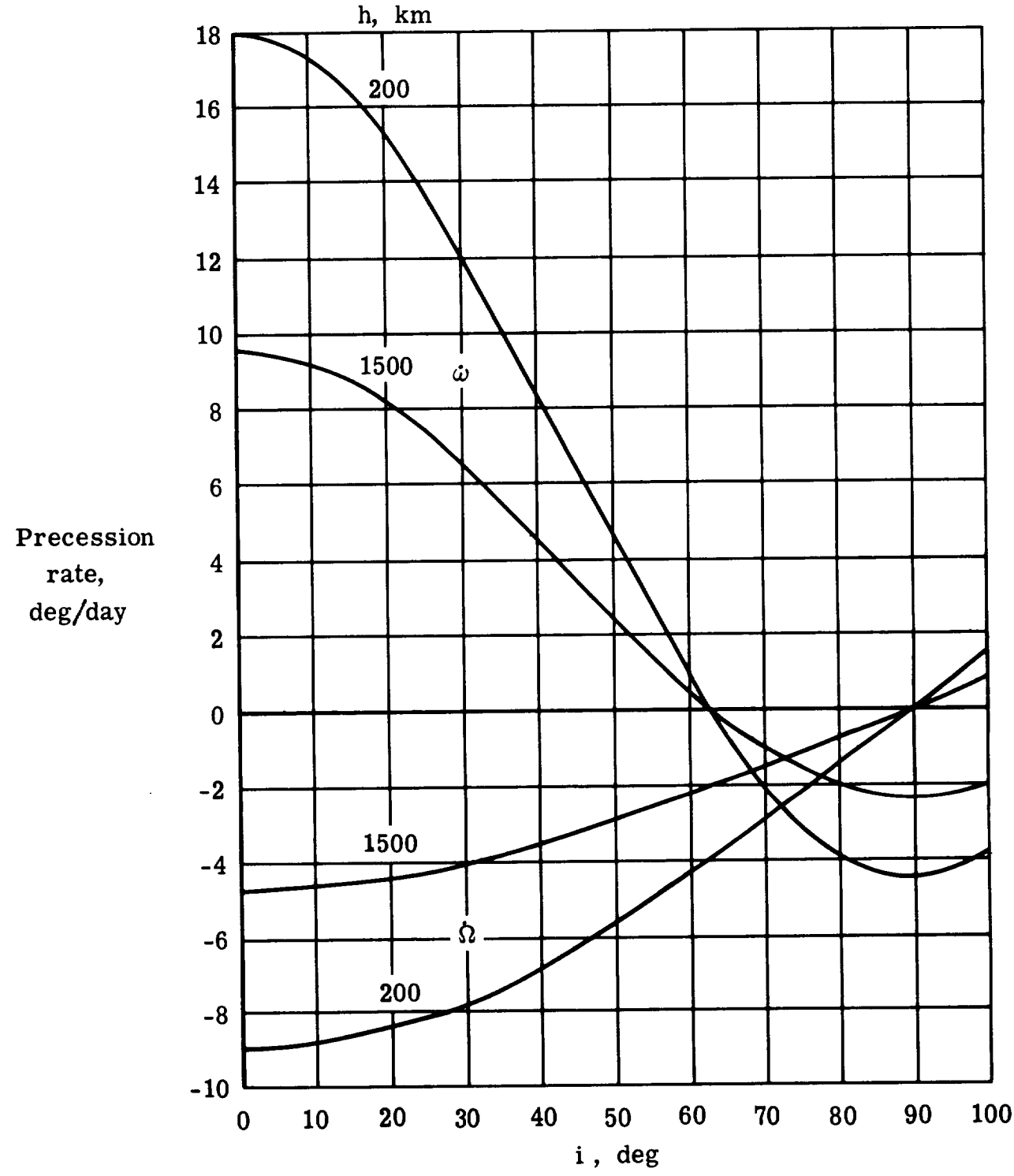

Figure 7.- Precession rates for perigee and right ascension of the ascending node for perturbed circular orbits, as a function of inclination.

Note that because of the minus sign appearing in the expression for $\dot{\Omega}$, the Sun-synchronous inclination will always be greater than 90°. For many purposes it may be sufficient to ignore the bracketed term in equation (17). As an example, for a = 7000 km and e = 0, the Sun-synchronous inclination i_s is found to be 97°.874474 with this term ignored. Iterating once by substituting this value for i in the bracketed term and recomputing yield i_s = 97°.879528. The single iteration procedure gives a Sun-synchronous orbit precession which matches the Sun's position after 1 year to better than 10^{-5} deg. The variation of Sun-synchronous orbit inclination for circular orbits up to an altitude of 1600 km is given in figure 8.

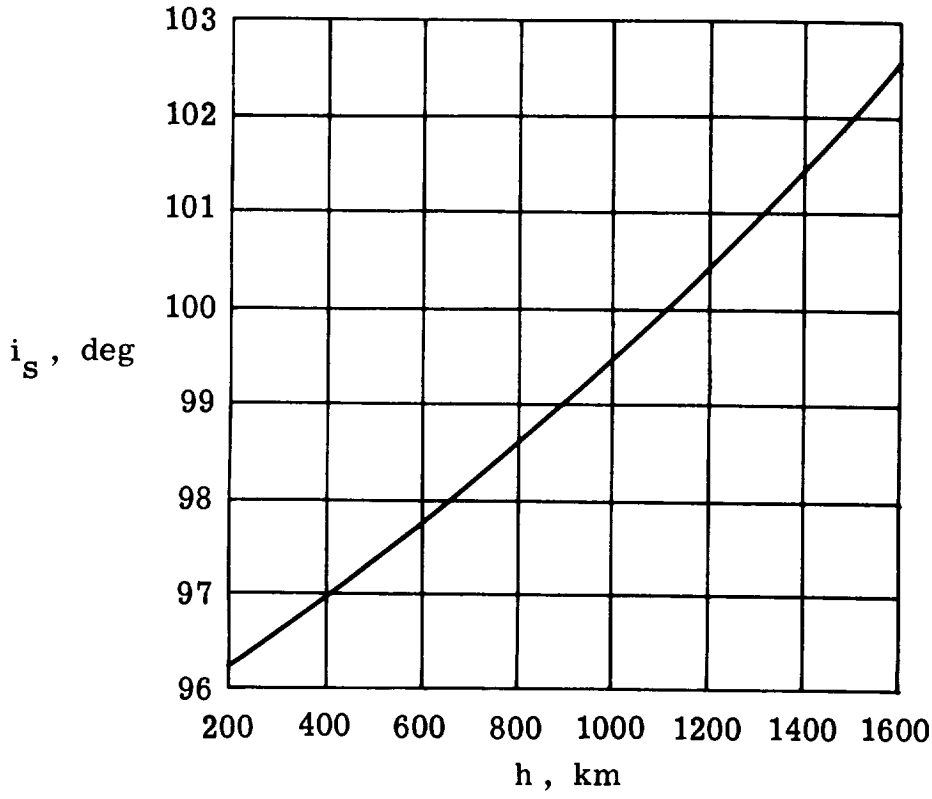

Figure 8.- Variation of Sun-synchronous orbit inclination for circular orbits as a function of altitude h.

It is interesting to consider how well a Sun-synchronous orbit actually maintains a constant relationship to the Sun throughout the year. To do this, first assume a fictitious sun[2] that travels at a constant rate along the ecliptic projection on the celestial sphere (fig. 3). This would mean that the fictitious sun travels around the celestial sphere at a constant rate of 0.9856473 deg/day. Figure 9 shows how to compare the right ascension of the ascending node of a satellite orbit with the right ascension of the fictitious subsolar

[2]This "fictitious sun" is an ad hoc mathematical entity for the purposes of this discussion, and is not the same as the fictitious mean sun which forms the basis for the mean solar time system. (See p. 6 and ref. 1.)

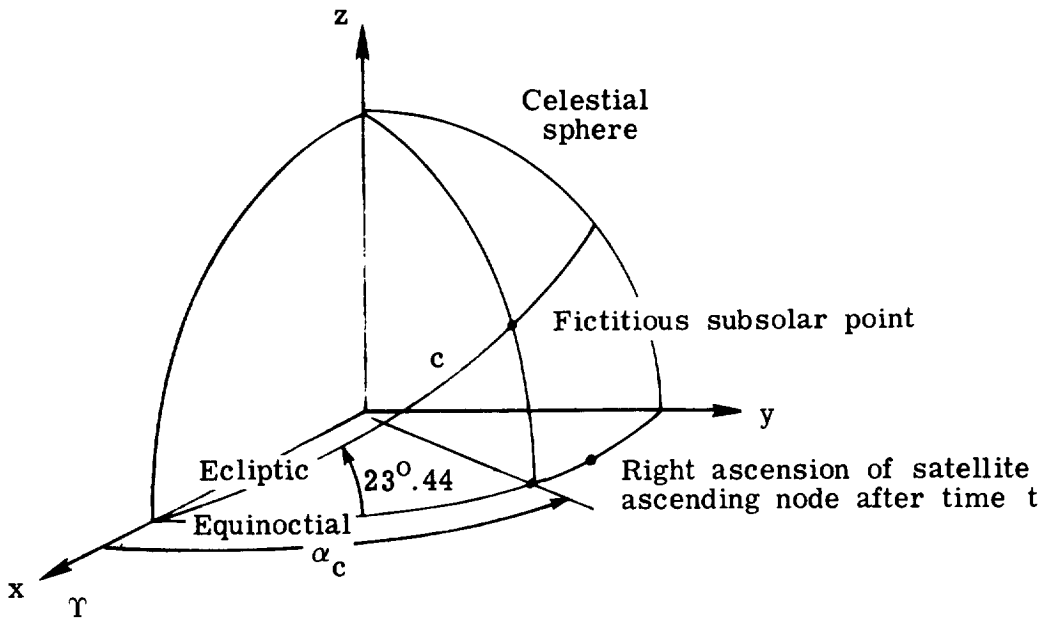

$c = 0.9856473t$

$\tan \alpha_c = \cos 23^{\circ}.44 \tan c$

α_c = right ascension of fictitious subsolar point after time t

Figure 9.- Relationship between a Sun-synchronous orbit and the subsolar point for a fictitious sun which moves at a constant rate along the ecliptic.

point. It assumes that a Sun-synchronous orbit is started at the vernal equinox, so that the subsolar point is initially in the orbital plane. For constant motion of this fictitious sun, the right ascensions must be equal at each equinox (where the ecliptic intersects the equinoctial) and at each solstice (where the ecliptic reaches its highest or lowest point relative to the equinoctial). For the fictitious sun in its circular orbit, the vernal equinox, summer solstice, autumnal equinox, and winter solstice occur at exactly 1/4-year intervals.

In figure 10 the dashed line gives the resulting difference between the right ascension of the ascending node of a Sun-synchronous orbit and that of the fictitious subsolar point for one-fourth of the yearly cycle. The solid line in figure 10 shows the difference between the same satellite quantity and the right ascension of the real subsolar point throughout 1 year. Also shown in the figure is the actual subsolar declination $\delta_{\odot}$ as the real Sun passes through the summer solstice, autumnal equinox, and winter solstice. The points at which $\delta_{\odot} = 0$ define the equinoxes, and the maximum and minimum values of $\delta_{\odot}$ define the summer and winter solstices, respectively. The three separate ordinates for $\delta_{\odot}$ in figure 10 show when these events occur during the year relative to 1/4, 1/2, and 3/4 of a year, as denoted by the three tick marks on the time axis. The greater than expected lagging of the real subsolar point is due to the eccentricity of the Earth's orbit around the Sun; the tick marks show

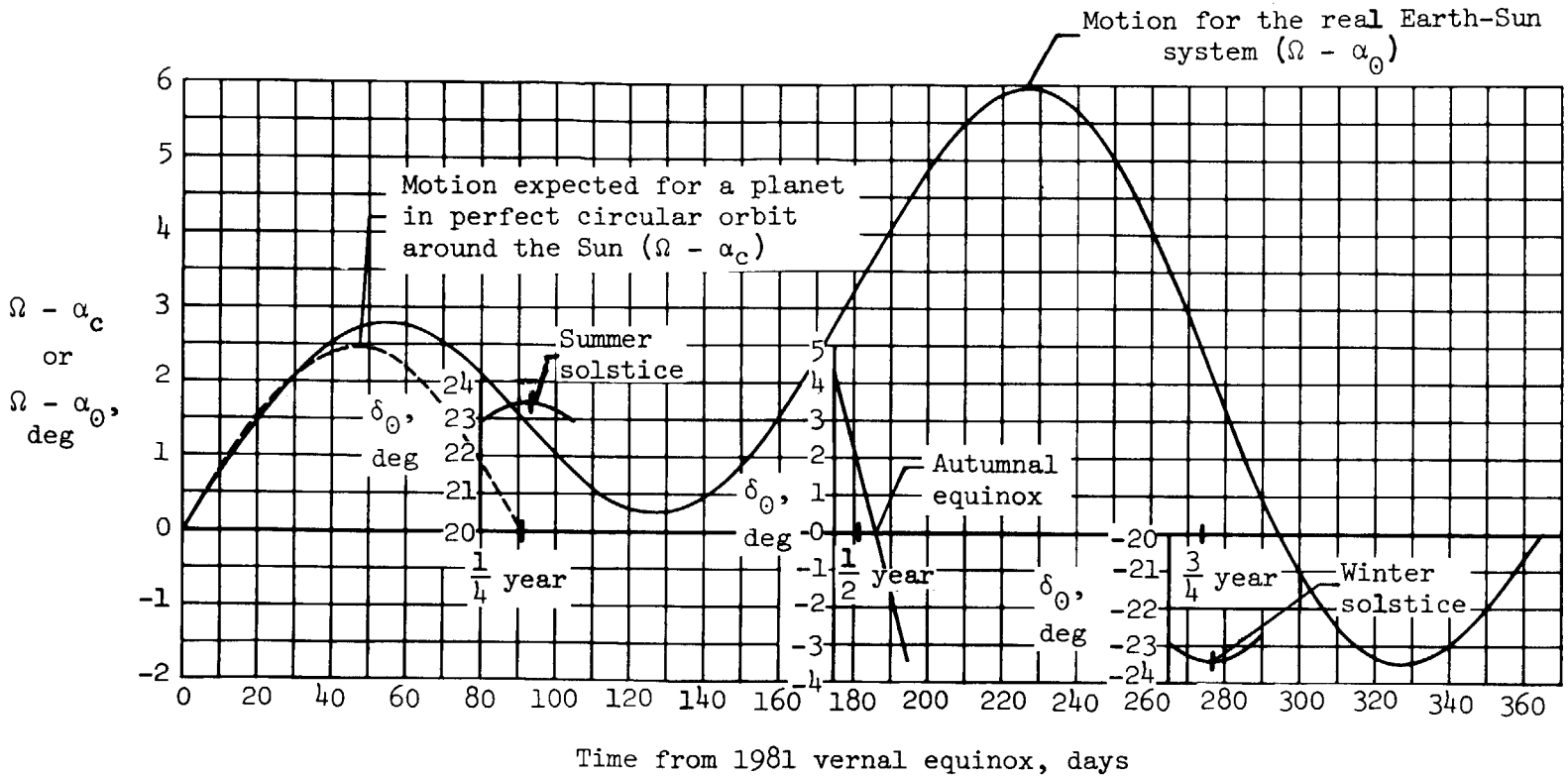

Figure 10.- Angle, as a function of time from the 1981 vernal equinox, between the right ascension of the ascending node of a high-noon Sun-synchronous satellite orbit minus the right ascension of the subsolar point.

that the autumnal equinox occurs more than 6 months after the vernal equinox, implying that the Earth moves through its aphelion (farthest point from the Sun) during this period. During the time between autumn and the next spring, the Sun "catches up" as the Earth moves through its perihelion (closest point to the Sun). Thus the satellite leads the Sun for most of the year, by as much as about 6°. Although these data are typical for the time periods of interest, they are, strictly speaking, a function of time, since the perihelion of the Earth is precessing around the Sun at a rate of approximately 1.7 degrees per century. Hence the year for which the calculations have been made (1981) is specified.

III. ESTABLISHING PATTERNS OF SURFACE COVERAGE FROM A SATELLITE

The underlying assumption for this section is that any Earth observation mission requires some type of repetitive surface coverage pattern to achieve its goals. To establish these patterns, it is necessary to couple the motion of a satellite in inertial space (that is, with respect to the inertial right-ascension—declination coordinate system) with its motion over the surface of the rotating Earth. For a randomly chosen orbit, there is no reason to expect the satellite ground track (that is, the longitude-latitude history) of the sub-satellite point to be repetitive. This is because, in general, the satellite period bears no useful relationship to the Earth's rotational period unless it is specifically selected for a particular purpose.

Ground Tracks for Circular Orbits

Several typical ground tracks are shown in figure 11 for circular orbits with a semimajor axis of 7000 km and varying inclinations. One-fourth of the

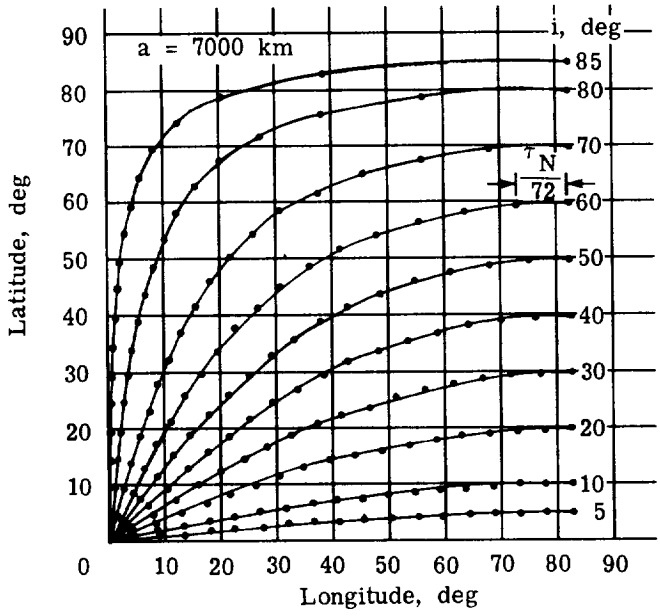

Figure 11.- Ground tracks for circular orbits, through one-fourth of a nodal period.

track is shown - the track over one-fourth of a nodal period. The satellite does not cover a longitude of 90° during this time because of the rotation of the Earth and, secondarily, the orbital precession terms. The longitude-latitude history relative to an initial point on the equator can be calculated as a function of mean-anomaly step ΔM (in degrees) according to the following equations:

$$\lambda = \sin^{-1}\left[\sin i \sin (\Delta M + \Delta\omega_{\Delta M})\right] \tag{18}$$

$$\Delta L = \tan^{-1}\left[\cos i \tan(\Delta M + \Delta\omega_{\Delta M})\right] + \Delta\Omega_{\Delta M} - \frac{\Delta M\, \tau_A (360.9856473)}{(360)(86\ 400)} \tag{19}$$

Note that these equations work only for circular orbits, or the mean motion for elliptical orbits, for the reasons discussed earlier in reference to the definition of nodal period (eq. (10)). Since orbits for coverage of the Earth's surface are commonly circular anyhow, for a variety of reasons, this is not a particularly restrictive limitation. The longitudes and latitudes are referenced to a fictitious spherical earth, even though the dynamical equations of the orbit reflect the fact that the Earth is oblate. Transformation of longitude-latitude data from a sphere to points on an oblate spheroidal surface is easily achieved (ref. 6) but is not considered necessary for the present objective of understanding and modifying patterns of surface coverage.

The cumulative effect of the apparent westward drift of the ground track is further illustrated in figure 12, which shows the longitude-latitude trace of

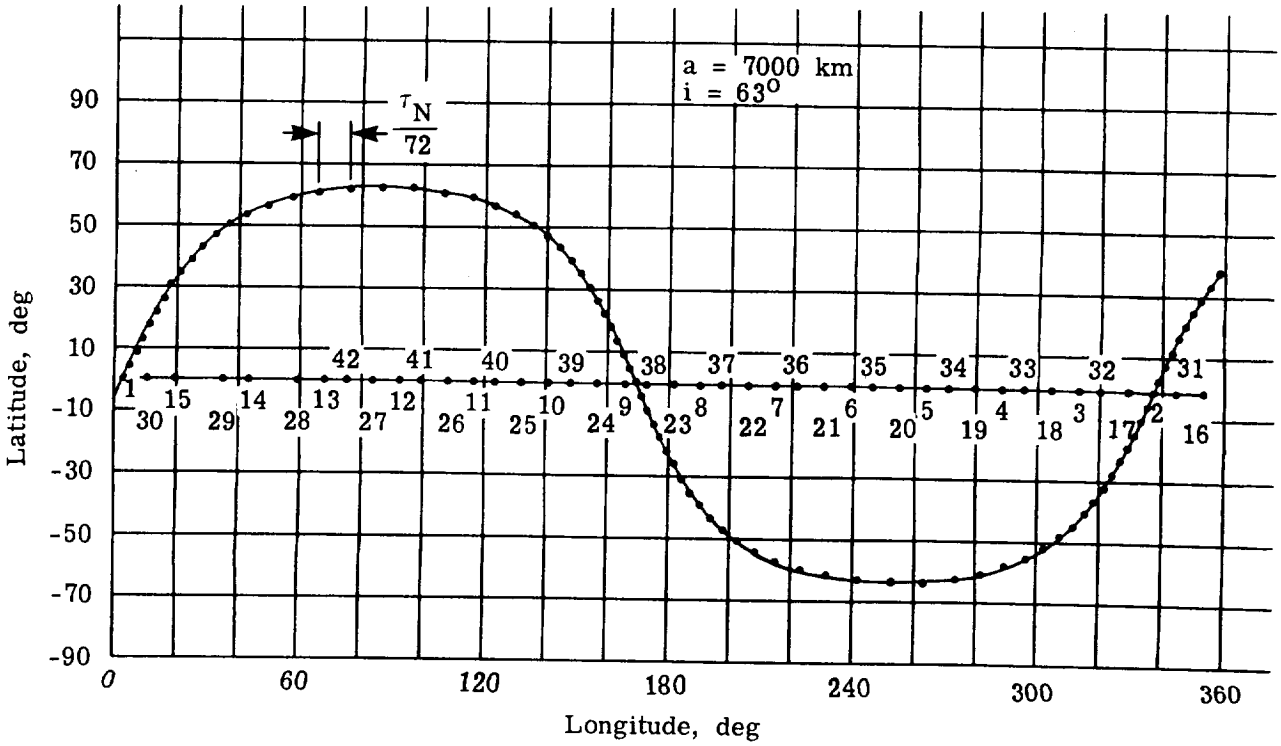

Figure 12.- Ground track for 1 revolution of a circular orbit and starting longitudes for subsequent orbits.

a circular orbit with $i = 63^\circ$ and $a = 7000$ km. (The reason for the choice of these particular orbit elements will be made clear in a subsequent section. It is immediately clear, however, that the 63° inclination covers, in latitude at least, most of the inhabited areas of the Earth.) The longitudes at which successive orbits cross the equator are shown in figure 12 by the numbered marks along the axis. The westward movement of each successive orbital track is, for any orbit, an obvious consequence of the Earth's rotation. The gaps in longitude between successive orbits constitute one of the basic restrictions in obtaining surface coverage. There is not much that can be done to alter the magnitude of the gaps, as can be seen from table 4. This shows, as a function of altitude, the change in longitude ΔL between successive orbital passes over the same latitude. To simplify construction of the table, the orbital precession effects, which are considerably less than 1 degree per orbit, have been neglected. Hence the quantity ΔL is the rotation of the Earth under a hypothetical unperturbed (Keplerian) circular orbit during one Keplerian period. More exact calculations would require the use of nodal periods and inclusion of the precession effects. Table 4 also illustrates the range of orbital periods available for Earth observation. In principle, any orbital period between about 16 and 1 or less orbits per day can be obtained; however, for reasons of sensor resolution and launch system capability, most Earth observation orbits will remain at below about 1500 km, or a period of less than about 7000 sec. The lower limit on period is set by the lowest altitude which is practical in terms of coping with atmospheric drag - about 200 km. The last nine columns of table 4 show the longitudinal displacement in kilometers at nine different latitudes for a spherical earth whose radius is equal to 6378.145 km (the mean equatorial radius of the Earth).

Designing Orbits for Repetitive Longitude-Latitude Coverage

The satellite ground track and successive equator crossings presented in figure 12 at least suggest that the longitude-latitude history will not repeat itself in any useful way; that is, there is no discernible repetitive coverage pattern for this particular orbit. According to table 4, the ground track cannot possibly repeat itself any more often than once a day, as it takes about 1 day for the Earth's surface to rotate once under the orbital trace. Except for that restriction, however, it is easy to redesign the orbit to pass over the same longitude-latitude points every day, every 2 days, and so forth. Again, because of the general differences between mean and true anomaly, this discussion is valid only for circular orbits, or the "mean" location of satellites in elliptical orbits.

Consider the geometry shown in figure 13. At some given time a satellite passes over longitude L, which is shown on the equator but could be at any latitude. For repetitive coverage of L, the point L must undergo n revolutions under the orbit trace in the time required for the satellite to undergo m nodal revolutions (where n and m are integers). The point L moves with respect to the orbit plane at an angular rate $\dot{\theta} - \dot{\Omega}$, and the satellite's orbital rate is $\dot{M} + \dot{\omega}$. (Recall that $\dot{\theta}$ is the Earth's rotational rate.) Therefore,

$$\frac{(m)(360)}{\dot{M} + \dot{\omega}} = \frac{(n)(360)}{\dot{\theta} - \dot{\Omega}} \tag{20}$$

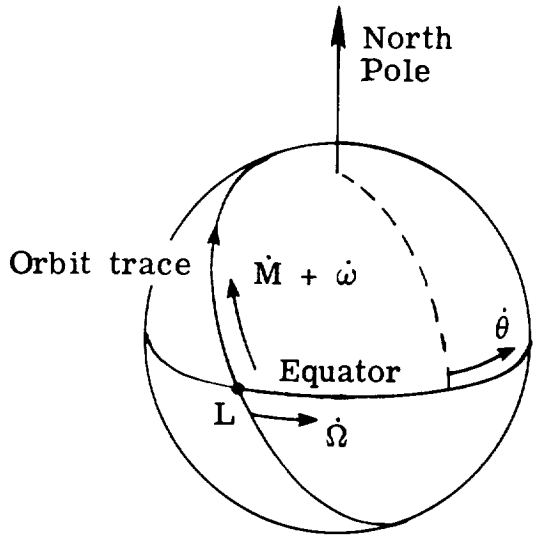

Figure 13.- Earth-orbit geometry for defining the repetition factor Q.

The repetition factor Q is defined as the number of satellite revolutions divided by the number of revolutions of the point L:

$$Q \equiv \frac{m}{n} = \frac{\dot{M} + \dot{\omega}}{\dot{\theta} - \dot{\Omega}} \tag{21}$$

Note that except for the $\dot{\omega}$ and $\dot{\Omega}$ terms, Q would be exactly equal to the number of orbits per day; however, because of the need to maintain repeated coverage over a long period of time, it is necessary to retain these small terms when designing for a particular repetition factor. An integer value of Q, for example, Q = 14/1, means that the longitude and latitude points covered by a particular ground track will be exactly duplicated 14 orbits later, the next day. What is lost to gain this advantage is that other longitudes, those not covered during the first day, will never be covered. If Q is given the value $\frac{29}{2} = 14\frac{1}{2}$, the initial longitude coverage will be duplicated on every other day after launch, with longitude points halfway in between being covered on the alternate days.

Sun-synchronous orbits present a special case in defining Q. Since the Earth's rotation rate $\dot{\theta}$ is 360° plus the average solar precession in one day, by definition, and the orbit is designed so that $\dot{\Omega}$ is the average solar precession in one day, the synchronous repetition factor is

$$Q_S = \frac{\dot{M} + \dot{\omega}}{360} \tag{22}$$

where the units of $\dot{M}$ and $\dot{\omega}$ are degrees per day. That is, for Sun-synchronous orbits, Q_S is numerically identical with the number of nodal revolutions per day.

The range of circular orbit altitudes required to produce specified values of Q (convertible to semimajor axis, in the average sense discussed previously) is shown in figure 14, which also illustrates the small inclination

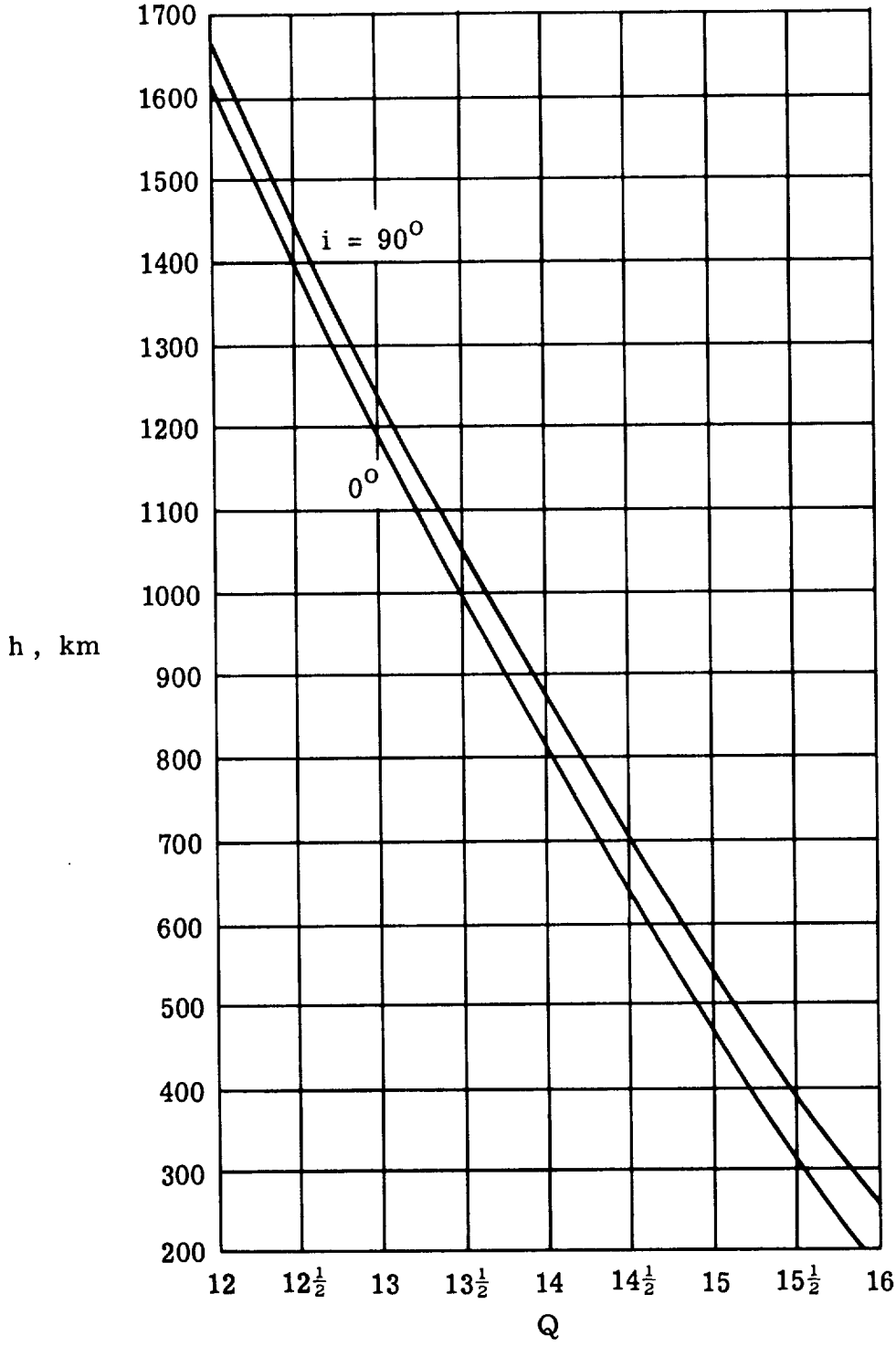

Figure 14.- Circular orbit altitudes h to achieve specified repetition factors.

dependence (through $\dot{\Omega}$). An extensive listing of circular orbit parameters for particular values of Q is given in table 5. Repetition rates of 1 to 10 days and 2 or 3 weeks are considered. Table 6 gives the same data for Sun-synchronous orbits, in which case both semimajor axis and inclination must have a particular value to satisfy two independent constraints: the correct precession rate, dependent on the satellite-Sun geometry, and repetitive ground coverage, dependent on the satellite-Earth geometry.

Appendix A presents several computing algorithms written in BASIC language for the Wang 2200 computer system. These can be used to calculate many useful orbit parameters based on the first-order perturbations discussed in the preceding sections. In particular, orbit parameters which produce orbits having desired repetition factors can be generated; the necessary computations are very tedious to do by hand to the accuracy required for internally self-consistent, long-term orbit propagation.

Solar Illumination Considerations in Satellite Orbit Analysis

Previously it has been shown that the apparent motion of the Sun about the Earth is not coupled in any discernible way with the Earth's rotation. As a result, the specification of orbit parameters for a particular type of repetitive ground coverage must be made independently of what the solar illumination conditions will be during the specified repeat cycle. Even for Sun-synchronous orbits, which maintain a "fixed" geometry with respect to the Sun, figure 4 serves as a reminder that the resulting illumination geometry is not really fixed at all and actually varies in a more complex way than might be expected.

As a basis for consideration of solar illumination patterns, table 7 presents a summary of solar position information, starting at the beginning of a calendar year and continuing through the vernal equinox of the following year. The calculations are based on equations for the Earth's motion around the Sun, presented in appendix B. Note that figure 10 can be obtained from these data. It should be emphasized that the large number of significant figures shown in the position data is merely for the sake of internal consistency when working with the data in other contexts (as in computer programs) and need not necessarily represent actual solar positions to the indicated accuracy.

As an illustration of the relationship between the Sun's apparent motion in its nearly inertial framework and the Earth's rotation about its own axis, consider the following problem: It is well known that local clock noon does not in general correspond to high noon - the instant at which the subsolar point crosses an observer's meridian. For an arbitrary date, say May 1, 1981, find the actual local clock time at which high noon occurs for an observer at a longitude L_m of -70°. The first step in the solution is to locate both the Sun and the observer in a common coordinate system. The latitude (declination) does not matter, as the location of high noon only involves lining up the observer's meridian with the subsolar point. The right ascension of the observer is calculated from equations (1) to (3). The Julian date for 0^h UT, May 1, 1981, is 244 4725.5. In the following calculations, note the practice of removing integer multiples of 360° from the angular values, and of converting negative angles to their positive equivalents between 0° and 360°:

$$T = \frac{244\ 4725.5 - 241\ 5020.0}{36\ 525} = 0.813292 \text{ Julian century}$$

$$\alpha_{g,o} = 99^{\circ}.6909833 + 36000^{\circ}.7689T + 0^{\circ}.00038708T^2 = 218^{\circ}.838139$$

$$\alpha_{obs} = \alpha_{g,o} + L_m = 148^{\circ}.838139$$

The right ascension of the Sun at 0^h UT is given in table 7:

$$\alpha_{\odot} = 38^{\circ}.127349$$

The observer's right ascension changes at a rate equal to the sidereal rotation of the Earth. The corresponding motion of the subsolar point is not constant but changes with the seasons and the position of the Earth in its heliocentric orbit. The rate can be determined to sufficient accuracy by examining the change in solar right ascension as given in table 7. The average of the 5-day changes prior to and following May 1, 1981, is

$$\dot{\alpha}_{\odot} = \frac{1}{2}\left[\frac{(42^{\circ}.927723 - 38^{\circ}.127349)}{5} + \frac{(38^{\circ}.127349 - 33^{\circ}.382532)}{5}\right] = 0.9545191 \text{ deg/day}$$

Finally, the time at which the Sun crosses the observer's meridian is given by

$$148^{\circ}.838139 + 360.9856473t = 38^{\circ}.127349 + 0.9545191t$$

$$360.0311282t = -110^{\circ}.71079 = 249^{\circ}.28921$$

$$t = 0.69241016 \text{ day}$$

Therefore, high noon occurs at J.D. 244 4726.19241016 = May 1, 1981, $16^h37^m04^s$ UT, or $11^h37^m04^s$ EST (local clock time).

Also of interest in table 7 is the variation of solar declination $\delta_{\odot}$ as a function of time. Clearly, this seasonal variation has a dominant effect on solar illumination during any Earth observing mission. Figure 15 illustrates the range of Sun elevation angles available throughout the year as a function of latitude. (A geometrical description of the elevation angle is given in the following section.) Variation of Sun elevation angle ξ with time is shown for summer, winter, and the equinoxes in table 8. The time system used in this table is an hour-angle (β) system; the elevation angle ξ is given at any latitude λ by

$$\xi = 90^{\circ} - \cos^{-1}(\cos \delta_{\odot} \cos \lambda \cos \beta + \sin \delta_{\odot} \sin \lambda) \qquad (23)$$

where β is the equatorial angle from the subsatellite meridian to the subsolar meridian. The reference (0 hours) is local high noon ($\beta = 0^{\circ}$). For example, at a relative time of +2 hours or -2 hours (10 a.m. or 2 p.m., respectively, in a "clock" terminology), the Sun is on a meridian $+30^{\circ}$ or -30° away from the local meridian. The use of this relative time system serves as a warning to exercise care when dealing with orbit timing. A "9:00 a.m." orbit could mean that a

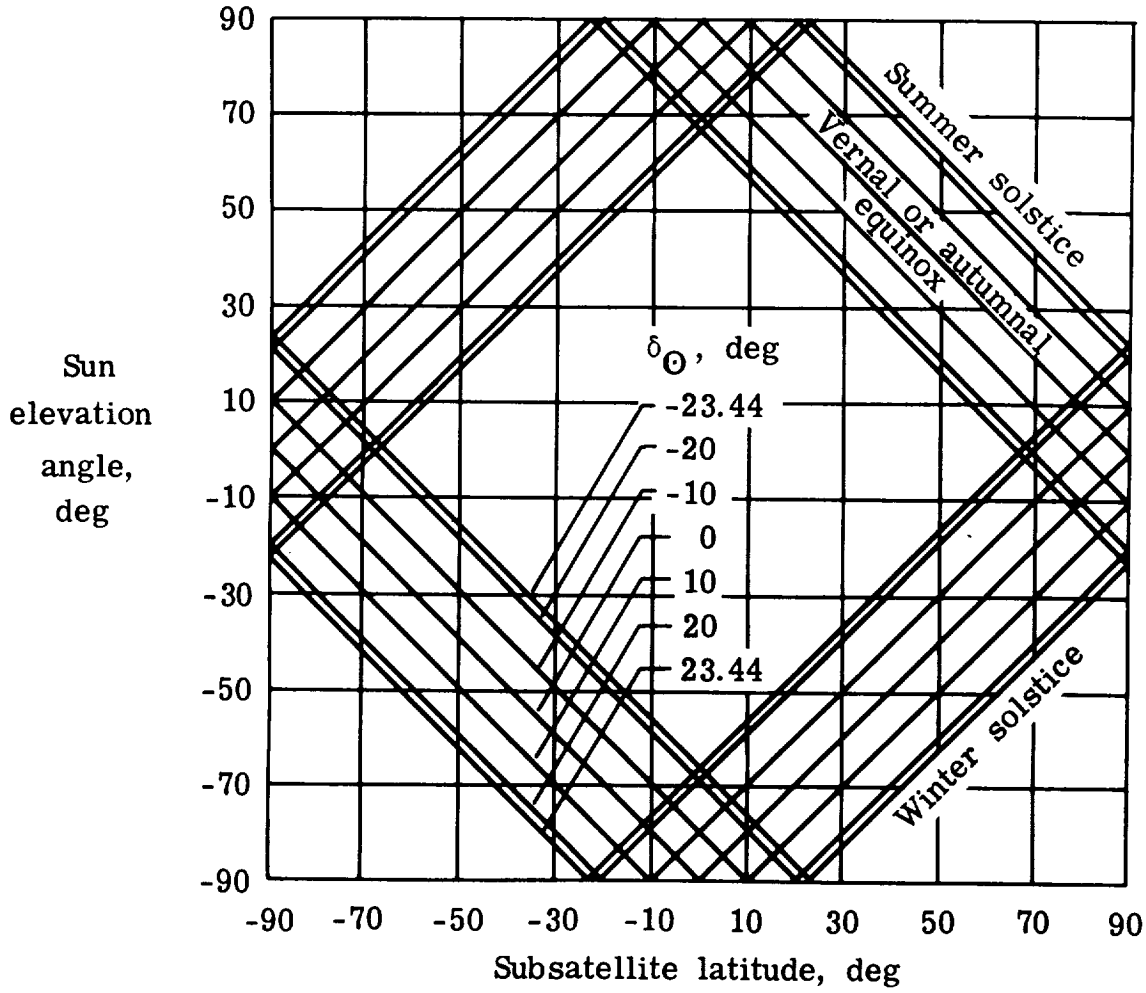

Figure 15.- Range of Sun elevation angles as a function of subsatellite latitude, with subsolar declination (time of year) as a parameter.

satellite crosses the equator at 9:00 a.m. local time, but such a description might just as well be loosely used to mean that at the equator crossing, the subsolar meridian is 45° to the east of the subsatellite meridian. These conditions are not, in general, exactly equivalent! The reason for belaboring these distinctions will be apparent in a later example, where care is taken to separate actual Sun lighting conditions at the Earth's surface from the intuitive feelings about sunlight that an observer from the northern temperate latitudes tends to associate with a given local clock time.

As an example of the use of figure 15 or equation (23) to provide limiting values for Sun lighting conditions, consider an observer at 50° latitude. The range of available elevation angles is bounded by the intersection of the edges of the rectangle appropriate to the subsolar declination at the date of observation with a vertical line at 50°. The subsolar declination is directly related to the date of observation. Using table 7, for example, the observer could relate a particular date to the corresponding subsolar declination for use with

figure 15, interpolating as required in the table and figure. Suppose the date is around June 20, near the summer solstice. Then the subsolar declination is at its maximum of $23^{o}.44$; there is an appropriate boundary indicated in figure 15 for this value which may be used without interpolation. The maximum and minimum values of ξ occur for $\beta = 0^{o}$ and $\beta = 180^{o}$, respectively (0 and 12 hours). Thus, either approximately from figure 15 or more accurately from equation (23), the maximum and minimum values of ξ at the time of the summer solstice are found to be $63^{o}.44$ and $-16^{o}.56$, respectively, for an observer at 50^{o} latitude.

Before examining solar illumination patterns during long-duration missions, it is first necessary to establish the reference systems for specifying solar position from the ground and from a satellite. Following that, some special attention will be given to the problem of solar occultation, since the observation of sunset and sunrise relative to a satellite - at the beginning and end of periods of darkness - has particular significance for many types of atmospheric profile measurements.

Pointing Angle Geometries for Locating the Sun

To account for the Sun's location relative to a satellite or its subpoint on the Earth's surface, it is necessary to have three pieces of information: (1) a reference system, (2) the solar elevation or zenith angle, and (3) the direction from which the Sun is shining. The geometry selected for locating the Sun from the Earth's surface is shown in figure 16. The point P is the

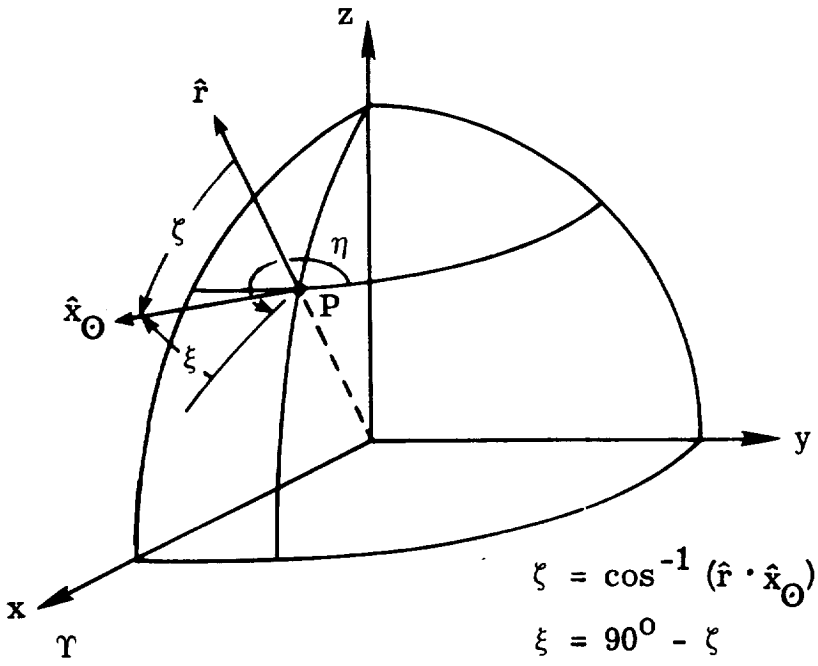

Figure 16.- Pointing angles for the Sun relative to the Earth's surface.

subsatellite point, $\hat{r}$ is the unit vector to the satellite, and $\hat{x}_\odot$ is a unit vector in the direction of the Sun. The zenith angle ζ is measured downward from the local vertical $\hat{r}$, and the elevation angle ξ is measured upward from the local horizon. The angle η, measured counterclockwise from the parallel of latitude through P (that is, from a unit vector pointing east from P), defines the direction from which the Sun is shining.

Note that P is a point of right ascension and declination, so that a subsatellite point given in terms of longitude and latitude must be transformed to the proper coordinate system. Note, too, that since the Sun appears to be infinitely far away, $\hat{x}_\odot$ has essentially constant components regardless of the location of P. Thus, P could just as well be at the satellite, in which case η and ξ or ζ could serve as pointing angles to the Sun from the satellite. However, for this purpose other reference systems, such as those described in the following paragraph, are more convenient.

Figure 17 illustrates a coordinate system for defining pointing angles relative to a satellite. The unit vector $\hat{N}$ is normal to the orbit, in the

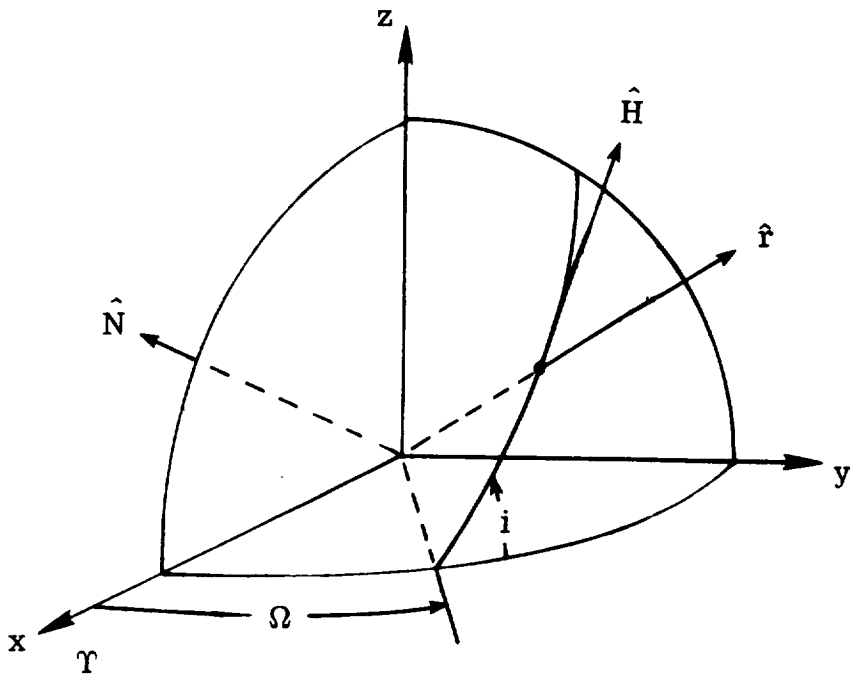

$$\hat{N} = (\sin \Omega \sin i, -\cos \Omega \sin i, \cos i)$$
$$\hat{H} = \hat{N} \times \hat{r}$$

Figure 17.- Definition of a Cartesian coordinate system for pointing relative to a satellite.

direction of the angular momentum vector. For circular orbits the heading vector $\hat{H}$ is in the same direction as the velocity vector. These two vectors, with $\hat{r}$, form a Cartesian coordinate system.

One way to find the Sun relative to $\hat{H}$, $\hat{N}$, and $\hat{r}$ is to rotate first about $\hat{r}$ and then about $\hat{N}$. Figure 18(a) shows the pointing angles A and B which result. Note that A is identical with the sun elevation angle ξ. Another useful way to find the Sun is to rotate first about $\hat{N}$, with results as shown in figure 18(b); I is rotation in the plane of satellite motion and O is rotation out of plane.

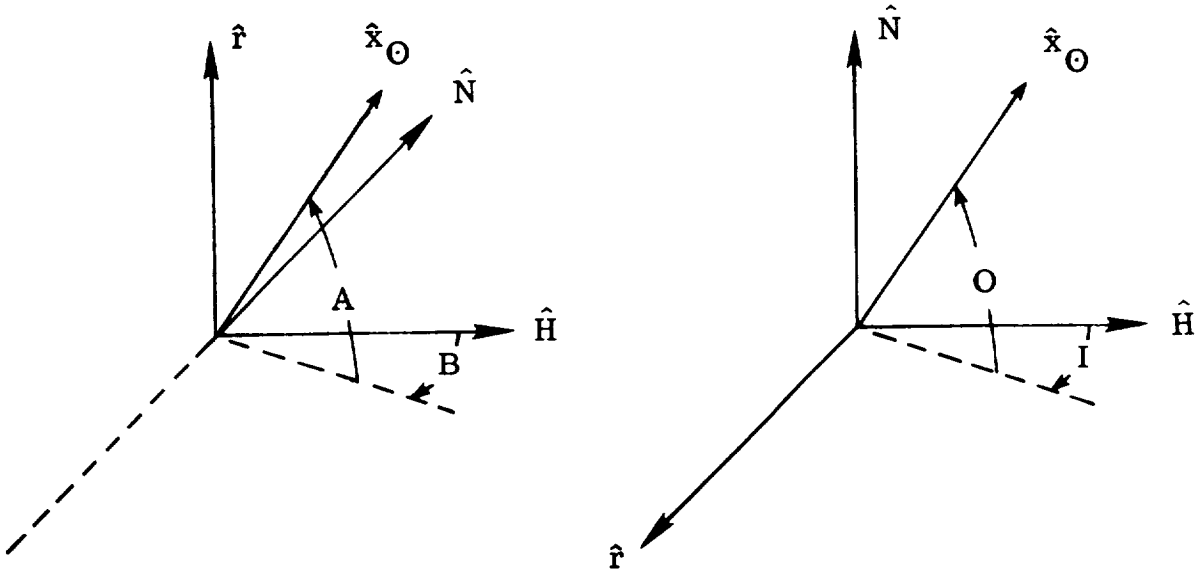

(a) $B = \tan^{-1}\left(-\hat{N} \cdot \hat{x}_\odot / \hat{H} \cdot \hat{x}_\odot\right)$;

$A = 90^\circ - \cos^{-1}(\hat{r} \cdot \hat{x}_\odot)$.

(b) $I = \tan^{-1}\left(\hat{r} \cdot \hat{x}_\odot / \hat{H} \cdot \hat{x}_\odot\right)$;

$O = 90^\circ - \cos^{-1}(\hat{N} \cdot \hat{x}_\odot)$.

Figure 18.- Pointing angles for locating the Sun relative to a satellite.

For noncircular orbits it may be useful to consider a coordinate system which retains $\hat{N}$, replaces $\hat{H}$ with the unit velocity vector $\hat{v}$, and replaces $\hat{r}$ with a new unit vector $\hat{v} \times \hat{N}$ to give a Cartesian system.

The Geometry of Sunrise and Sunset as Viewed From a Satellite

As previously mentioned, the times during which the Sun rises and sets on the Earth's horizon as viewed from a satellite have a special significance for many types of atmospheric observations. The usual astronomical definitions of sunrise or sunset, based on the appearance of the solar image to an observer on the ground, are not the same as employed here. It is perfectly satisfactory for the present to define sunrise or sunset as the instant at which the center of the solar image (as located by a unit vector $\hat{x}_\odot$ in the right-ascension—declination system) is coincident with the horizon of a spherical earth of radius 6378.145 km. During sunrise or sunset it is, in principle, possible to obtain vertical profiles of many different atmospheric constituents which attenuate the Sun's radiation. Of interest during these measurements is the tangent point on the Earth (or on a concentric spherical shell) at which the measurement is made. The geometry is shown in sketch (a). A vector $\vec{r}_T$ from the Earth's

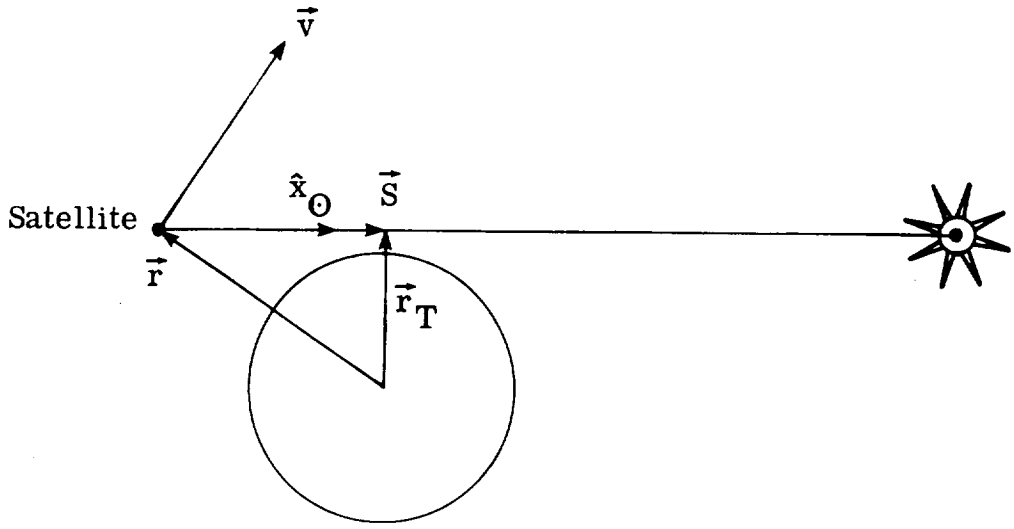

Sketch (a)

center is constructed perpendicular to the line from the satellite to the Sun (along $\hat{x}_\odot$). The path from the satellite to the point of intersection of $\vec{r}_T$ along $\hat{x}_\odot$ is given by the vector $\vec{S}$. The tangent latitude and longitude are the coordinates of the point at which $\vec{r}_T$ pierces the Earth's surface. Depending on the orbit parameters (and hence the apparent sunrise or sunset rate) and the time required for measurements, the tangent point may or may not change significantly during the course of a series of measurements made as the Sun's image passes through the atmosphere. Thus, although the problem of interpreting solar occultation measurements is, per se, beyond the scope of this paper, the orbital information necessary for taking these effects into account can easily be supplied.

Since $\vec{r}$ and $\hat{x}_\odot$ are known, the triangular geometry for finding $\vec{S}$ and $\vec{r}_T$ is straightforward:

$$\vec{S} = (-\vec{r} \cdot \hat{x}_\odot)\hat{x}_\odot \tag{24}$$

$$\vec{r}_T = \vec{r} + \vec{S} \tag{25}$$

The apparent sunrise or sunset rate along $\vec{r}_T$ is given by

$$R = \vec{v} \cdot \hat{r}_T \tag{26}$$

which can conveniently be expressed as the rate, in kilometers per second, at which the solar image appears to move vertically with respect to the horizon at the tangent point, or as an angular rate by using the magnitude of $\vec{S}$.

To provide a feeling for the magnitude of the sunrise and sunset rates, assume that the Sun is just rising directly in front of and below a satellite in a circular orbit with a radius of 7000 km. In terms of the angles defined in

figure 18, B and O are zero and A and I are negative. The geometry is given in sketch (b).

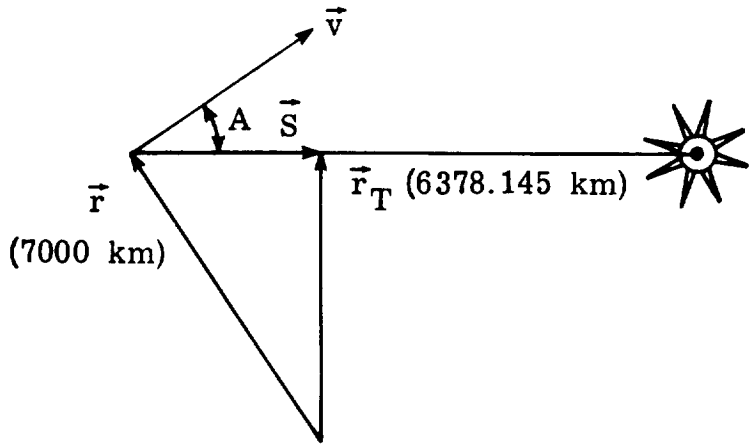

Sketch (b)

For this simple case:

$$S = \sqrt{7000^2 - 6378.145^2} = 2884 \text{ km}$$

and

$$I = A = -\left[90^o - \cos^{-1}(S/7000)\right] = -24^o.3$$

The Keplerian period of this orbit τ_o is 5828.5 sec, so that (to a good approximation even for the perturbed case):

$$v = 2\pi(7000/5828.5) = 7.546 \text{ km/sec}$$

The projection of this velocity onto $\hat{r}_T$ is $\vec{v} \cdot \hat{r}_T$, given by

$$R = v \sin A = 3.11 \text{ km/sec} = 0.062 \text{ deg/sec}$$

It is easy to see from this case that the Sun's image appears to pass through 50 km or so of atmosphere in less than 20 sec. At the other extreme, however, when the satellite is travelling along the terminator, as when the orbit is entering a period of no occultation for several orbits, the sunrise or sunset rate approaches zero. Then vertical profiles of the atmosphere become more difficult to obtain because the tangent point as previously defined undergoes large excursions across the Earth's surface.

The equations for determining the time of sunrise and sunset relative to perigee in an inertially fixed orbit are worked out in appendix C. Strictly speaking, this procedure must be an iterative one, since the orbit actually moves in inertial space between the instant of perigee passage and the calculated time of entry into and exit from a period of darkness. As a practical matter, the iteration is usually not worth the effort. With appendix C, it is

possible to propagate an orbit in steps of one anomalistic period, from perigee to perigee, computing the sunrises and sunsets at each step and determining those periods of continuous solar exposure. This information has obvious importance for the scientific objectives of any mission as well as for the engineering design of the satellite and its systems.

IV. SOME EXAMPLES OF GEOGRAPHICAL COVERAGE AND SOLAR ILLUMINATION PATTERNS FOR LONG-DURATION EARTH MONITORING MISSIONS

It should be clear from the preceding sections that the discussions of orbit analysis were intended to encompass mission situations extending for a year or so - long enough for orbits to precess completely through several cycles, for the Sun to go through an annual illumination cycle, and for repetitive coverage of locations on the Earth's surface. The dynamic relationships between a satellite and the targets of its sensors are often decisive factors in assessing the worth of a mission. It is not so much a question of establishing a particular set of viewing conditions at a particular time as it is a question of assessing and optimizing the total output from all measurement opportunities over the nominal course of the mission. This section presents some representative patterns of coverage based on actual orbit analysis experience with several proposed Earth observation missions. The examples are intended to illustrate some important types of coverage and their associated problems. They include (1) yearly illumination patterns over a single site, (2) yearly variations in illumination angle as a function of latitude, (3) solar illumination effects on global surface coverage, and (4) tangent-point distributions for solar occultation experiments.

Establishing a Need for Repetitive Coverage Patterns

Each of the following examples requires, in some form, the establishment of repeatable patterns; therefore, it is appropriate at this point to consider the general necessity for repetition. The quantities or features of interest for measuring or viewing from a spacecraft have one property in common: they all vary in at least three dimensions - longitude, latitude, and time. If they did not, there would be little justification for viewing them from spaceborne platforms. In order to separate the contributions of each dimension, it is clearly necessary to have repetition - repetition of two quantities to isolate the third. Repeated measurements over the same location (longitude and latitude) to isolate a dependence on time is one important example. Note that other desirable repetitive pairings - longitude or latitude with time to isolate the dependence on a space dimension - are not possible with a single satellite, which can repeat itself in space but not in time. Thus, it must be sufficient to match repetition in space coordinates with later but presumably identical conditions in the time coordinate. If the time dependence is obvious or dominating, as in a diurnal cycle, identical conditions may be easy to establish. Otherwise, interpretation of a set of sequential measurements is one of the major problems in utilizing spacecraft data.

A less obvious reason for repetitive measurements is the need to determine error associated with measurements. Assuming that the errors resulting from making and interpreting measurements are randomly distributed, multiple measurements under the same conditions are required to isolate error from the other factors influencing the value of the measured quantity. The extent to which this can be done depends on the feasibility of substituting equivalent values in the time dimension for identical ones. Spatially distributed quantities are not exempt from similar considerations, as it is often necessary to group nearly identical spatial coordinates with the assumption that variations of interest exist only over spatial scales that are large compared with the differences among such a grouping of available data points.

Yearly Illumination Patterns Over a Single Site

A straightforward application of the previous analyses is to establish a satellite orbit that gives repetitive coverage over a selected site or group of sites, determine one or more parameters of interest, and study their behavior over the course of a year. This type of parametric study has practical applications in Earth resource management; pollution monitoring; land-use planning; and many other research, survey, or inventory tasks. The example in this section is based on a 1973 study of orbit requirements for observing the eastern coast of the continental United States (ref. 7). In this study, an orbit was selected that gives good coverage of the entire east coast and its performance was assessed by reference to a single site at Norfolk, Virginia, which is roughly midway along the Atlantic Coast.

The orbit inclination of 63° was selected by minimizing the off-nadir pointing required to cover 25 east coast sites of interest. This orbit has been noted previously, in the section "Establishing Patterns of Surface Coverage From a Satellite," as covering in latitude most of the inhabited areas of the Earth. A ground track is plotted in figure 12; however, it is a "random" orbit in the sense that its other elements were not selected to give a particular repetition factor for regular coverage of a selected site. For a circular orbit, this means just changing the semimajor axis to the appropriate value. This is easily done with the algorithms described in appendix A. Table 9 gives a list of orbit parameters for a 63° circular orbit which gives daily coverage over a particular site ($Q = 15$). The list includes the starting conditions which will cause the satellite to pass over Norfolk at the desired time on its initial orbit (local clock noon). Note that the anomalistic and nodal periods are nearly identical, as the inclination of 63° is very close to the value at which perigee precession is zero. (See fig. 7.) The ground track of this orbit is plotted for the first 15 revolutions in figure 19, as seen from a vantage point in space directly over Norfolk.

The parameter of interest in reference 7, and of general interest for any similar mission, is the variation of Sun elevation angle during the repeated passages over the site. Clearly, some of the passes will take place in darkness because of the nodal precession of the orbit. The precession rate relative to the Sun is about $4\frac{1}{2}$ deg/day; therefore, it would be reasonable to expect a complete illumination cycle to take about 80 days. "On top" of this cycle should

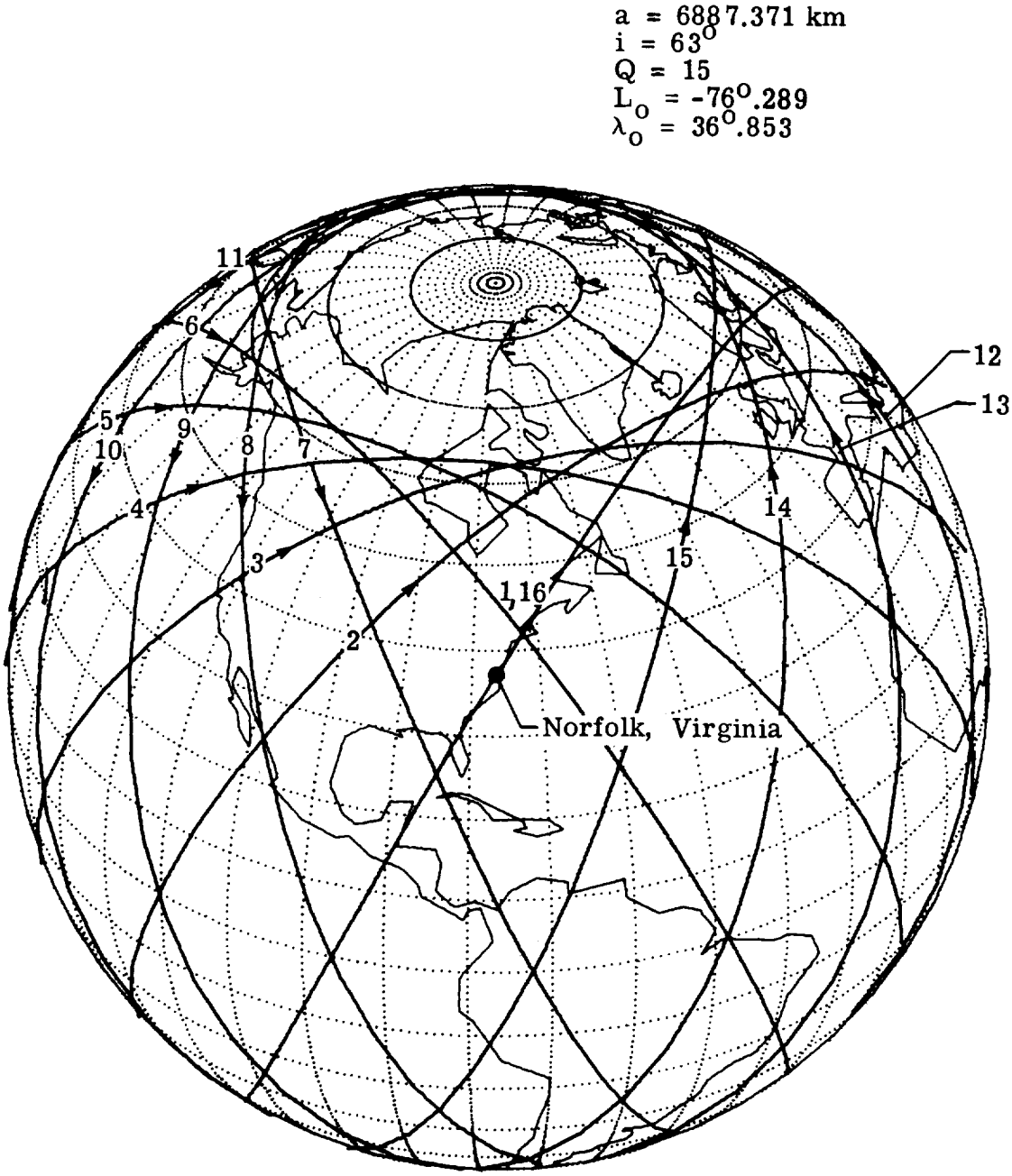

Figure 19.- Ground track history of a 63° orbit started at Norfolk, Virginia, with a 1-day repeat cycle. Q = 15.

be an elevation-angle envelope resulting from the seasonal variation of the Sun's declination. The actual variation in Sun elevation angle over Norfolk at the time of satellite passage is illustrated in figure 20. The points show the elevation angle for an orbit initially passing over Norfolk on Jan. 1, 1981, at 17^h UT (12:00 noon EST). Bear in mind that the curve is really not continuous but is a set of 365 discrete points, one for each pass over Norfolk during the year. The solid lines show the maximum and minimum available Sun elevation

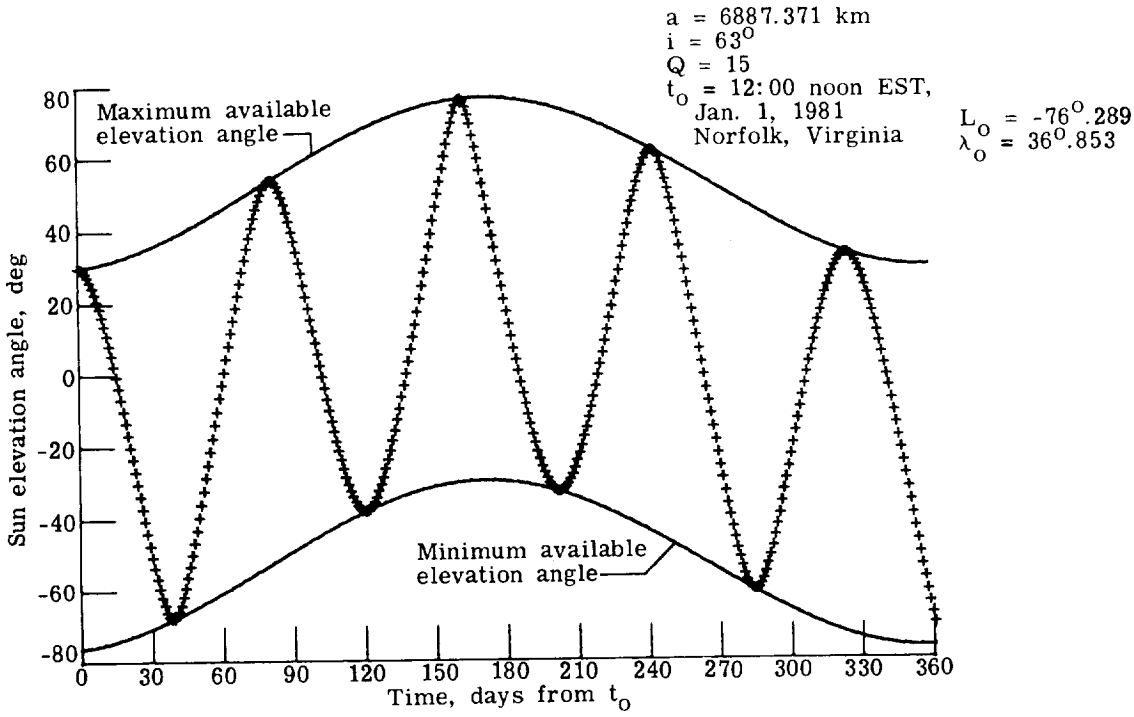

Figure 20.- Sun elevation angle over Norfolk, Virginia, for a satellite in a 63° circular orbit.

angles at this site as calculated from equation (23). It is interesting to consider how little control can be exercised over the resulting illumination pattern. By starting the orbit at a different time of day, the patterns can be shifted within the envelope of available elevation angles; except for this, there are no available parameters for altering the pattern in any significant way. A different inclination will speed up or slow down the illumination cycle without altering its basic behavior. A different value of Q will alter the coverage of other places, all of which will have their own latitude-dependent illumination patterns similar to those in figure 20. The price for repetitive coverage over more sites is, as always, less frequent coverage of each site. The resulting trade-off is a standard study for any Earth-oriented mission with multiple objectives, each of which may have to be compromised for the total optimization of the mission.

There is also the possibility of using a Sun-synchronous orbit. Then, most of the rest of the east coast coverage will be lost because orbits at synchronous inclination no longer follow the coastline. In this case, the initial timing of the orbit is important, as it can be used to regulate the Sun elevation pattern for the rest of the year, within the allowable envelope. If it is desired to view the nadir at the maximum Sun elevation angle (not necessarily a desirable situation), this condition can be approximately met by starting the orbit at local clock noon. Indeed, the elevation angle for such an orbit started at Norfolk would follow the top solid line in figure 20 and would be indistinguishable from it on the scale of this figure. Curves for other local times would have the same shape as the maximum-minimum envelopes in figure 20 but

would be displaced within these envelopes by an amount proportional to the local time, between noon and midnight.

Yearly Variations in Illumination Angle as a Function of Latitude

The specific example of a 63° orbit discussed in the previous section can easily be generalized to predict the illumination conditions encountered by any orbit. The envelope of available Sun elevation angles apparent in figure 20 is but one of a family of such curves which are a function of latitude and time. Figure 21 gives 10 such yearly curves for latitudes from 0° to 90° in 10° incre-

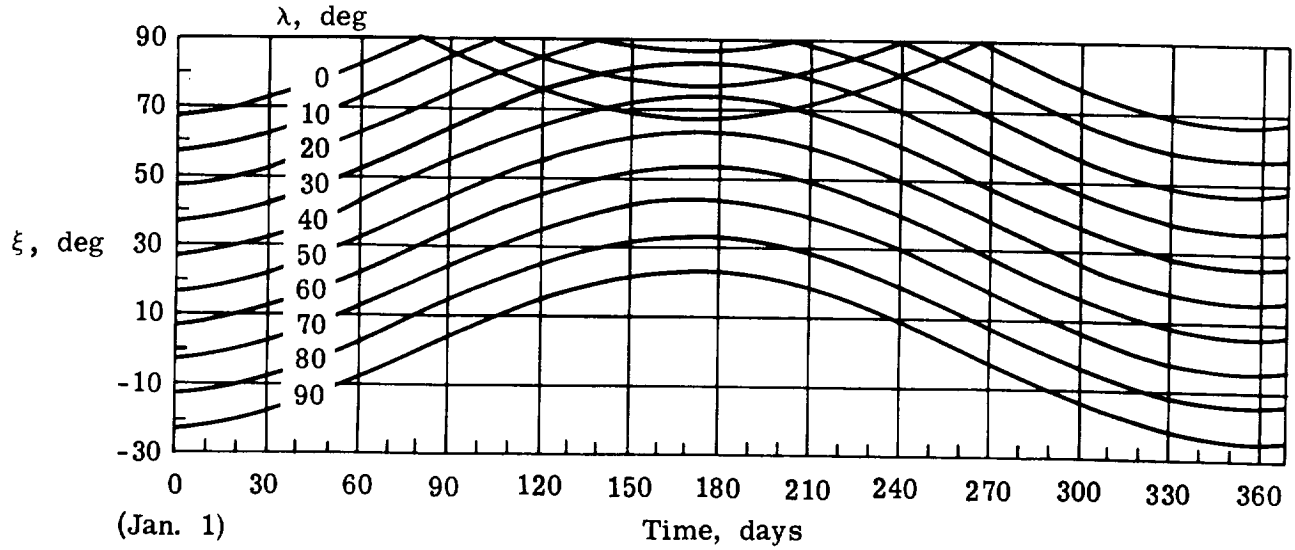

Figure 21.- Available Sun elevation angle as a function of time at various latitudes.

ments. The data may be calculated with the aid of equation (23); they are an extension of the data listed in table 8. It is within these envelopes, and of course their corresponding southern hemisphere equivalents, that the Sun elevation angles vary.

As usual, Sun-synchronous orbits present a special case, as their orbital planes do not precess on the average relative to the Sun. Assume that a satellite in a Sun-synchronous orbit has been started on the equator at the point and time of the vernal equinox. The Sun elevation angles observed as the satellite passes several different latitudes are recorded in figure 22. These curves, for a "high noon" configuration, closely resemble the elevation-angle envelopes of figure 21, but small differences are detectable, especially at lower latitudes. These differences arise from the peculiarities of the Sun's apparent motion around the Earth, as previously discussed in conjunction with figure 10. It is often of interest to adjust the initial geometry of Sun-synchronous orbits away from high noon to accommodate sensors - photographic, for example - for which longer shadows might be desired to provide contrast in the observed surface features.

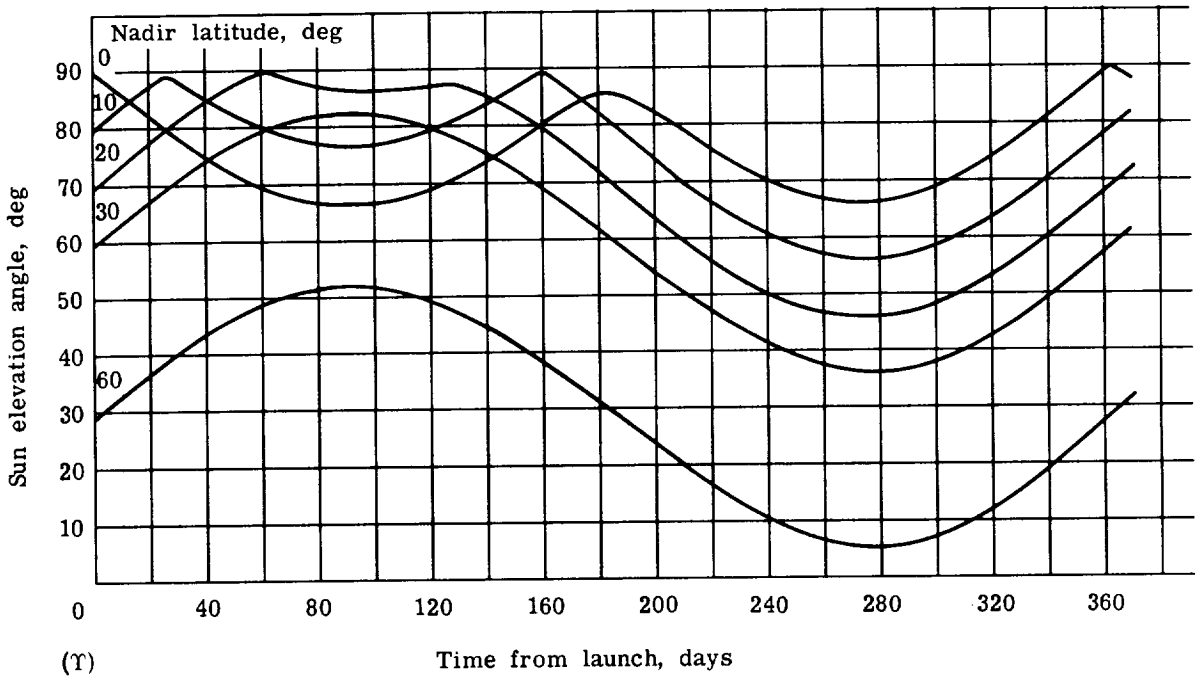

Figure 22.- History of observed Sun elevation angle for a Sun-synchronous orbit started at the location and time of the vernal equinox.

Solar Illumination Effects on Global Surface Coverage

One possible line of background justification for the examples in this section is the desire to monitor, on a global scale, the radiation balance of the Earth. It is a problem which has widespread appeal because of the importance of the radiation balance in predicting long-term trends in the Earth's weather and climate. The present state of knowledge of the Earth's radiation processes is such that significant advances require accurate measurements on a global scale of the emitted and reflected radiation, in particular. At least one of these, the reflected radiation, presents an exceedingly complex problem in data interpretation and requires not just global coverage on a longitude-latitude grid of 5° or so but repetitive coverage of the same locations over a wide range of Sun geometries. This particular problem has been explored in an analysis of orbit requirements for Earth radiation monitoring (ref. 8). It can be viewed more generally as a problem that imposes the most severe possible requirements on the ability to extract adequate data from Earth-orbiting satellites.

For the moment, consider the performance of a single nadir-viewing satellite in covering longitude, latitude, and time (or equivalently, illumination angle). At the outset it can be stated that coverage of the longitude-latitude grid, within the latitude limits of the orbit, is easy to obtain. In fact, by appropriately specifying the repetition factor Q, it is possible to get extensive coverage in these two dimensions over as fine a grid as required. The problem lies in the time coverage, for reasons which are made qualitatively clear by considering the relative slowness with which a satellite orbit moves with respect to the Sun or, put another way, the slowness with which the satel-

lite orbit plane changes its position relative to the plane of the solar terminator. It has already been demonstrated in previous sections that it is possible to cover a particular site at most on a once per day basis, thereby giving up a fine longitude-latitude grid in favor of a coarse one (with longitude points roughly 25° apart according to table 4). The illumination on subsequent passes will change daily (recall the coverage of Norfolk, Virginia, detailed in fig. 20), but the coverage does not even approach the requirements for establishing diurnal changes in radiation patterns. The best that can be hoped for is that over a sufficiently long period of time, say a month, adequate coverage will be achieved to allow extrapolation in both space and time to the desired quantities. This process requires extensive modeling of (for example) the radiation environment and an appreciation for the orbit constraints; it poses a problem sufficiently complex to have defied satisfactory solution up to the present time.

Since it is really the Sun elevation angle which is of interest for the radiation problem, rather than clock time per se, the single satellite coverage is first expressed in terms of an hour-angle system relative to the satellite, as a function of latitude. (It is the same system previously defined for use in eq. (23), where β is the hour angle.) For each part of table 10, the globe has been divided into thirty-six 5° latitude strips and the horizontal scale is divided into twenty-four "1-hour" segments. Thus, each step on the horizontal scale represents 15° of separation between the subsatellite and subsolar meridians. The contents of a latitude-time "box" are increased by one each time a measurement at the satellite nadir point is assumed to have been made within the space and time boundaries of that box. It is assumed that measurements are made from orbit at a constant rate, which amounts to one measurement every 5° of mean anomaly. The results of 30 000 such measurements (about 30 days) are given in tables 10(a), (b), and (c), for 50°, 80°, and Sun-synchronous orbits, respectively, at an altitude of 800 km.

To make the orbit geometry as easy as possible to visualize, the initial conditions are very special ones: in each case the satellite starts on the equator at the location and time of a vernal equinox so that the first measurement records an hour angle of zero. The boxing algorithm truncates hour-angle values rather than rounding them off, so that the hour-angle equivalent time of "zero" might go into either the first or last box, depending on its precise value. It can be seen that with the given initial condition, the hour angle will then be 6 (a zenith angle of 90°) at a mean anomaly of 90°; 12, at 180°; 18, at 270°; and 0(24) again, at 360°. The imprecision of ignoring the distinction between anomalistic and nodal revolutions is of no noticeable consequence for making this point. The change in the coverage pattern over 30 days is due to orbital plane precession relative to the Sun and, to a smaller extent over this short period of time, the seasonal motion of the Sun into the northern hemisphere. For the 50° orbit this relative precession rate is about -5.2 deg/day; for the 80° orbit it is about -2.1 deg/day; and for the Sun-synchronous orbit it is, by design, zero.

Eventually, the nonsynchronous satellites will make measurements at all *hour angles for* each *available latitude*. The question is whether or not the necessary extrapolations can be made to determine diurnal variations and average out or otherwise account for their effects. The difficulty in doing this over the required time scale (say, within 30 days) provides the argument in

favor of multiple satellites, which will cause the latitude-time grid to be filled in much more quickly than will a single satellite. The trade-off between the cost of additional satellites and increased mission capability is at the heart of the justification process for this type of spaceborne monitoring program. One attempt at presenting the options for multiple satellite missions may be found in reference 8, where the ability of various satellite systems to fill in the latitude-time grid in 30 days is examined. A two-satellite configuration of one 50° and one 80° orbit was recommended in this study for "zonal" coverage over latitude bands, but such a system still may not be able to provide total latitude-time coverage as quickly as desired for accurate interpretation of radiation data. Another solution to this problem is to use multiple Sun-synchronous satellites to give continuous coverage of a particular local illumination condition. Four such satellites might be sufficient to allow confident modeling of the diurnal radiation cycle. However, the expense of such an extensive system has so far been an insurmountable obstacle to its implementation.

There is another way of looking at the latitude-illumination grid. It can be argued that not only is clock time an insufficient measure of illumination coverage, but relative solar time (hour angle) by itself is not much better, as it still does not unambiguously specify the illumination conditions at the nadir point.[3] Thus, an additional parameter of real interest is the solar zenith angle. These data are shown in table 11 for the same three orbits previously used - 50°, 80°, and Sun-synchronous - and may be compared with the corresponding parts of table 10. The pattern of zenith-angle coverage can best be visualized by first considering the Sun-synchronous orbit from which is viewed a dawn or dusk condition (zenith angle of 90°) near the South or North Pole, respectively. The other orbits initially have the same type of pattern, but they precess away from this geometry. In 30 days the 50° orbit has precessed about -156° relative to the Sun, and thus has viewed dawn and dusk conditions over every available latitude. The 80° orbit will fill in its "hole in the middle" in a similar fashion if given enough time - it has precessed only about -63° in 30 days.

The foregoing discussion of the problem of radiation-balance coverage may appear quite discouraging from the point of view of the mission analyst, who apparently cannot exercise sufficient control over orbital properties to achieve the desired results with reasonable satellite systems. However, the definition of global coverage is to some extent a flexible one which can be expected to relax considerably under different circumstances. (Such a situation will be dealt with in the following section.) In the present case, it is clear that sensors with sufficiently wide fields of view will allow global coverage in some sense. Then, the problem becomes not one of obtaining sufficient data but one of interpreting the available information in an unambiguous way. The implied trade-off between flight hardware for measurements and computer software for analysis is an important consideration in mission planning but lies outside the scope of this analysis.

---

[3]Interpretation of the reflections of solar energy by the Earth's surface requires such an unambiguous two-parameter specification of solar position.

Tangent-Point Distributions For Solar Occultation Experiments

The three previous sections have dealt with some of the coverage patterns resulting from a nadir-looking satellite system. Another basic type of sensing involves looking not at the Earth but at the Sun under specialized conditions. It has long been recognized that in studies of atmospheric constituents, it is profitable to use the Sun as a radiation source. It is easy to visualize a process whereby solar radiation received by a satellite when the Sun is well above the horizon is compared with the radiation attenuated by the atmosphere as the Sun rises or sets through the Earth's atmosphere. In keeping with previous general discussions, it is important to examine not just one or a few of these measurements in isolation, but to view a set of such measurements in the context of a total mission.

The data to be presented here are applicable to any solar occultation experiment; they were generated originally in support of a proposed mission for measuring halogens in the stratosphere (ref. 9). The question in this case is a typical one: Is the coverage resulting from a flight project (assumed to last 1 year) sufficient in space and time to permit useful interpretation of the underlying distributions of the variable of interest? The particular example of stratospheric halogens allows an immediate but qualified "yes" to this question, as do many other proposed experiments, since information of any kind about the distribution of many stratospheric constituents is virtually nonexistent. However, the problem of justifying the return of the mission relative to its cost is another obstacle which must be overcome.

Because of the paucity of worldwide stratospheric data, the definition of global coverage can indeed be relaxed, as suggested in the previous section. It may at first be sufficient merely to establish average levels over various parts of the globe, taking note of only the coarsest features of the underlying factors which drive the distributions. But it is at this point that the qualification of the "yes" becomes apparent: What is "coarse"? How well can time averages be made? Can spatial and temporal distributions be separated, and to what extent? To help answer these questions, several pertinent sets of solar occultation data are presented in figure 23. In figure 23(a) the distribution of tangent latitudes during 1 year is presented for a 70° orbit, chosen because it is approximately the lowest orbit inclination at this moderate altitude ($a = 6978$ km) which will allow some polar coverage. The curves appear to be continuous, but in reality they are made up of the discrete contributions of the sunrises and sunsets viewed from the satellite throughout the year: 9600 separate occurrences at the rate of about 14.9 per day. The orbit is deliberately started during a period of total solar exposure, and its subsequent precession through cycles of occultation and exposure is dependent in a complex way on the time of year of the launch and the precession rate of the orbit relative to the Sun. The small dots represent sunrises; the crosses, sunsets, a convention which also applies to the rest of figure 23. Note that in contrast to nadir-looking coverage, the latitude limits of the tangent point are not restricted to $\pm 70^{\circ}$, but extend northward and southward depending on the solar position. The length of the cycles can be altered, similarly to surface illumination cycles previously discussed, by choosing orbits with faster or slower precession rates. However, since the precession rate is mostly a function of inclination, this choice cannot be made independently of the coverage in

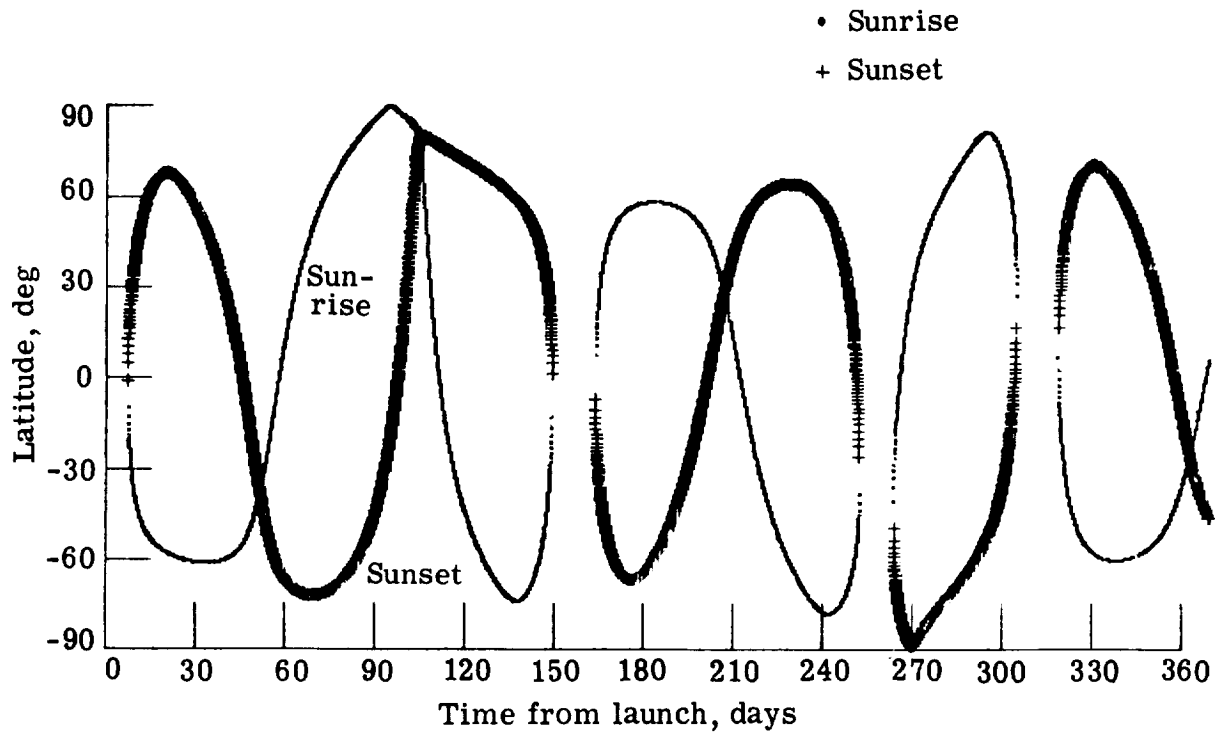

(a) Tangent latitude on the Earth's surface at sunrise or sunset.

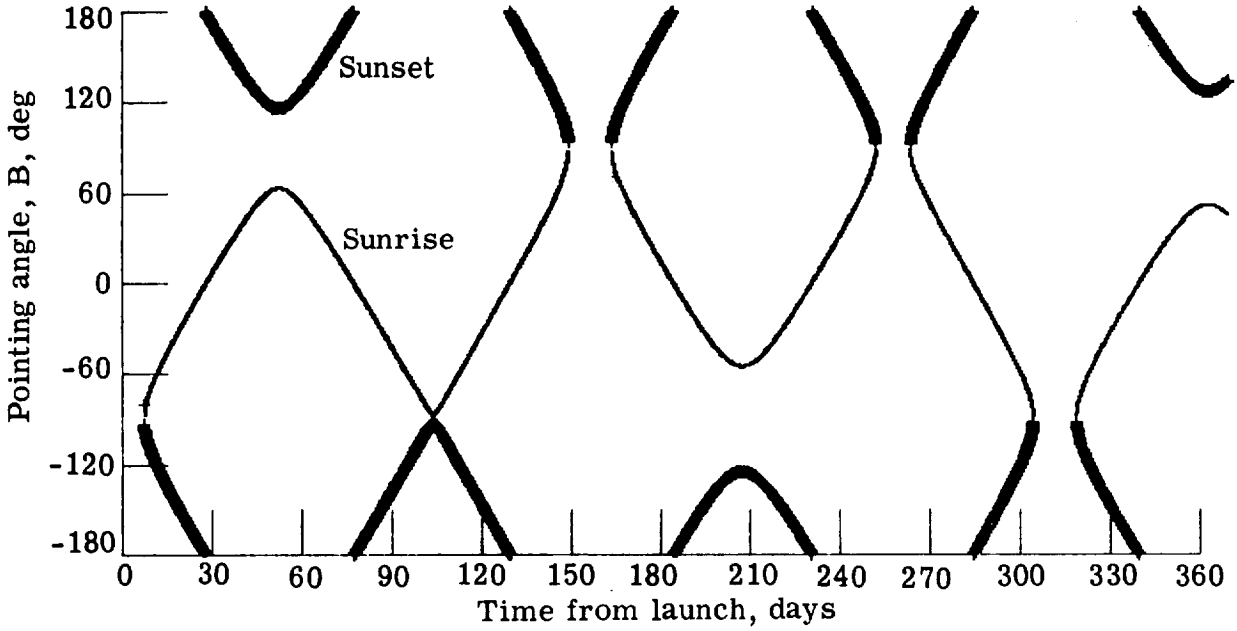

(b) Pointing (yaw) angle to the Sun relative to the plane of satellite motion at sunrise or sunset.

Figure 23.- Solar occultation data during a 1-year flight for a 70° orbit at h = 600 km.

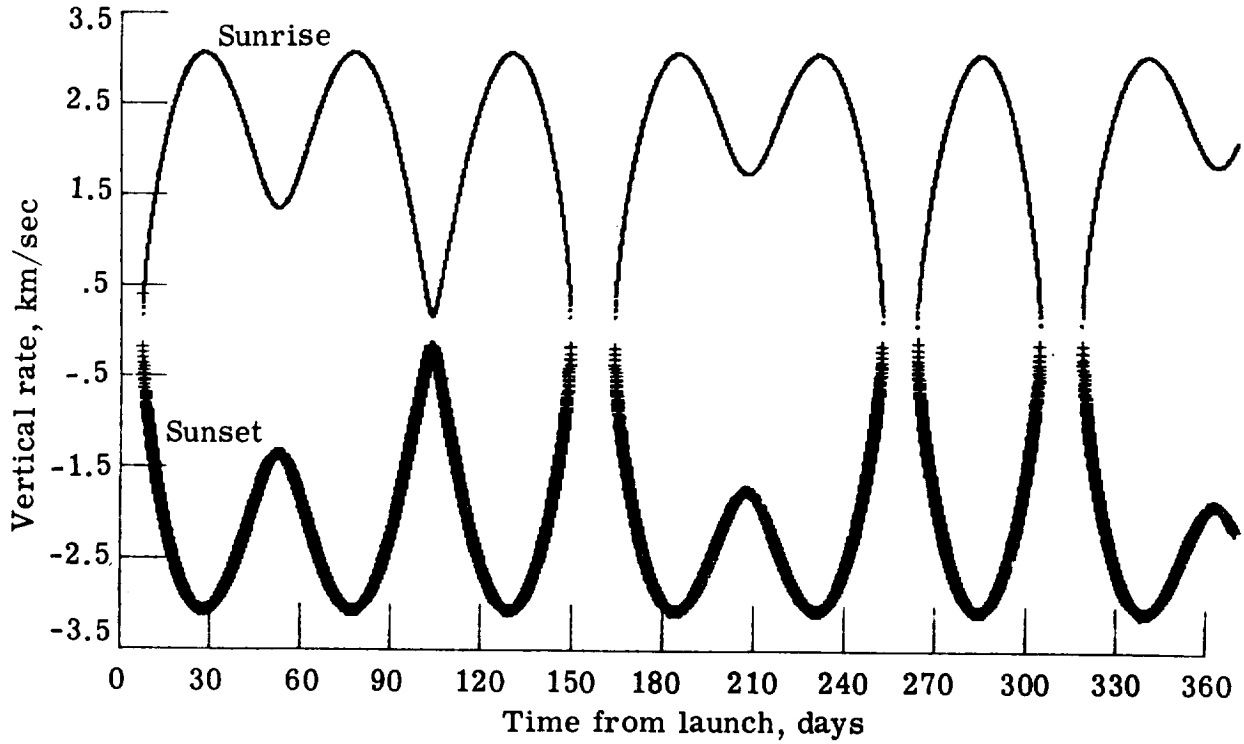

(c) Apparent vertical rate of the solar image through the atmosphere at sunrise and sunset.

Figure 23.- Concluded.

latitude. Also, the exact shape of the cycles and the location of the periods of total sunlight are determined by the timing and initial geometry of the launch. Therefore, figure 23 must be considered to be only representative in details, while retaining generality in overall cyclic patterns.

Figure 23(b) illustrates another important facet of solar occultation experiments which must be considered in mission design: tracking the Sun. The quantity plotted is a "yaw" angle, previously defined as B, which locates the solar image on the Earth's horizon relative to the direction of satellite motion. The constantly changing satellite-Sun geometry causes an expected variation of B over a range of $\pm 180^{\circ}$, a characteristic feature of Sun-tracking measurements. A question clearly framed by the figure is: What level of sophistication is warranted in designing a Sun tracker? The problem of finding the Sun when it is "up" and following it as it sets is easier than predicting where it will be just as it rises - a differentiation which carries with it the prospect of losing half of all the occultation opportunities. The sunrise-sunset symmetry evident in the pointing requirements relative to 90° and -90° is encouraging, however, with the possibility of utilizing a sunset to predict the value of B for the following sunrise.

A third cyclic pattern of interest during the mission is the variation in the vertical rate R at which the Sun rises or sets. A useful approximation is to consider the value of R at the horizon as characteristic of a particu-

lar measurement opportunity, even though the rate is not actually constant during the entire residence time of the solar image within the vertical limits of the atmosphere. This quantity is plotted in figure 23(c). It is clear from previous discussions that the maximum values of $|R|$ occur when the Sun is ahead of or behind the satellite ($B = 0^{o}$ or $\pm 180^{o}$) and that the minimum values occur at $B = 90^{o}$ or -90^{o}. Whereas the significance of this number depends on the nature of the experiment being performed, it is easy to see that vertical profiles of the atmosphere over a well-defined spot on the Earth can best be achieved when $|R|$ is as large as possible. At the other extreme the longitude-latitude coordinates can vary considerably during the passage of the solar image through the stratosphere. Without going into details of data reduction, it is reasonable to conclude that the distribution of R over the life of a mission will affect the overall accuracy of the resulting global distributions. The distribution of measurements of $|R|$ in 0.5 km/sec intervals is given in figure 24 for the 9600 measurements of this 1-year mission.

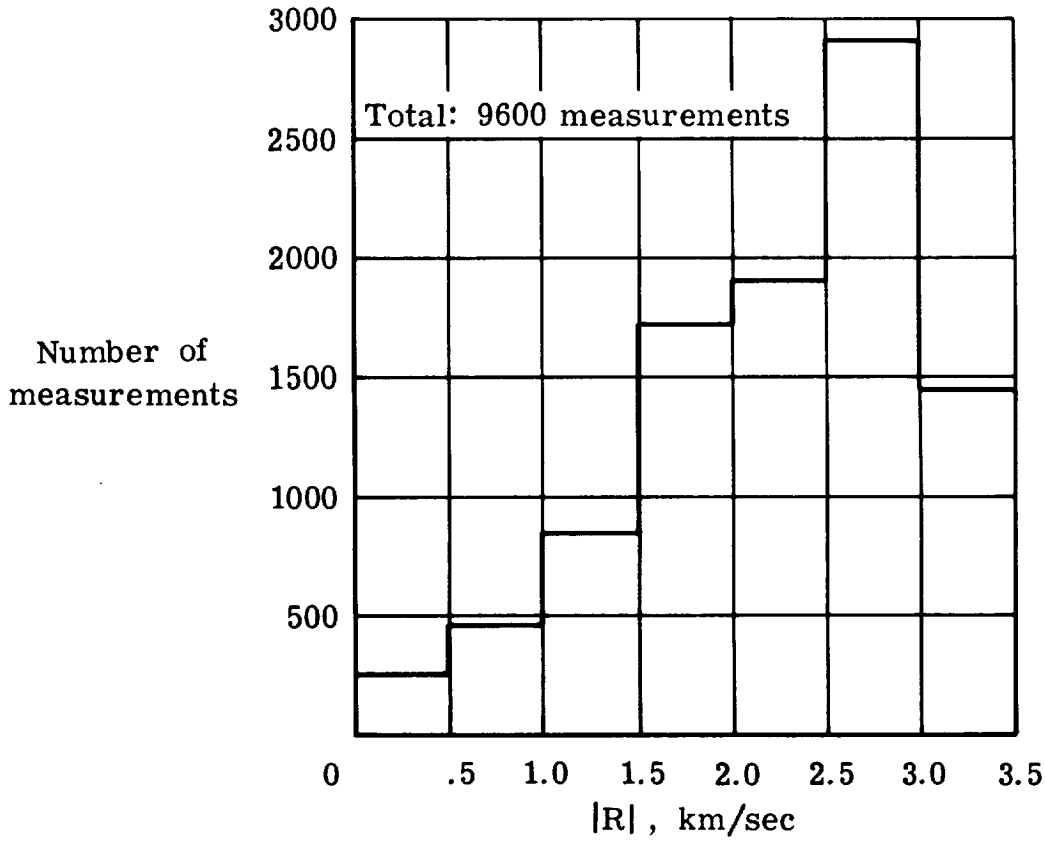

Figure 24.- Distribution of apparent rate of the solar image vertically through the atmosphere as viewed from a satellite during sunrise or sunset.

Up to now, no mention has been made of longitude coverage; in the previous section it has been assumed to be less critical than latitude coverage. Tangent latitude is plotted against tangent longitude in figure 25, where it is clear that in some sense the coverage in longitude is uniform at least over a time span of 1 year; that is, there are no obvious gaps in this plot. It is useful

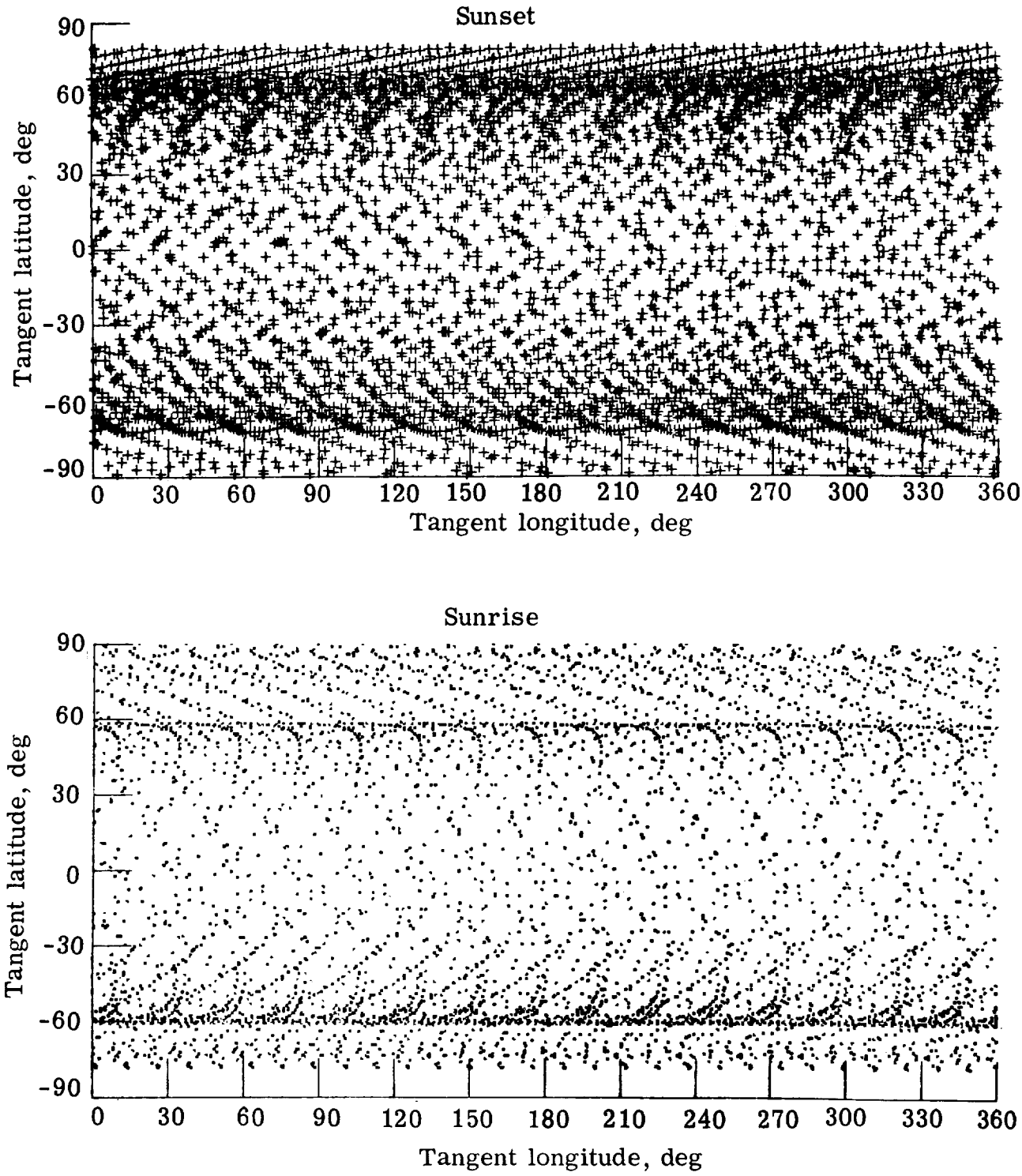

Figure 25.- Distribution of tangent longitude and latitude on the Earth's surface at sunrise or sunset after a 1-year, solar occultation mission for a 70°, 600-km orbit.

to look at smaller time intervals, however, to see how the longitude-latitude coverage is built up. In figure 26, about 400 orbits from the beginning of the

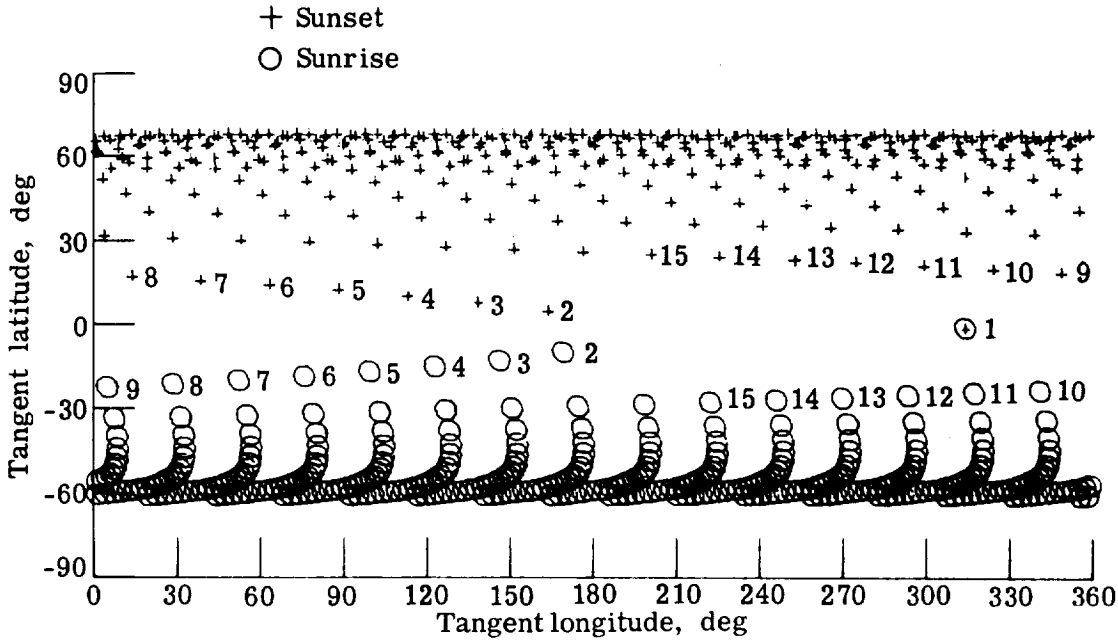

Figure 26.- Distribution of tangent longitude and latitude at sunrise and sunset for about 400 orbits during the first period of occultation.

first period of occultation are considered. The first 15 occulted orbits are numbered, starting from the point where the Sun just reaches the horizon so that sunrise and sunset occur at essentially the same time and place. It can be seen that the longitude points are fairly regularly spaced throughout a day - a time interval during which the latitude changes relatively little. This is encouraging from the point of view of taking averages over bands of latitude, a procedure which is commonly used for modeling the stratosphere.

The ability of this mission to achieve yearly averages of a single stratospheric quantity as a function of latitude is shown in figure 27. The solid line gives the actual yearly averages of a dimensionless parameter F, produced by a hypothetical stratospheric model which varies in longitude, latitude, and time and has random components to account for measurement and analysis errors and natural random fluctuations. (It can be thought of as representing a total vertical burden of some stratospheric constituent.) A 1-year mission which extracts 9600 measurements from this model is flown, and the resulting 36 latitude band averages are calculated with standard statistical procedures for grouping and weighting the available data. Although a detailed statistical analysis of the measurements is beyond the scope of this report, the lack of agreement in figure 27 between "theory" (perfect sampling) and "experiment" (available sampling) near both poles can readily be attributed to an insufficient number of temporally spaced measurements near the poles, as is evident in figure 23(a). In any event, the solar occultation technique has obvious potential for space-based stratospheric measurements and may allow global modeling in certain restricted circumstances.

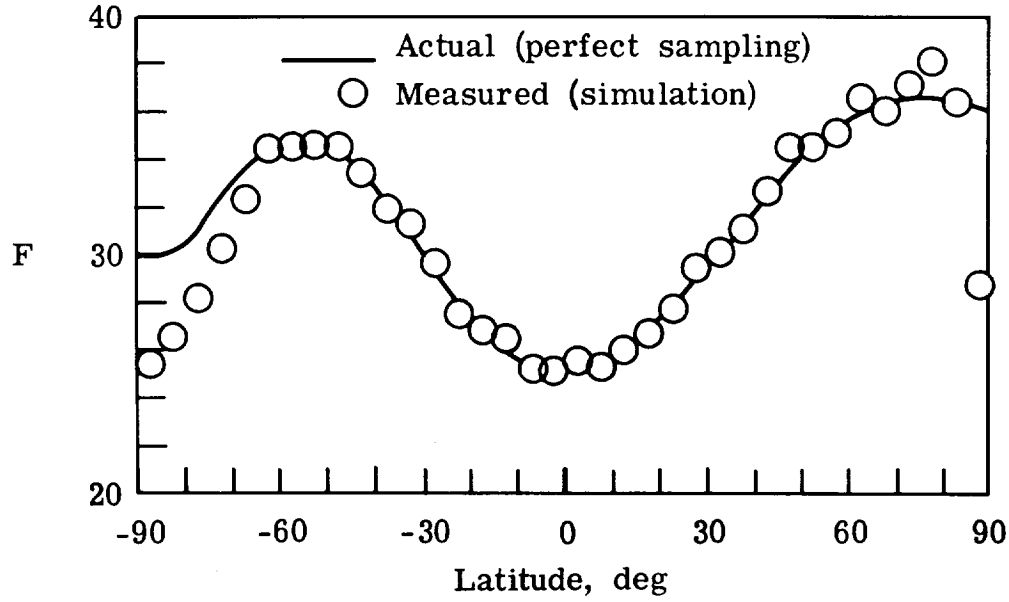

Figure 27.- Actual and measured (simulated) yearly averages of a hypothetical stratospheric constituent as a function of latitude.

V. SYMBOLS

a	semimajor axis, km
A,B	pointing angles to Sun relative to a satellite, deg (see fig. 18(a))
c	location of a fictitious sun along the celestial ecliptic, deg (see fig. 9)
d	Julian days since Jan. 1.0, 1900
D	= d/10000
e	eccentricity
E	eccentric anomaly, rad
f	true anomaly, deg or rad
F	dimensionless parameter used for evaluating ability of a solar occultation mission to extract information on global distribution of stratospheric constituents
h	altitude above surface of a fictitious spherical earth of radius $r_{\oplus}$, km
$\hat{H}$	unit heading vector (see fig. 17)

i	inclination of an orbit, deg
I,O	pointing angles to Sun relative to a satellite, deg (see fig. 18(b))
J_2	term in expansion of Earth's gravitational potential (see eqs. (5))
J.D.	Julian date or day
L	longitude, deg
m,n	integers (see eq. (20))
M	mean anomaly, deg or rad
$\hat{N}$	unit vector normal to an orbit (see fig. 17)
p	semilatus rectum, km
P	point on Earth's surface, along a satellite orbit, or on the celestial sphere
Q	orbit repetition factor
$r,\vec{r}$	satellite distance from center of Earth or a position vector, km
$r_\oplus$	Earth's mean equatorial radius, 6378.145 km
R	rate at which solar image appears to rise or set on the horizon as viewed from a satellite; km/sec or deg/sec
$\vec{S}$	vector in direction of Sun as viewed from a satellite, with length as defined in sketch (a), km
t	time; days, min, or sec, as defined in context
T	Julian centuries since Jan. 1.0, 1900
$v,\vec{v}$	speed, km/sec, or a velocity vector
$\hat{x}_\odot$	unit vector pointing toward Sun, defined in right-ascension—declination coordinate system
x,y,z	Cartesian coordinates
α	right ascension, deg
β	hour angle of subsolar meridian relative to a satellite meridian, deg
δ	declination, deg
ϵ	obliquity of Earth's equator to the ecliptic, deg

ζ	solar zenith angle, deg (see fig. 16)
η	direction from which Sun is shining relative to Earth's surface, deg (see fig. 16)
$\dot{\theta}$	rotation rate of Earth, 0.25068447 deg/min or 360.9856473 deg/day
λ	latitude, deg
μ	Earth's gravitational constant, 398601.2 km^3/sec^2
ξ	Sun elevation angle, deg (see fig. 16)
τ	period, sec or orbits/day
Υ	referring to vernal equinox (as when indicating direction of the first point of Aries)
ω	argument of perihelion, deg
Ω	right ascension of ascending node, deg

Subscripts:

A	anomalistic periods
g	Greenwich meridian
m	meridian
ΔM	evaluated for a mean-anomaly step size of ΔM degrees
N	nodal periods
o	initial or unperturbed (Keplerian) quantities
s	Sun-synchronous quantities
$\oplus$	Earth
$\odot$	Sun
obs	observer
x,y,z	components of a position vector

Superscripts:

h,m,s	hours, minutes, seconds
	d/dt

$\vec{\ }$	dimensioned vector
$\hat{\ }$	unit vector

APPENDIX A

"BASIC" LANGUAGE ALGORITHMS FOR CALCULATING ORBIT PARAMETERS

Many of the equations of previous sections on orbital dynamics may easily be incorporated into small computer programs for calculating relevant orbit properties. Table A1 gives a BASIC language algorithm written for the Wang 2200 computer system. With an input of semimajor axis, eccentricity, and inclination, plus the desired mean-anomaly step size, the precession rates and other data are calculated. The Sun-synchronous inclination is also calculated; all the orbit data can be obtained for synchronous orbits by setting I = S and rerunning the program. The last two lines of printout will show that the inclination for synchronous orbits as calculated from just one iteration does, in fact, give very nearly the desired result. An example of the output is given in the table.

Table A2 lists another useful BASIC algorithm. With inputs of Q (in terms of an integer plus a fraction), eccentricity, inclination, and a guess at the semimajor axis, a simple iterative technique causes the semimajor axis to converge to the correct value for the desired Q. For Sun-synchronous orbits the inclination is calculated internally and adjusted to maintain the synchronous precession rate as semimajor axis is varied. This algorithm will generate data such as those presented in tables 5 and 6. It can be modified to vary eccentricity instead of semimajor axis, but simultaneous freedom of these two variables would lead to an infinite number of solutions for each value of Q.

TABLE A1.- "BASIC" ALGORITHM FOR GENERATING ORBIT PARAMETERS

ON THE WANG 2200 SYSTEM

```
10SELECT D
20X1=66058.33128
30X2=6.283185308
40X3=398601.2
50X4=57.29577951
60X5=.9856473
70INPUT "MEAN ANOMALY STEP",D
80INPUT "UNPERTURBED SEMIMAJOR AXIS",A0
90INPUT "ECCENTRICITY",E
100INPUT "INCLINATION",I
110PRINT "D ",D
120PRINT "A0",A0
130PRINT "E ",E
140PRINT "I ",I
150P0=(A0*(1-E*E))!2
160T0=X2*A0*SQR(A0/X3)
170M0=X2/T0
180M1=M0*(1+X1/P0*SQR(1-E*E)*(1-1.5*SIN(I)!2))*X4*86400
190D1=X1/P0*M1*(2-2.5*SIN(I)!2)
200D2=-X1/P0*M1*COS(I)
210T1=X2/M1*180/#PI*86400
220T2=X2/(M1+D1)*180/#PI*86400
230S0=-A0!1.5*P0*X5/X1/SQR(X3)/X4/86400
240S=S0/(1+X1/P0*SQR(1-E*E)*(1-1.5*SIN(ARCCOS(S0))!2))
250S0=ARCCOS(S0)
260S=ARCCOS(S)
270D3=X1/P0*(2-2.5*SIN(I)!2)*D
280D4=-X1/P0*COS(I)*D
290D5=M0*(1+X1/P0*SQR(1-E*E)*(1-1.5*SIN(S)!2))
300D6=-X1/P0*D5*COS(S)*X4*86400
310D7=D6*365.2422
320Q=(M1+D1)/(.7292115061E-4*180/#PI*86400-D2)
340PRINT "UNPERTURBED PERIOD,SEC                    ",T0
350PRINT "UNPERTURBED MEAN MOTION,RAD/SEC           ",M0
360PRINT "MEAN MOTION,DEG/DAY                       ",M1
370PRINT "PERIGEE RATE,DEG/DAY                      ",D1
380PRINT "NODE RATE,DEG/DAY                         ",D2
390PRINT "PERIGEE STEP,DEG/MEAN ANOMALY STEP        ",D3
400PRINT "NODE STEP,DEG/MEAN ANOMALY STEP           ",D4
410PRINT "ANOMALISTIC PERIOD                        ",T1
420PRINT "NODAL PERIOD                              ",T2
430PRINT "REPETITION FACTOR Q                       ",Q
440PRINT "UNPERTURBED SYNCHRONOUS INCLINATION       ",S0
450PRINT "SYNCHRONOUS INCLINATION                   ",S
455M1=M0*(1+X1/P0*SQR(1-E*E)*(1-1.5*SIN(S)!2))*X4*86400
460D1=X1/P0*M1*(2-2.5*SIN(S)!2)
470Q1=(M1+D1)/360
480PRINT "SYNCHRONOUS REPETITION FACTOR             ",Q1
490PRINT "DAILY SYNCHRONOUS ORBIT PRECESSION        ",D6
500PRINT "YEARLY SYNCHRONOUS ORBIT PRECESSION       ",D7
```

TABLE A1.- Concluded

D	360
A0	7000
E	0
I	60
UNPERTURBED PERIOD,SEC	5828.5110951
UNPERTURBED MEAN MOTION,RAD/SEC	1.07800863E-03
MEAN MOTION,DEG/DAY	5335.626538
PERIGEE RATE,DEG/DAY	.8991392485551
NODE RATE,DEG/DAY	-3.596556994221
PERIGEE STEP,DEG/MEAN ANOMALY STEP	6.06658144E-02
NODE STEP,DEG/MEAN ANOMALY STEP	-.2426632577633
ANOMALISTIC PERIOD	5829.493459208
NODAL PERIOD	5828.511260928
REPETITION FACTOR Q	14.63737447681
UNPERTURBED SYNCHRONOUS INCLINATION	97.87448384351
SYNCHRONOUS INCLINATION	97.87952788402
SYNCHRONOUS REPETITION FACTOR	14.80520669859
DAILY SYNCHRONOUS ORBIT PRECESSION	.9856473476633
YEARLY SYNCHRONOUS ORBIT PRECESSION	360.0000056847

(Set I=S and rerun - RUN10 - to get synchronous orbit data)

D	360
A0	7000
E	0
I	97.87952788402
UNPERTURBED PERIOD,SEC	5828.5110951
UNPERTURBED MEAN MOTION,RAD/SEC	1.07800863E-03
MEAN MOTION,DEG/DAY	5333.131479134
PERIGEE RATE,DEG/DAY	-3.25706764226
NODE RATE,DEG/DAY	.9856473476636
PERIGEE STEP,DEG/MEAN ANOMALY STEP	-.2198603870542
NODE STEP,DEG/MEAN ANOMALY STEP	6.65337141E-02
ANOMALISTIC PERIOD	5832.22073668
NODAL PERIOD	5835.78478641
REPETITION FACTOR Q	14.80520831492
UNPERTURBED SYNCHRONOUS INCLINATION	97.87448384351
SYNCHRONOUS INCLINATION	97.87952788402
SYNCHRONOUS REPETITION FACTOR	14.80520669859
DAILY SYNCHRONOUS ORBIT PRECESSION	.9856473476633
YEARLY SYNCHRONOUS ORBIT PRECESSION	360.0000056847

APPENDIX A

TABLE A2.- "BASIC" ALGORITHM FOR GENERATING ORBITS WITH SPECIFIED REPETITION FACTORS ON THE WANG 2200 SYSTEM

```
10  PRINT
20  SELECT D
30  X1=66053.33128:X2=6.283185308:X3=398601.2:X4=57.29577951
40  INPUT "REPETITION FACTOR:INTEGER,NUM,DENOM",Q,N,U
50  F0=Q+N/U
60  INPUT "GUESS AT SEMIMAJOR AXIS",A1
70  A2=A1+10
80  INPUT "ECCENTRICITY",E
90  INPUT "INCLINATION-USE 999 FOR SUN SYNC",I
100 IF I=999THEN 130
110 I1=I:I2=I:I3=I
120 PRINT
130 PRINTUSING 390,F0,N,U;
140 P1=(A1*(1-E*E))!2:P2=(A2*(1-E*E))!2
150 T1=X2*A1*SQR(A1/X3):T2=X2*A2*SQR(A2/X3)
160 M1=X2/T1:M2=X2/T2:IF I[]999THEN 190
170 GOSUB '1(A1,P1):I1=S
180 GOSUB '1(A2,P2):I2=S
190 S1=M1*(1+X1/P1*SQR(1-E*E)*(1-1.5*SIN(I1)!2))*X4*86400
200 S2=M2*(1+X1/P2*SQR(1-E*E)*(1-1.5*SIN(I2)!2))*X4*86400
210 D1=X1/P1*S1*(2-2.5*SIN(I1)!2):D2=X1/P2*S2*(2-2.5*SIN(I2)!2)
220 C1=-X1/P1*S1*COS(I1):C2=-X1/P2*S1*COS(I2)
230 F1=(S1+D1)/(.729211506E-4*180/#PI*86400-C1)-F0
240 F2=(S2+D2)/(.729211506E-4*180/#PI*86400-C2)-F0
250 IF ABS(F1)[1E-6 THEN 360:IF ABS(F2)[1E-6 THEN 370
260 A3=(A2-A1)*F2/(F1-F2)+A2
270 P3=(A3*(1-E*E))!2:T3=X2*A3*SQR(A3/X3):M3=X2/T3:IF I[]999THEN 290
280 GOSUB '1(A3,P3):I3=S
290 S3=M3*(1+X1/P3*SQR(1-E*E)*(1-1.5*SIN(I3)!2))*X4*84600
300 D3=X1/P3*S3*(2-2.5*SIN(I3)!2):C3=-X1/P3*S3*COS(I3)
310 F3=(S3+D3)/(.7292115061E-4*180/#PI*86400-C3)-F0
320 IF ABS(F3)[1E-6 THEN 340
330 A1=A2:A2=A3:GOTO 140
340 A=A3:F=F3+F0
350 GOTO 380
360 A=A1:F=F1+F0:GOTO 380
370 A=A2:F=F2+F0
380 I=I3:PRINTUSING 400,A+.0000005;I+.0000005
390%## ##/##
400% ####.######   ###.######
410 GOTO 40
420 END
430DEFFN'1(A,P)
440 S0=-A!1.5*P*.9856473/X1/SQR(X3)/X4/86400
450 S=S0/(1+X1/P*SQR(1-E*E)*(1-1.5*SIN(ARCCOS(S0))!2))
460 S=ARCCOS(S)
470 RETURN
```

(Sample case for a = 7000, e = 0, i = 60, Q = 13 1/2)

```
13  1/ 2 7396.373144    60.000000
  (i = 999)
13  1/ 2 7445.166714    99.793197
```

APPENDIX B

ORBIT ELEMENTS FOR THE EARTH'S MOTION AROUND THE SUN

The equations for the Earth's orbit elements can be obtained by inverting the equations for the apparent motion of the Sun obtained from astronomical observation. The time-varying orbit elements of the Sun can be found in reference 1, and inverted orbit elements for the Earth, or more specifically, mean elements for the gravitational center of the Earth-Moon system (barycenter) are given explicitly in reference 6:

$$d = \text{J.D.} - 241\ 5020.0$$

$$D = d/10000$$

$$T = d/36\ 525$$

$$a_{\oplus} = 1.00000023 \text{ AU}$$

$$e_{\oplus} = 0.01675104 - 0.0000418T - 0.000000126T^2$$

$$\omega_{\oplus} = 101^{\circ}.220833 + 0^{\circ}.0000470684d + 0^{\circ}.0000339D^2 + 0^{\circ}.00000007D^3$$

$$M_{\oplus} = 358^{\circ}.475845 + 0^{\circ}.985600267d - 0^{\circ}.0000112D^2 - 0^{\circ}.00000007D^3$$

$$\varepsilon_{\oplus} = 23^{\circ}.452294 - 0^{\circ}.0035626D - 0^{\circ}.000000123D^2 + 0^{\circ}.0000000103D^3$$

Reference 6 gives the value of 1 AU (astronomical unit) as 149 597 893 ± 5 km. The true anomaly of the Earth can be obtained from implementation of any of the many available iterative solutions to Kepler's equation, or by expansion (ref. 3, eq. (6-15)):

$$f = M + 2e \sin M + \frac{5e^2}{4} \sin 2M + \frac{e^3}{12}(13 \sin 3M - 3 \sin M) + \frac{e^4}{96}(103 \sin 4M - 44 \sin 2M) + \frac{e^5}{960}(1097 \sin 5M - 645 \sin 3M + 50 \sin M) + \frac{e^6}{960}(1223 \sin 6M - 902 \sin 4M + 85 \sin 2M) + \ldots$$

In this expression, both f and M must be in radians.

APPENDIX C

DETERMINING THE CONDITIONS UNDER WHICH THE SUN IS OCCULTED BY THE EARTH RELATIVE TO A SATELLITE HAVING FIXED ORBIT ELEMENTS

Solution of the occultation problem involves determining the points on its orbit at which a satellite enters or leaves the Earth's shadow. The geometry is shown in sketch (C1). The symbols used for this appendix form a self-

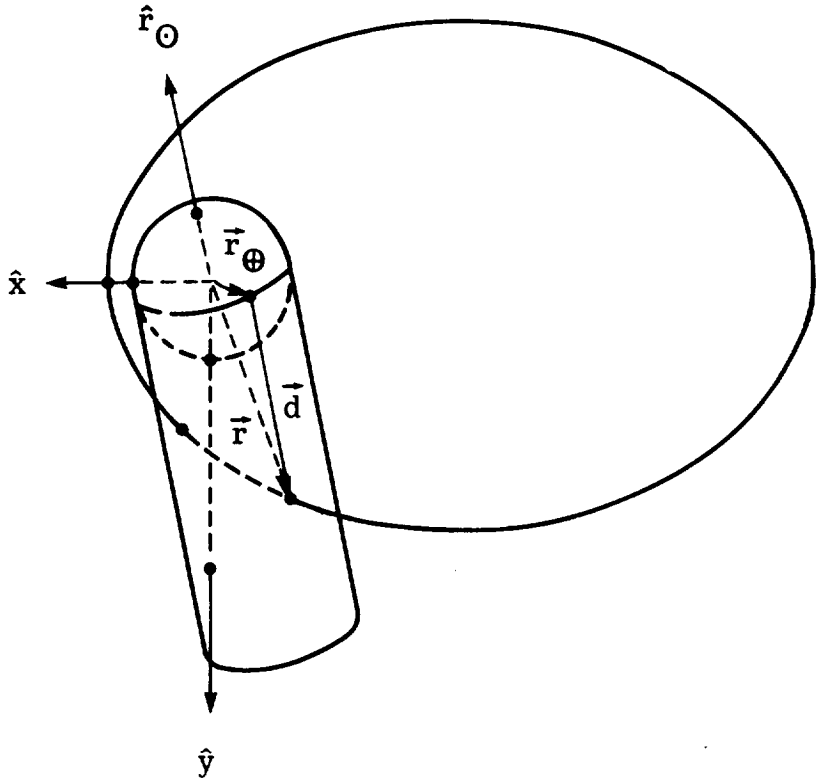

Sketch (C1)

contained set, and they are not all defined in or consistent with the symbol list in the body of the report. All the vector quantities are expressed in a system whose x-y plane lies in the plane of the satellite orbit, with x and y oriented as indicated in sketch (C1). Such a coordinate system is called the PQW system. Vectors can be rotated into the PQW system by standard procedures. (See, for example, ref. 2.)

A_0 to A_4 constants as defined below

$\vec{d}$ vector perpendicular to the terminator, extending from the terminator to the satellite, km

e eccentricity

f true anomaly, deg

p semilatus rectum, km

$\vec{r}$ radius vector to satellite, km

$\hat{r}_\odot$ unit vector to the Sun

$\vec{r}_\oplus$ Earth radius vector to the terminator, km

$\hat{x}$ unit vector in direction of the perigee of the satellite orbit

$\hat{y}$ unit vector at right angles to $\hat{x}$ along the semilatus rectum

ψ angle between $\hat{r}_\odot$ and $\vec{r}$, deg

The geometric constraint is the requirement that at a point where the satellite enters or leaves the Earth's shadow,

$$\hat{r}_\odot \cdot \vec{d} = -d = -(r^2 - r_\oplus^2)^{1/2} = r \cos \psi$$

That is, $\hat{r}_\odot$ and $\vec{d}$ are antiparallel. This restriction can be written in another way:

$$\hat{r}_\odot \cdot \vec{d} = \hat{r}_\odot \cdot (\vec{r} - \vec{r}_\oplus) = \hat{r}_\odot \cdot \vec{r} = r\hat{r}_\odot \cdot (\hat{x} \cos f + \hat{y} \sin f) = r \cos \psi$$

The x- and y-components of the unit vector to the Sun are

$$r_{\odot x} = \hat{r}_\odot \cdot \hat{x}$$

$$r_{\odot y} = \hat{r}_\odot \cdot \hat{y}$$

Then,

$$r_{\odot x} \cos f + r_{\odot y} \sin f = - \frac{(r^2 - r_\oplus^2)^{1/2}}{r}$$

Since $r = p/(1 + e \cos f)$,

$$\frac{p}{(1 + e \cos f)}(r_{\odot x} \cos f + r_{\odot y} \sin f) + \left[\frac{p^2}{(1 + e \cos f)^2} - r_\oplus^2\right]^{1/2} = 0$$

This can be rewritten in terms of $\cos f$:

$$A_0 \cos^4 f + A_1 \cos^3 f + A_2 \cos^2 f + A_3 \cos f + A_4 = 0$$

The constants are

$$A_0 = \left(\frac{r_\oplus}{p}\right)^4 e^4 - 2\left(\frac{r_\oplus}{p}\right)^2 (r_{\odot y}^2 - r_{\odot x}^2)e^2 + (r_{\odot x}^2 + r_{\odot y}^2)^2$$

APPENDIX C

$$A_1 = 4\left(\frac{r_\oplus}{p}\right)^4 e^3 - 4\left(\frac{r_\oplus}{p}\right)^2 (r_{\odot y}^2 - r_{\odot x}^2)e$$

$$A_2 = 6\left(\frac{r_\oplus}{p}\right)^4 e^2 - 2\left(\frac{r_\oplus}{p}\right)^2 (r_{\odot y}^2 - r_{\odot x}^2) - 2\left(\frac{r_\oplus}{p}\right)^2 (1 - r_{\odot y}^2)e^2 + 2(r_{\odot y}^2 - r_{\odot x}^2)(1 - r_{\odot y}^2)$$

$$-4r_{\odot x}^2 r_{\odot y}^2$$

$$A_3 = 4\left(\frac{r_\oplus}{p}\right)^4 e - 4\left(\frac{r_\oplus}{p}\right)^2 (1 - r_{\odot y}^2)e$$

$$A_4 = \left(\frac{r_\oplus}{p}\right)^4 - 2\left(\frac{r_\oplus}{p}\right)^2 (1 - r_{\odot y}^2) + (1 - r_{\odot y}^2)^2$$

The fourth-order equation may be solved by standard procedures. The two spurious roots may be rejected by noting that $|\hat{r}_\odot \times \vec{r}| = r \sin \psi = |\vec{r}_\oplus|$ and $\hat{r}_\odot \cdot \vec{r}/r \leq 0$ for occultation to occur.

REFERENCES

1. Explanatory Supplement to the Astronomical Ephemeris and the American Ephemeris and Nautical Almanac. H.M. Naut. Alm. Off., 1961.

2. Escobal, Pedro Ramon: Methods of Orbit Determination. John Wiley & Sons, Inc., c.1965.

3. Orbital Flight Handbook. Part 1 - Basic Techniques and Data. NASA SP-33, Pt. 1, 1963.

4. Kozai, Yoshihide: The Motion of a Close Earth Satellite. Astron. J., vol. 64, no. 9, Nov. 1959, pp. 367-377.

5. McCuskey, S. W.: Introduction to Celestial Mechanics. Addison-Wesley Pub. Co., Inc., c.1963.

6. Melbourne, William G.; Mulholland, J. Derral; Sjogren, William L.; and Sturms, Francis M., Jr.: Constants and Related Information for Astrodynamic Calculations, 1968. Tech. Rep. No. 32-1306 (Contract NAS 7-100), Jet Propulsion Lab., California Inst. Technol., July 15, 1968.

7. Harrison, Edwin F.; and Green, Richard N.: Orbit Analysis for Coastal Zone Oceanography Observations. AIAA Paper No. 73-207, Jan. 1973.

8. Harrison, Edwin F.; Brooks, David R.; and Gibson, Gary G.: Mission Analysis To Define Satellite Orbits for Earth Radiation Budget Measurements. AIAA Paper 76-811, Aug. 1976.

9. Russell, James M., III; Park, Jae H.; and Drayson, S. Roland: Global Monitoring of Stratospheric Halogen Compounds From a Satellite Using Gas Filter Spectroscopy in the Solar Occultation Mode. Appl. Opt., vol. 16, no. 3, Mar. 1977, pp. 607-612.

TABLE 1.- JULIAN DAY NUMBER, 1950-1999, OF DAY COMMENCING

AT GREENWICH NOON ON:

Year	Jan. 0.5[a]	Feb. 0.5	Mar. 0.5	Apr. 0.5	May 0.5	June 0.5	July 0.5	Aug. 0.5	Sept. 0.5	Oct. 0.5	Nov. 0.5	Dec. 0.5
1950	243 3282	3313	3341	3372	3402	3433	3463	3494	3525	3555	3586	3616
1951	3647	3678	3706	3737	3767	3798	3828	3859	3890	3920	3951	3981
1952	4012	4043	4072	4103	4133	4164	4194	4225	4256	4286	4317	4347
1953	4378	4409	4437	4468	4498	4529	4559	4590	4621	4651	4682	4712
1954	4743	4774	4802	4833	4863	4894	4924	4955	4986	5016	5047	5077
1955	243 5108	5139	5167	5198	5228	5259	5289	5320	5351	5381	5412	5442
1956	5473	5504	5533	5564	5594	5625	5655	5686	5717	5747	5778	5808
1957	5839	5870	5898	5929	5959	5990	6020	6051	6082	6112	6143	6173
1958	6204	6235	6263	6294	6324	6355	6385	6416	6447	6477	6508	6538
1959	6569	6600	6628	6659	6689	6720	6750	6781	6812	6842	6873	6903
1960	243 6934	6965	6994	7025	7055	7086	7116	7147	7178	7208	7239	7269
1961	7300	7331	7359	7390	7420	7451	7481	7512	7543	7573	7604	7634
1962	7665	7696	7724	7750	7785	7816	7846	7877	7908	7938	7969	7999
1963	8030	8061	8089	8120	8150	8181	8211	8242	8273	8303	8334	8364
1964	8395	8426	8455	8486	8516	8547	8577	8608	8639	8669	8700	8730
1965	243 8761	8792	8820	8851	8881	8912	8942	8973	9004	9034	9065	9095
1966	9126	9157	9185	9216	9246	9277	9307	9338	9369	9399	9430	9460
1967	9491	9522	9550	9581	9611	9642	9672	9703	9734	9764	9795	9825
1968	9856	9887	9916	9947	9977	*0008	*0038	*0069	*0100	*0130	*0161	*0191
1969	244 0222	0253	0281	0312	0342	0373	0403	0434	0465	0495	0526	0556
1970	244 0587	0618	0646	0677	0707	0738	0768	0799	0830	0860	0891	0921
1971	0952	0983	1011	1042	1072	1103	1133	1164	1195	1225	1256	1286
1972	1317	1348	1377	1408	1438	1469	1499	1530	1561	1591	1622	1652
1973	1683	1714	1742	1773	1803	1834	1864	1895	1926	1956	1987	2017
1974	2048	2079	2107	2138	2168	2199	2229	2260	2291	2321	2352	2382
1975	244 2413	2444	2472	2503	2533	2564	2594	2625	2656	2686	2717	2747
1976	2778	2809	2838	2869	2899	2930	2960	2991	3022	3052	3083	3113
1977	3144	3175	3203	3234	3264	3295	3325	3356	3387	3417	3448	3478
1978	3509	3540	3568	3599	3629	3660	3690	3721	3752	3782	3813	3843
1979	3874	3905	3933	3964	3994	4025	4055	4086	4117	4147	4178	4208
1980	244 4239	4270	4299	4330	4360	4391	4421	4452	4483	4513	4544	4574
1981	4605	4636	4664	4695	4725	4756	4786	4817	4848	4878	4909	4939
1982	4970	5001	5029	5060	5090	5121	5151	5182	5213	5243	5274	5304
1983	5335	5366	5394	5425	5455	5486	5516	5547	5578	5608	5639	5669
1984	5700	5731	5760	5791	5821	5852	5882	5913	5944	5974	6005	6035
1985	244 6066	6097	6125	6156	6186	6217	6247	6278	6309	6339	6370	6400
1986	6431	6462	6490	6521	6551	6582	6612	6643	6674	6704	6735	6765
1987	6796	6827	6855	6886	6916	6947	6977	7008	7039	7069	7100	7130
1988	7161	7192	7221	7252	7282	7313	7343	7374	7405	7435	7466	7496
1989	7527	7558	7586	7617	7647	7678	7708	7739	7770	7800	7831	7861
1990	244 7892	7923	7951	7982	8012	8043	8073	8104	8135	8165	8196	8226
1991	8257	8288	8316	8347	8377	8408	8438	8469	8500	8530	8561	8591
1992	8622	8653	8682	8713	8743	8774	8804	8835	8866	8896	8927	8957
1993	8988	9019	9047	9078	9108	9139	9169	9200	9231	9261	9292	9322
1994	9353	9384	9412	9443	9473	9504	9534	9565	9596	9626	9657	9687
1995	244 9718	9749	9777	9808	9838	9869	9899	9930	9961	9991	*0022	*0052
1996	245 0083	0114	0143	0174	0204	0235	0265	0296	0327	0357	0388	0418
1997	0449	0480	0508	0539	0569	0600	0630	0661	0692	0722	0753	0783
1998	0814	0845	0873	0904	0934	0965	0995	1026	1057	1087	1118	1148
1999	245 1179	1210	1238	1269	1299	1330	1360	1391	1422	1452	1483	1513
2000	245 1544	1575	1604	1635	1665	1696	1726	1757	1788	1818	1849	1879

[a]Jan. 0.5 = Greenwich noon (12^h) UT, Dec. 31.

TABLE 2.- KEPLERIAN AND PERTURBED ORBITAL PERIODS AS A FUNCTION OF ALTITUDE AND INCLINATION

h, km	τ_O, sec	τ_A, τ_N, $\tau_A - \tau_O$, and $\tau_N - \tau_O$,[a] sec, for i, deg, of -									
		0	10	20	30	40	50	60	70	80	90
200	5309.6	5301.6	5301.9	5303.0	5304.6	5306.6	5308.7	5310.7	5312.3	5313.3	5313.7
		-8.1	-7.7	-6.7	-5.1	-3.1	-1.0	1.0	2.6	3.7	4.1
		5285.4	5286.4	5289.2	5293.5	5298.7	5304.4	5309.6	5314.0	5316.8	5317.8
		-24.2	-23.3	-20.5	-16.2	-10.9	-5.3	0.0	4.3	7.1	8.1
300	5431.2	5423.1	5423.5	5424.6	5426.2	5428.1	5430.2	5432.2	5433.8	5434.8	5435.2
		-8.0	-7.7	-6.6	-5.0	-3.1	-1.0	1.0	2.6	3.7	4.0
		5407.1	5408.1	5410.9	5415.1	5420.4	5425.9	5431.2	5435.5	5438.3	5439.2
		-24.1	-23.1	-20.3	-16.1	-10.8	-5.2	0.0	4.3	7.1	8.1
400	5553.6	5545.7	5546.0	5547.1	5548.6	5550.6	5552.7	5554.6	5556.2	5557.3	5557.6
		-8.0	-7.6	-6.6	-5.0	-3.0	-1.0	1.0	2.6	3.6	4.0
		5529.8	5530.7	5533.5	5537.7	5542.9	5548.4	5553.6	5557.9	5560.7	5561.6
		-23.9	-22.9	-20.2	-15.9	-10.7	-5.2	0.0	4.3	7.0	8.0
500	5677.0	5669.1	5669.4	5670.5	5672.0	5674.0	5676.0	5678.0	5679.6	5680.6	5680.9
		-7.9	-7.6	-6.5	-4.9	-3.0	-0.9	1.0	2.6	3.6	4.0
		5653.3	5654.2	5657.0	5661.2	5666.3	5671.8	5677.0	5681.2	5684.0	5684.9
		-23.7	-22.8	-20.0	-15.8	-10.7	-5.2	0.0	4.2	7.0	7.9
600	5801.2	5793.4	5793.7	5794.8	5796.3	5798.2	5800.3	5802.2	5803.8	5804.8	5805.2
		-7.9	-7.5	-6.5	-4.9	-3.0	-0.9	1.0	2.6	3.6	3.9
		5777.7	5778.6	5781.4	5785.5	5790.6	5796.1	5801.2	5805.4	5808.2	5809.1
		-23.5	-22.6	-19.9	-15.7	-10.6	-5.1	0.0	4.2	6.9	7.9
700	5926.4	5918.6	5918.9	5919.9	5921.5	5923.4	5925.4	5927.4	5928.9	5929.9	5930.3
		-7.8	-7.5	-6.4	-4.9	-3.0	-0.9	1.0	2.5	3.6	3.9
		5903.0	5904.0	5906.6	5910.8	5915.9	5921.3	5926.4	5930.5	5933.3	5934.2
		-23.4	-22.4	-19.7	-15.6	-10.5	-5.1	0.0	4.2	6.9	7.8
800	6052.4	6044.7	6045.0	6046.0	6047.6	6049.5	6051.5	6053.4	6054.9	6055.9	6056.3
		-7.7	-7.4	-6.4	-4.8	-2.9	-0.9	1.0	2.5	3.5	3.9
		6029.2	6030.1	6032.8	6036.9	6042.0	6047.4	6052.4	6056.5	6059.2	6060.2
		-23.2	-22.3	-19.6	-15.5	-10.4	-5.1	0.0	4.1	6.8	7.8
900	6179.3	6171.6	6172.0	6173.0	6174.5	6176.4	6178.4	6180.3	6181.8	6182.8	6183.2
		-7.7	-7.3	-6.3	-4.8	-2.9	-0.9	1.0	2.5	3.5	3.9
		6156.3	6157.2	6159.9	6164.0	6169.0	6174.3	6179.3	6183.4	6186.1	6187.0
		-23.1	-22.1	-19.5	-15.4	-10.4	-5.0	0.0	4.1	6.8	7.7
1000	6307.1	6299.5	6299.8	6300.8	6302.3	6304.2	6306.2	6308.1	6309.6	6310.6	6311.0
		-7.6	-7.3	-6.3	-4.8	-2.9	-0.9	1.0	2.5	3.5	3.8
		6284.2	6285.1	6287.8	6291.8	6296.8	6302.1	6307.1	6311.2	6313.9	6314.8
		-22.9	-22.0	-19.3	-15.3	-10.3	-5.0	0.0	4.1	6.7	7.7
1100	6435.3	6428.2	6428.5	6429.5	6431.0	6432.9	6434.9	6436.7	6438.3	6439.2	6439.6
		-7.6	-7.3	-6.3	-4.7	-2.9	-0.9	1.0	2.5	3.5	3.8
		6413.0	6414.0	6416.6	6420.6	6425.6	6430.8	6435.8	6439.8	6442.5	6443.4
		-22.7	-21.8	-19.2	-15.2	-10.2	-5.0	0.0	4.0	6.7	7.6
1200	6565.3	6557.8	6558.1	6559.1	6560.6	6562.4	6564.4	6566.2	6567.8	6563.7	6569.1
		-7.5	-7.2	-6.2	-4.7	-2.9	-0.9	0.9	2.5	3.4	3.8
		6542.7	6543.6	6546.2	6550.2	6555.1	6560.4	6565.3	6569.3	6572.0	6572.9
		-22.6	-21.7	-19.1	-15.1	-10.2	-4.9	0.0	4.0	6.6	7.6
1300	6695.7	6688.2	6688.5	6689.5	6691.0	6692.8	6694.8	6696.6	6698.1	6699.1	6699.4
		-7.5	-7.2	-6.2	-4.7	-2.9	-0.9	0.9	2.4	3.4	3.8
		6673.2	6674.1	6676.7	6680.7	6685.6	6690.8	6695.7	6699.7	6702.3	6703.2
		-22.4	-21.5	-19.0	-15.0	-10.1	-4.9	0.0	4.0	6.6	7.5
1400	6826.9	6819.5	6819.8	6820.8	6822.3	6824.1	6826.0	6827.8	6829.3	6830.3	6830.6
		-7.4	-7.1	-6.1	-4.7	-2.8	-0.9	0.9	2.4	3.4	3.7
		6804.6	6805.5	6808.1	6812.0	6816.9	6822.1	6826.9	6830.9	6833.5	6834.4
		-22.3	-21.4	-18.8	-14.9	-10.0	-4.9	0.0	4.0	6.6	7.5
1500	6959.0	6951.6	6951.9	6952.9	6954.4	6956.2	6958.1	6959.9	6961.4	6962.4	6962.7
		-7.4	-7.1	-6.1	-4.6	-2.8	-0.9	0.9	2.4	3.4	3.7
		6936.8	6937.7	6940.3	6944.2	6949.0	6954.2	6959.0	6962.9	6965.5	6966.4
		-22.2	-21.3	-18.7	-14.8	-10.0	-4.8	0.0	3.9	6.5	7.4

[a]At each value of altitude h, the first line of data is τ_A; the second line, $\tau_A - \tau_O$; the third line, τ_N; and the fourth line, $\tau_N - \tau_O$, all in seconds.

TABLE 3.- NODAL PRECESSION RATES FOR PERTURBED CIRCULAR ORBITS AS A FUNCTION OF ALTITUDE AND INCLINATION

i, deg	$\dot{\omega}$,[a] deg/day, and $\dot{\Omega}$,[a] deg/day, at altitude, h, km, of -													
	200	300	400	500	600	700	800	900	1000	1100	1200	1300	1400	1500
0	17.913 -8.956	16.991 -8.495	16.129 -8.064	15.322 -7.661	14.567 -7.283	13.859 -6.929	13.194 -6.597	12.570 -6.235	11.983 -5.992	11.431 -5.716	10.912 -5.456	10.422 -5.211	9.960 -4.980	9.524 -4.762
10	17.236 -8.820	16.349 -8.366	15.520 -7.941	14.744 -7.544	14.017 -7.172	13.335 -6.824	12.696 -6.496	12.095 -6.189	11.531 -5.900	11.000 -5.629	10.500 -5.373	10.029 -5.132	9.584 -4.904	9.165 -4.690
20	15.289 -8.414	14.502 -7.981	13.767 -7.576	13.079 -7.197	12.434 -6.842	11.829 -6.510	11.262 -6.198	10.730 -5.905	10.229 -5.629	9.758 -5.370	9.314 -5.126	8.896 -4.896	8.502 -4.679	8.130 -4.474
30	12.308 -7.752	11.675 -7.353	11.083 -6.980	10.528 -6.631	10.010 -6.304	9.523 -5.998	9.067 -5.710	8.638 -5.440	8.235 -5.187	7.856 -4.948	7.499 -4.723	7.162 -4.511	6.845 -4.311	6.545 -4.123
40	8.653 -6.355	8.208 -6.502	7.792 -6.172	7.402 -5.864	7.038 -5.575	6.696 -5.304	6.375 -5.050	6.073 -4.811	5.790 -4.586	5.523 -4.375	5.272 -4.176	5.036 -3.989	4.813 -3.812	4.602 -3.646
50	4.767 -5.749	4.522 -5.454	4.292 -5.177	4.078 -4.918	3.877 -4.676	3.689 -4.449	3.512 -4.236	3.346 -4.035	3.190 -3.847	3.043 -3.670	2.905 -3.503	2.774 -3.346	2.652 -3.198	2.536 -3.058
60	1.118 -4.471	1.060 -4.241	1.006 -4.026	0.956 -3.825	0.909 -3.636	0.865 -3.460	0.823 -3.294	0.785 -3.133	0.748 -2.992	0.714 -2.854	0.681 -2.724	0.651 -2.602	0.622 -2.487	0.595 -2.378
70	-1.355 -3.057	-1.760 -2.900	-1.671 -2.753	-1.587 -2.615	-1.509 -2.487	-1.436 -2.366	-1.367 -2.252	-1.302 -2.146	-1.242 -2.046	-1.184 -1.952	-1.131 -1.863	-1.080 -1.780	-1.032 -1.701	-0.987 -1.626
80	-3.795 -1.552	-3.599 -1.472	-3.417 -1.397	-3.246 -1.328	-3.087 -1.262	-2.937 -1.201	-2.796 -1.143	-2.664 -1.089	-2.540 -1.039	-2.423 -0.991	-2.313 -0.946	-2.209 -0.903	-2.111 -0.863	-2.019 -0.826
90	-4.463 0.000	-4.233 0.000	-4.023 0.000	-3.823 0.000	-3.634 0.000	-3.458 0.000	-3.292 0.000	-3.137 0.000	-2.990 0.000	-2.853 0.000	-2.723 0.000	-2.601 0.000	-2.486 0.000	-2.377 0.000
100	-3.795 1.552	-3.599 1.472	-3.417 1.397	-3.246 1.328	-3.087 1.262	-2.937 1.201	-2.796 1.143	-2.664 1.089	-2.540 1.039	-2.423 0.991	-2.313 0.946	-2.209 0.903	-2.111 0.863	-2.019 0.826

[a]For each value of i the first line of data is $\dot{\omega}$; the second line, $\dot{\Omega}$. (Note: $\dot{\omega} = 0$ at $i = 63.435^{\circ}$; $\dot{\Omega} = 0$ at $i = 90^{\circ}$.)

TABLE 4.- LONGITUDE DISPLACEMENTS FOR ONE REVOLUTION OF A CIRCULAR KEPLERIAN ORBIT

Altitude, km	Keplerian period		ΔL, deg/orbit	ΔL, km/orbit, at specified latitude, deg, of -								
	orbits/day	sec		0	10	20	30	40	50	60	70	80
200	16.27	5310	22.18	2470	2432	2321	2139	1892	1587	1235	845	429
300	15.91	5431	22.69	2526	2488	2374	2188	1935	1624	1263	864	439
400	15.56	5554	23.20	2583	2544	2427	2237	1979	1660	1292	883	449
500	15.22	5677	23.72	2640	2600	2481	2287	2023	1697	1320	903	458
600	14.89	5801	24.24	2698	2657	2535	2337	2067	1734	1349	923	469
700	14.58	5926	24.76	2756	2714	2590	2387	2112	1772	1378	943	479
800	14.28	6052	25.29	2815	2772	2645	2438	2156	1809	1407	963	489
900	13.98	6179	25.82	2874	2830	2701	2489	2202	1847	1437	983	499
1000	13.70	6307	26.35	2933	2889	2757	2540	2247	1886	1467	1003	509
1100	13.42	6436	26.89	2993	2948	2813	2592	2293	1924	1497	1024	520
1200	13.16	6565	27.43	3054	3007	2869	2644	2339	1963	1527	1044	530
1300	12.90	6696	27.98	3114	3067	2926	2697	2386	2002	1557	1065	541
1400	12.66	6827	28.52	3175	3127	2984	2750	2432	2041	1588	1086	551
1500	12.42	6959	29.08	3237	3187	3041	2803	2479	2080	1618	1107	562

TABLE 5.- CIRCULAR ORBIT PARAMETERS FOR SPECIFIED REPETITION FACTORS

Q	Orbit altitude, km, for inclination, i, deg, of -									
	0	10	20	30	40	50	60	70	80	90
12	1616.2	1616.5	1617.6	1619.6	1622.7	1627.1	1633.0	1640.6	1649.9	1660.7
12 1/ 2	1395.9	1396.3	1397.5	1399.8	1403.3	1408.2	1414.7	1423.0	1433.0	1444.6
12 1/ 3	1467.7	1468.1	1469.3	1471.5	1474.8	1479.5	1485.9	1493.9	1503.7	1515.0
12 2/ 3	1325.6	1326.0	1327.3	1329.7	1333.3	1338.3	1345.1	1353.6	1363.8	1375.7
12 1/ 4	1504.2	1504.6	1505.8	1507.9	1511.2	1515.8	1522.0	1530.0	1539.6	1550.8
12 3/ 4	1291.0	1291.4	1292.8	1295.2	1298.8	1304.0	1310.8	1319.4	1329.8	1341.8
12 1/ 5	1526.3	1526.7	1527.8	1529.9	1533.2	1537.8	1543.9	1551.8	1561.4	1572.5
12 4/ 5	1270.4	1270.8	1272.2	1274.6	1278.3	1283.6	1290.4	1299.1	1309.6	1321.7
12 1/ 6	1541.1	1541.5	1542.6	1544.7	1547.9	1552.5	1558.6	1566.4	1575.9	1587.0
12 5/ 6	1256.7	1257.2	1258.6	1261.0	1264.8	1270.0	1276.9	1285.7	1296.2	1308.3
12 1/ 7	1551.7	1552.1	1553.2	1555.3	1558.5	1563.0	1569.1	1576.9	1586.4	1597.4
12 6/ 7	1247.0	1247.5	1248.9	1251.3	1255.1	1260.4	1267.3	1276.1	1286.6	1298.8
12 1/ 8	1559.7	1560.1	1561.2	1563.3	1566.5	1571.0	1577.1	1584.8	1594.3	1605.3
12 7/ 8	1239.8	1240.2	1241.6	1244.1	1247.9	1253.1	1260.1	1268.9	1279.5	1291.7
12 1/ 9	1565.9	1566.3	1567.4	1569.5	1572.7	1577.2	1583.2	1591.0	1600.4	1611.4
12 8/ 9	1234.1	1234.6	1236.0	1238.5	1242.2	1247.5	1254.5	1263.3	1274.0	1286.2
12 1/10	1570.9	1571.3	1572.4	1574.5	1577.6	1582.1	1588.2	1595.9	1605.3	1616.3
12 9/10	1229.6	1230.1	1231.5	1234.0	1237.8	1243.1	1250.1	1258.9	1269.5	1281.8
12 1/11	1575.0	1575.4	1576.5	1578.5	1581.7	1586.2	1592.2	1599.9	1609.3	1620.3
12 10/11	1225.9	1226.4	1227.8	1230.3	1234.1	1239.4	1246.4	1255.3	1265.9	1278.2
12 1/12	1578.4	1578.8	1579.9	1581.9	1585.1	1589.6	1595.6	1603.3	1612.7	1623.6
12 11/12	1222.9	1223.3	1224.7	1227.2	1231.0	1236.4	1243.4	1252.2	1262.9	1275.2
12 1/13	1581.3	1581.7	1582.8	1584.8	1588.0	1592.5	1598.5	1606.2	1615.6	1626.5
12 12/13	1220.3	1220.7	1222.1	1224.7	1228.5	1233.8	1240.8	1249.7	1260.4	1272.6
12 1/14	1583.8	1584.1	1585.3	1587.3	1590.4	1594.9	1600.9	1608.6	1618.0	1628.9
12 13/14	1218.1	1218.5	1219.9	1222.4	1226.3	1231.6	1238.6	1247.5	1258.2	1270.5
12 1/15	1585.9	1586.3	1587.4	1589.4	1592.6	1597.1	1603.1	1610.7	1620.1	1631.0
12 14/15	1216.1	1216.6	1218.0	1220.5	1224.3	1229.7	1236.7	1245.6	1256.3	1268.6
12 1/16	1587.8	1588.2	1589.3	1591.3	1594.5	1598.9	1604.9	1612.6	1622.0	1632.9
12 15/16	1214.4	1214.9	1216.3	1218.8	1222.7	1228.0	1235.1	1243.9	1254.6	1267.0
12 1/17	1589.5	1589.8	1591.0	1593.0	1596.1	1600.6	1606.6	1614.2	1623.6	1634.5
12 16/17	1213.0	1213.4	1214.8	1217.4	1221.2	1226.5	1233.6	1242.5	1253.2	1265.5
12 1/18	1591.0	1591.3	1592.4	1594.4	1597.6	1602.0	1608.0	1615.7	1625.1	1636.0
12 17/18	1211.6	1212.1	1213.5	1216.1	1219.9	1225.2	1232.3	1241.2	1251.9	1264.2
12 1/19	1592.3	1592.6	1593.7	1595.8	1598.9	1603.4	1609.4	1617.0	1626.4	1637.2
12 18/19	1210.5	1210.9	1212.4	1214.9	1218.7	1224.1	1231.1	1240.0	1250.7	1263.1
12 1/20	1593.5	1593.8	1594.9	1597.0	1600.1	1604.5	1610.5	1618.2	1627.5	1638.4
12 19/20	1209.4	1209.9	1211.3	1213.8	1217.7	1223.0	1230.1	1239.0	1249.7	1262.0
12 1/21	1594.5	1594.9	1596.0	1598.0	1601.2	1605.6	1611.6	1619.3	1628.6	1639.5
12 20/21	1208.5	1208.9	1210.3	1212.9	1216.7	1222.1	1229.1	1238.0	1248.7	1261.1

TABLE 5.- Continued

Q	Orbit altitude, km, for inclination, i, deg, of -									
	0	10	20	30	40	50	60	70	80	90
13	1189.3	1189.8	1191.2	1193.8	1197.7	1203.1	1210.2	1219.2	1230.0	1242.4
13 1/ 2	995.2	995.7	997.4	1000.2	1004.5	1010.5	1018.2	1027.9	1039.5	1052.8
13 1/ 3	1058.6	1059.1	1060.7	1063.4	1067.6	1073.4	1080.9	1090.4	1101.7	1114.7
13 2/ 3	933.0	933.6	935.3	938.2	942.7	948.8	956.8	966.7	978.6	992.1
13 1/ 4	1090.8	1091.3	1092.8	1095.5	1099.6	1105.3	1112.7	1122.1	1133.2	1146.1
13 3/ 4	902.4	903.0	904.7	907.7	912.2	918.4	926.5	936.6	948.6	962.3
13 1/ 5	1110.3	1110.8	1112.3	1115.0	1119.0	1124.6	1132.0	1141.3	1152.3	1165.1
13 4/ 5	884.2	884.7	886.5	889.5	894.1	900.4	908.5	918.7	930.7	944.5
13 1/ 6	1123.3	1123.8	1125.3	1128.0	1132.0	1137.6	1144.9	1154.1	1165.1	1177.8
13 5/ 6	872.1	872.7	874.4	877.5	882.1	888.4	896.6	906.3	918.9	932.7
13 1/ 7	1132.7	1133.1	1134.6	1137.3	1141.3	1146.8	1154.1	1163.3	1174.3	1187.0
13 6/ 7	863.5	864.0	865.8	868.9	873.5	879.8	888.1	898.3	910.4	924.3
13 1/ 8	1139.7	1140.2	1141.7	1144.3	1148.3	1153.8	1161.1	1170.2	1181.2	1193.9
13 7/ 8	857.0	857.6	859.4	862.5	867.1	873.4	881.7	891.9	904.1	918.0
13 1/ 9	1145.2	1145.7	1147.1	1149.8	1153.7	1159.2	1166.5	1175.6	1186.6	1199.2
13 8/ 9	852.0	852.6	854.4	857.5	862.1	868.5	876.8	887.0	899.2	913.2
13 1/10	1149.6	1150.0	1151.5	1154.1	1158.1	1163.6	1170.9	1180.0	1190.9	1203.5
13 9/10	848.0	848.6	850.4	853.5	858.1	864.5	872.8	883.1	895.3	909.3
13 1/11	1153.2	1153.6	1155.1	1157.7	1161.7	1167.2	1174.4	1183.5	1194.4	1207.0
13 10/11	844.8	845.3	847.1	850.2	854.9	861.3	869.6	879.9	892.1	906.1
13 1/12	1156.2	1156.6	1158.1	1160.7	1164.7	1170.2	1177.4	1186.5	1197.4	1209.9
13 11/12	842.0	842.6	844.4	847.5	852.2	858.6	866.9	877.2	889.5	903.4
13 1/13	1158.7	1159.2	1160.6	1163.2	1167.2	1172.7	1179.9	1189.0	1199.9	1212.4
13 12/13	839.7	840.3	842.1	845.2	849.9	856.3	864.6	874.9	887.2	901.2
13 1/14	1160.9	1161.3	1162.8	1165.4	1169.3	1174.8	1182.1	1191.1	1202.0	1214.6
13 13/14	837.8	838.4	840.1	843.3	847.9	854.3	862.7	873.0	885.3	899.3
13 1/15	1162.8	1163.2	1164.7	1167.3	1171.2	1176.7	1183.9	1193.0	1203.9	1216.4
13 14/15	836.1	836.6	838.4	841.6	846.2	852.7	861.0	871.3	883.6	897.6
13 1/16	1164.4	1164.9	1166.4	1169.0	1172.9	1178.4	1185.6	1194.6	1205.5	1218.0
13 15/16	834.6	835.2	836.9	840.1	844.8	851.2	859.5	869.9	882.2	896.2
13 1/17	1165.9	1166.4	1167.8	1170.4	1174.3	1179.8	1187.0	1196.1	1206.9	1219.5
13 16/17	833.3	833.8	835.6	838.8	843.4	849.9	858.2	868.6	880.9	894.9
13 1/18	1167.2	1167.7	1169.1	1171.7	1175.6	1181.1	1188.3	1197.3	1208.2	1220.7
13 17/18	832.1	832.7	834.5	837.6	842.3	848.7	857.1	867.4	879.7	893.8
13 1/19	1168.3	1168.8	1170.3	1172.9	1176.8	1182.2	1189.4	1198.5	1209.4	1221.9
13 18/19	831.0	831.6	833.4	836.6	841.2	847.7	856.0	866.4	878.7	892.7
13 1/20	1169.4	1169.9	1171.3	1173.9	1177.8	1183.3	1190.5	1199.5	1210.4	1222.9
13 19/20	830.1	830.7	832.5	835.6	840.3	846.7	855.1	865.5	877.8	891.8
13 1/21	1170.3	1170.8	1172.3	1174.9	1178.8	1184.2	1191.4	1200.5	1211.3	1223.8
13 20/21	829.3	829.8	831.6	834.8	839.5	845.9	854.3	864.6	877.0	891.0

TABLE 5.- Continued

Q	Orbit altitude, km, for inclination, i, deg, of -									
	0	10	20	30	40	50	60	70	80	90
14	812.3	812.9	814.7	817.9	322.6	829.1	837.5	348.0	860.3	874.5
14 1/ 2	639.5	640.1	642.2	645.7	650.9	657.9	667.0	678.2	691.5	706.5
14 1/ 3	696.0	696.7	698.6	702.0	707.0	713.9	722.3	733.7	746.7	761.4
14 2/ 3	584.0	584.7	586.7	590.4	595.7	603.0	612.3	623.8	637.3	652.6
14 1/ 4	724.7	725.3	727.2	730.6	735.5	742.3	751.1	761.9	774.7	789.3
14 3/ 4	556.6	557.3	559.4	563.1	568.5	575.9	585.3	596.9	610.6	626.1
14 1/ 5	742.0	742.6	744.5	747.8	752.7	759.4	768.1	778.9	791.6	806.1
14 4/ 5	540.3	541.0	543.1	546.8	552.3	559.7	569.3	580.9	594.7	610.3
14 1/ 6	753.6	754.2	756.1	759.4	764.3	770.9	779.6	790.3	803.0	817.4
14 5/ 6	529.5	530.2	532.3	536.1	541.6	549.0	558.6	570.3	584.1	599.8
14 1/ 7	761.9	762.5	764.4	767.7	772.5	779.2	787.8	798.5	311.1	825.5
14 6/ 7	521.8	522.5	524.6	528.4	533.9	541.4	551.0	562.8	576.6	592.3
14 1/ 8	768.2	768.8	770.6	773.9	778.7	785.4	794.0	804.6	817.2	831.5
14 7/ 8	516.0	516.7	518.9	522.6	528.2	535.7	545.3	557.1	571.0	586.7
14 1/ 9	773.0	773.6	775.5	778.8	783.6	790.2	798.8	809.4	822.0	836.3
14 8/ 9	511.5	512.2	514.4	518.2	523.7	531.3	540.9	552.7	566.6	582.4
14 1/10	776.9	777.5	779.4	782.6	787.5	794.1	802.6	813.2	825.8	840.1
14 9/10	507.9	508.6	510.8	514.6	520.2	527.7	537.4	549.2	563.2	578.9
14 1/11	780.1	780.7	782.6	785.8	790.6	797.2	805.8	816.4	828.9	843.2
14 10/11	505.0	505.7	507.9	511.7	517.3	524.8	534.5	546.4	560.3	576.1
14 1/12	782.8	783.4	785.3	788.5	793.3	799.9	808.4	819.0	831.5	845.8
14 11/12	502.6	503.3	505.5	509.3	514.8	522.4	532.1	544.0	557.9	573.7
14 1/13	785.1	785.7	787.5	790.7	795.5	802.1	810.6	821.2	833.7	848.0
14 12/13	500.5	501.2	503.4	507.2	512.8	520.4	530.1	542.0	555.9	571.7
14 1/14	787.0	787.6	789.4	792.7	797.5	804.0	812.6	823.1	835.6	849.9
14 13/14	498.8	499.5	501.7	505.5	511.0	518.6	528.3	540.2	554.2	570.0
14 1/15	788.7	789.3	791.1	794.3	799.1	805.7	814.2	824.8	837.3	851.5
14 14/15	497.2	497.9	500.1	503.9	509.5	517.1	526.8	538.7	552.7	568.5
14 1/16	790.1	790.7	792.6	795.8	800.6	807.2	815.7	826.2	838.7	852.9
14 15/16	495.9	496.6	498.8	502.6	508.2	515.8	525.5	537.4	551.4	567.2
14 1/17	791.4	792.0	793.9	797.1	801.9	808.4	816.9	827.5	840.0	854.2
14 16/17	494.7	495.4	497.6	501.4	507.0	514.6	524.4	536.3	550.3	566.1
14 1/18	792.6	793.2	795.0	798.2	803.0	809.6	818.1	828.6	841.1	855.3
14 17/18	493.7	494.4	496.6	500.4	506.0	513.6	523.3	535.2	549.3	565.1
14 1/19	793.6	794.2	796.1	799.3	804.1	810.6	819.1	829.6	842.1	856.3
14 18/19	492.7	493.4	495.6	499.5	505.1	512.7	522.4	534.3	548.3	564.2
14 1/20	794.6	795.2	797.0	800.2	805.0	811.5	820.0	830.5	843.0	857.2
14 19/20	491.9	492.6	494.8	498.6	504.2	511.8	521.6	533.5	547.5	563.3
14 1/21	795.4	796.0	797.8	801.0	805.8	812.4	820.9	831.4	843.8	858.0
14 20/21	491.1	491.8	494.0	497.9	503.5	511.1	520.8	532.8	546.8	562.6

TABLE 5.- Concluded

Q	Orbit altitude, km, for inclination, i, deg, of -									
	0	10	20	30	40	50	60	70	80	90
15	475.9	476.6	478.9	482.7	488.4	496.0	505.9	517.9	532.0	547.9
15 1/ 2	320.3	321.6	324.0	328.2	334.3	342.6	353.2	366.0	381.0	397.3
15 1/ 3	371.6	372.4	374.7	378.8	384.8	392.9	403.2	415.7	430.4	447.0
15 2/ 3	270.3	271.6	274.1	278.4	284.8	293.2	304.0	317.2	332.4	349.6
15 1/ 4	397.3	398.1	400.4	404.4	410.4	418.3	428.5	440.9	455.5	471.8
15 3/ 4	246.1	246.9	249.5	253.9	260.3	268.9	279.3	293.0	303.5	325.3
15 1/ 5	412.9	413.6	415.9	419.9	425.8	433.7	443.8	456.1	470.6	486.9
15 4/ 5	231.4	232.2	234.8	239.2	245.7	254.3	265.3	278.7	294.2	311.6
15 1/ 6	423.3	424.1	426.3	430.3	436.1	444.0	454.1	466.3	480.7	497.0
15 5/ 6	221.6	222.5	225.1	229.5	236.0	244.7	255.7	269.1	284.7	302.2
15 1/ 7	430.3	431.5	433.8	437.7	443.5	451.4	461.4	473.6	488.0	504.2
15 6/ 7	214.7	215.5	218.1	222.6	229.1	237.8	248.9	262.3	278.0	295.5
15 1/ 8	436.4	437.1	439.4	443.3	449.1	456.9	466.9	479.1	493.4	509.6
15 7/ 8	209.5	210.3	212.9	217.4	223.9	232.7	243.8	257.3	272.9	290.5
15 1/ 9	440.7	441.5	443.7	447.7	453.4	461.2	471.2	483.4	497.7	513.8
15 8/ 9	205.4	206.3	208.9	213.4	219.9	228.7	239.8	253.3	269.0	286.6
15 1/10	444.2	445.0	447.2	451.2	456.9	464.7	474.7	486.8	501.1	517.2
15 9/10	202.2	203.0	205.7	210.2	216.7	225.5	236.7	250.2	265.9	283.5
15 1/11	447.1	447.8	450.1	454.0	459.8	467.5	477.5	489.6	503.9	520.0
15 10/11	199.6	200.4	203.0	207.5	214.1	222.9	234.1	247.6	263.3	281.0
15 1/12	449.5	450.2	452.5	456.4	462.1	469.9	479.8	492.0	506.2	522.3
15 11/12	197.4	198.2	200.8	205.3	211.9	220.7	231.9	245.4	261.2	278.8
15 1/13	451.5	452.3	454.5	458.4	464.1	471.9	481.8	494.0	508.2	524.3
15 12/13	195.5	196.4	199.0	203.5	210.1	218.9	230.1	243.6	259.4	277.0
15 1/14	453.3	454.0	456.2	460.1	465.9	473.6	483.5	495.7	509.9	525.9
15 13/14	193.9	194.8	197.4	201.9	208.5	217.3	228.5	242.1	257.8	275.5
15 1/15	454.8	455.5	457.7	461.6	467.4	475.1	485.0	497.1	511.4	527.4
15 14/15	192.5	193.4	196.0	200.5	207.1	216.0	227.2	240.7	256.5	274.2
15 1/16	456.1	456.8	459.1	463.0	468.7	476.4	486.3	498.4	512.6	528.7
15 15/16	191.3	192.2	194.8	199.3	205.9	214.8	226.0	239.6	255.3	273.0
15 1/17	457.2	458.0	460.2	464.1	469.8	477.6	487.5	499.6	513.8	529.8
15 16/17	190.3	191.1	193.8	198.3	204.9	213.7	224.9	238.5	254.3	272.0
15 1/18	458.3	459.0	461.3	465.1	470.9	478.6	488.5	500.6	514.8	530.3
15 17/18	189.3	190.2	192.8	197.3	203.9	212.8	224.0	237.6	253.4	271.1
15 1/19	459.2	459.9	462.2	466.1	471.8	479.5	489.4	501.5	515.7	531.7
15 18/19	188.5	189.3	192.0	196.5	203.1	212.0	223.2	236.8	252.6	270.3
15 1/20	460.0	460.8	463.0	466.9	472.6	480.3	490.2	502.3	516.5	532.5
15 19/20	187.7	188.6	191.2	195.7	202.4	211.2	222.4	236.0	251.8	269.5
15 1/21	460.8	461.5	463.8	467.6	473.4	481.1	491.0	503.0	517.2	533.2
15 20/21	187.0	187.9	190.5	195.1	201.7	210.5	221.8	235.3	251.2	268.9

TABLE 6.- CIRCULAR SUN-SYNCHRONOUS ORBIT PARAMETERS FOR SPECIFIED REPETITION FACTORS

Q		a_s, km	i_s, deg
12		8054.630	102.944
12	1/ 2	7837.948	101.748
12	1/ 3	7908.546	102.128
12	2/ 3	7768.903	101.385
12	1/ 4	7944.445	102.325
12	3/ 4	7734.946	101.210
12	1/ 5	7966.181	102.445
12	4/ 5	7714.749	101.106
12	1/ 6	7980.754	102.526
12	5/ 6	7701.357	101.038
12	1/ 7	7991.204	102.585
12	6/ 7	7691.827	100.990
12	1/ 8	7999.064	102.629
12	7/ 8	7684.698	100.954
12	1/ 9	8005.190	102.663
12	8/ 9	7679.165	100.926
12	1/10	8010.100	102.691
12	9/10	7674.746	100.904
12	1/14	8022.761	102.762
12	13/14	7663.412	100.847
12	1/21	8033.349	102.822
12	20/21	7653.999	100.800
13		7635.259	100.706
13	1/ 2	7445.167	99.793
13	1/ 3	7507.209	100.085
13	2/ 3	7384.389	99.514
13	1/ 4	7538.717	100.235
13	3/ 4	7354.462	99.378
13	1/ 5	7557.781	100.327
13	4/ 5	7336.650	99.298
13	1/ 6	7570.558	100.389
13	5/ 6	7324.835	99.246
13	1/ 7	7579.717	100.433
13	6/ 7	7316.425	99.208
13	1/ 8	7586.604	100.467
13	7/ 8	7310.133	99.180
13	1/ 9	7591.972	100.493
13	8/ 9	7305.248	99.159
13	1/10	7596.273	100.514
13	9/10	7301.347	99.141
13	1/14	7607.361	100.569
13	13/14	7291.338	99.097
13	1/21	7616.632	100.614
13	20/21	7283.023	99.061

TABLE 6.- Concluded

Q	a_s, km	i_s, deg
14	7266.465	98.988
14 1/ 2	7098.096	98.275
14 1/ 3	7153.130	98.504
14 2/ 3	7044.107	98.056
14 1/ 4	7181.049	98.621
14 3/ 4	7017.493	97.949
14 1/ 5	7197.932	98.693
14 4/ 5	7001.646	97.886
14 1/ 6	7209.242	98.741
14 5/ 6	6991.130	97.844
14 1/ 7	7217.348	98.776
14 6/ 7	6983.643	97.815
14 1/ 8	7223.442	98.802
14 7/ 8	6978.040	97.793
14 1/ 9	7228.191	98.822
14 8/ 9	6973.691	97.776
14 1/10	7231.996	98.839
14 9/10	6970.216	97.762
14 1/14	7241.802	98.881
14 13/14	6961.301	97.727
14 1/21	7250.000	98.917
14 20/21	6953.893	97.698
15	6939.136	97.641
15 1/ 2	6788.770	97.074
15 1/ 3	6837.983	97.256
15 2/ 3	6740.430	96.899
15 1/ 4	6862.926	97.350
15 3/ 4	6716.580	96.813
15 1/ 5	6878.001	97.407
15 4/ 5	6702.371	96.763
15 1/ 6	6888.097	97.445
15 5/ 6	6692.940	96.729
15 1/ 7	6895.331	97.473
15 6/ 7	6686.224	96.706
15 1/ 8	6900.769	97.493
15 7/ 8	6681.197	96.688
15 1/ 9	6905.005	97.510
15 8/ 9	6677.294	96.674
15 1/10	6908.400	97.523
15 9/10	6674.176	96.663
15 1/14	6917.147	97.556
15 13/14	6666.175	96.635
15 1/21	6924.457	97.584
15 20/21	6659.525	96.612
16	6646.276	96.566

TABLE 7.- SOLAR POSITION DATA AS A FUNCTION OF TIME

J.D. 244 xxxx.5	Calendar day	Days from 1981T	Days from Jan. 1.0, 1981	x-, y-, and z-components of $\hat{x}_{\odot}$;[a] right ascension and declination[b]
4605.5	81/ 1/ 1/ 0	-78.6992631	0	0.1821703 -0.9021130 -0.3911599 -78.583370 -23.026691
4610.5	81/ 1/ 6/ 0	-73.6992631	5	0.2687963 -0.8836995 -0.3831757 -73.081722 -22.530532
4615.5	81/ 1/11/ 0	-68.6992631	10	0.3532844 -0.8583031 -0.3721637 -67.627542 -21.849120
4620.5	81/ 1/16/ 0	-63.6992631	15	0.4349470 -0.8261368 -0.3582162 -62.233954 -20.990690
4625.5	81/ 1/21/ 0	-58.6992631	20	0.5131237 -0.7874736 -0.3414516 -56.911432 -19.965343
4630.5	81/ 1/26/ 0	-53.6992631	25	0.5871874 -0.7426430 -0.3220129 -51.667547 -18.784701
4635.5	81/ 1/31/ 0	-48.6992631	30	0.6565507 -0.6920272 -0.3000657 -46.506911 -17.461549
4640.5	81/ 2/ 5/ 0	-43.6992631	35	0.7206715 -0.6360570 -0.2757967 -41.431279 -16.009503
4645.5	81/ 2/10/ 0	-38.6992631	40	0.7790581 -0.5752062 -0.2494116 -36.439765 -14.442697
4650.5	81/ 2/15/ 0	-33.6992631	45	0.8312727 -0.5099864 -0.2211320 -31.529148 -12.775533
4655.5	81/ 2/20/ 0	-28.6992631	50	0.8769352 -0.4409415 -0.1911938 -26.694212 -11.022466
4660.5	81/ 2/25/ 0	-23.6992631	55	0.9157256 -0.3686411 -0.1598441 -21.928099 -9.197850
4665.5	81/ 3/ 2/ 0	-18.6992631	60	0.9473857 -0.2936752 -0.1273386 -17.222644 -7.315830
4670.5	81/ 3/ 7/ 0	-13.6992631	65	0.9717197 -0.2166476 -0.0939392 -12.568691 -5.390267
4675.5	81/ 3/12/ 0	-8.6992631	70	0.9885947 -0.1381703 -0.0599111 -7.956371 -3.434713
4680.5	81/ 3/17/ 0	-3.6992631	75	0.9979401 -0.0588577 -0.0255209 -3.375349 -1.462399
4685.5	81/ 3/22/ 0	1.3007369	80	0.9997459 0.0206790 0.0089665 1.184954 0.513750
4690.5	81/ 3/27/ 0	6.3007369	85	0.9940616 0.0998369 0.0432896 5.735175 2.481089
4695.5	81/ 4/ 1/ 0	11.3007369	90	0.9809934 0.1780259 0.0771926 10.285819 4.427217
4700.5	81/ 4/ 6/ 0	16.3007369	95	0.9607014 0.2546732 0.1104271 14.847094 6.339941
4705.5	81/ 4/11/ 0	21.3007369	100	0.9333973 0.3292274 0.1427541 19.428741 8.207247
4710.5	81/ 4/16/ 0	26.3007369	105	0.8993399 0.4011617 0.1739450 24.039855 10.017274
4715.5	81/ 4/21/ 0	31.3007369	110	0.8588327 0.4699771 0.2037836 28.688705 11.758304
4720.5	81/ 4/26/ 0	36.3007369	115	0.8122196 0.5352049 0.2320666 33.382532 13.418772
4725.5	81/ 5/ 1/ 0	41.3007369	120	0.7598813 0.5964090 0.2586048 38.127349 14.987297
4730.5	81/ 5/ 6/ 0	46.3007369	125	0.7022320 0.6531877 0.2832242 42.927723 16.452734
4735.5	81/ 5/11/ 0	51.3007369	130	0.6397148 0.7051751 0.3057661 47.786575 17.804262
4740.5	81/ 5/16/ 0	56.3007369	135	0.5727992 0.7520423 0.3260878 52.704987 19.031497
4745.5	81/ 5/21/ 0	61.3007369	140	0.5019768 0.7934983 0.3440633 57.682053 20.124629
4750.5	81/ 5/26/ 0	66.3007369	145	0.4277578 0.8292908 0.3595830 62.714788 21.074589

[a]Respectively (top line).
[b]In degrees (bottom line).

TABLE 7.- Continued

J.D. 244 xxxx.5	Calendar day	Days from 1981T	Days from Jan. 1.0, 1981	x-, y-, and z-components of $\hat{x}_\odot$;[a] right ascension and declination[b]
4755.5	81/ 5/31/ 0	71.3007369	150	0.3506685 0.8592059 0.3725542 67.798107 21.873232
4760.5	81/ 6/ 5/ 0	76.3007369	155	0.2712473 0.8830692 0.3829014 72.924913 22.513521
4765.5	81/ 6/10/ 0	81.3007369	160	0.1900419 0.9007454 0.3905658 78.086287 22.989713
4770.5	81/ 6/15/ 0	86.3007369	165	0.1076068 0.9121381 0.3955057 83.271794 23.297518
4775.5	81/ 6/20/ 0	91.3007369	170	0.0244998 0.9171809 0.3976961 88.469887 23.434235
4780.5	81/ 6/25/ 0	96.3007369	175	-0.0587201 0.9158823 0.3971291 93.668393 23.398829
4785.5	81/ 6/30/ 0	101.3007369	180	-0.1414958 0.9082346 0.3938130 98.855048 23.191968
4790.5	81/ 7/ 5/ 0	106.3007369	185	-0.2232742 0.8943046 0.3877729 104.018036 22.815995
4795.5	81/ 7/10/ 0	111.3007369	190	-0.3035090 0.8741872 0.3790499 109.146491 22.274847
4800.5	81/ 7/15/ 0	116.3007369	195	-0.3816632 0.8480146 0.3677014 114.230930 21.573926
4805.5	81/ 7/20/ 0	121.3007369	200	-0.4572113 0.8159553 0.3538003 119.263594 20.719940
4810.5	81/ 7/25/ 0	126.3007369	205	-0.5296418 0.7782138 0.3374355 124.238676 19.720709
4815.5	81/ 7/30/ 0	131.3007369	210	-0.5984601 0.7350298 0.3187108 129.152429 18.584977
4820.5	81/ 8/ 4/ 0	136.3007369	215	-0.6631906 0.6866775 0.2977450 134.003190 17.322218
4825.5	81/ 8/ 9/ 0	141.3007369	220	-0.7233793 0.6334647 0.2746718 138.791302 15.942462
4830.5	81/ 8/14/ 0	146.3007369	225	-0.7785967 0.5757321 0.2496388 143.518981 14.456144
4835.5	81/ 8/19/ 0	151.3007369	230	-0.8284401 0.5138519 0.2228074 148.190143 12.873981
4840.5	81/ 8/24/ 0	156.3007369	235	-0.8725366 0.4482265 0.1943521 152.810199 11.206878
4845.5	81/ 8/29/ 0	161.3007369	240	-0.9105459 0.3792875 0.1644599 157.385851 9.465863
4850.5	81/ 9/ 3/ 0	166.3007369	245	-0.9421629 0.3074934 0.1333298 161.924887 7.662054
4855.5	81/ 9/ 8/ 0	171.3007369	250	-0.9671206 0.2333281 0.1011716 166.435989 5.806641
4860.5	81/ 9/13/ 0	176.3007369	255	-0.9851929 0.1572987 0.0682051 170.928554 3.910901
4865.5	81/ 9/18/ 0	181.3007369	260	-0.9961975 0.0799329 0.0346590 175.412528 1.986217
4870.5	81/ 9/23/ 0	186.3007369	265	-0.9999981 0.0017759 0.0007700 179.898247 0.044119
4875.5	81/ 9/28/ 0	191.3007369	270	-0.9965074 -0.0766122 -0.0332192 -175.603707 -1.903671
4880.5	81/10/ 3/ 0	196.3007369	275	-0.9856891 -0.1546602 -0.0670610 -171.082670 -3.845198
4885.5	81/10/ 8/ 0	201.3007369	280	-0.9675600 -0.2317897 -0.1005044 -166.528047 -5.768222
4890.5	81/10/13/ 0	206.3007369	285	-0.9421917 -0.3074189 -0.1332974 -161.929496 -7.660183
4895.5	81/10/18/ 0	211.3007369	290	-0.9097123 -0.3809676 -0.1651883 -157.277130 -9.508174
4900.5	81/10/23/ 0	216.3007369	295	-0.8703065 -0.4518614 -0.1959279 -152.561749 -11.298939

[a]Respectively (top line).
[b]In degrees (bottom line).

TABLE 7.- Concluded

J.D. 244 xxxx.5	Calendar day	Days from 1981T	Days from Jan. 1.0, 1981	x-, y-, and z-components of $\hat{r}_{\odot}$;[a] right ascension and declination[b]
4905.5	81/10/28/ 0	221.3007369	300	-0.8242168 -0.5195372 -0.2252723 -147.775111 -13.018892
4910.5	81/11/ 2/ 0	226.3007369	305	-0.7717430 -0.5834481 -0.2529841 -142.910226 -14.654172
4915.5	81/11/ 7/ 0	231.3007369	310	-0.7132410 -0.6430690 -0.2788359 -137.961694 -16.190740
4920.5	81/11/12/ 0	236.3007369	315	-0.6491219 -0.6979018 -0.3026114 -132.926046 -17.614522
4925.5	81/11/17/ 0	241.3007369	320	-0.5798494 -0.7474810 -0.3241090 -127.802092 -18.911607
4930.5	81/11/22/ 0	246.3007369	325	-0.5059370 -0.7913788 -0.3431431 -122.591224 -20.068490
4935.5	81/11/27/ 0	251.3007369	330	-0.4279443 -0.8292102 -0.3595469 -117.297654 -21.072375
4940.5	81/12/ 2/ 0	256.3007369	335	-0.3464723 -0.8606381 -0.3731740 -111.928537 -21.911505
4945.5	81/12/ 7/ 0	261.3007369	340	-0.2621588 -0.8853772 -0.3839009 -106.493941 -22.575527
4950.5	81/12/12/ 0	266.3007369	345	-0.1756723 -0.9031980 -0.3916280 -101.006626 -23.055840
4955.5	81/12/17/ 0	271.3007369	350	-0.0877057 -0.9139303 -0.3962815 -95.481630 -23.345926
4960.5	81/12/22/ 0	276.3007369	355	0.0010301 -0.9174653 -0.3978143 -89.935665 -23.441613
4965.5	81/12/27/ 0	281.3007369	360	0.0898142 -0.9137579 -0.3962067 -84.386367 -23.341258
4970.5	82/ 1/ 1/ 0	286.3007369	365	0.1779221 -0.9028273 -0.3914671 -78.851454 -23.045923
4975.5	82/ 1/ 6/ 0	291.3007369	370	0.2646340 -0.8847572 -0.3836319 -73.347886 -22.558835
4980.5	82/ 1/11/ 0	296.3007369	375	0.3492419 -0.8596954 -0.3727650 -67.891082 -21.886248
4985.5	82/ 1/16/ 0	301.3007369	380	0.4310573 -0.8278519 -0.3589576 -62.494286 -21.036198
4990.5	82/ 1/21/ 0	306.3007369	385	0.5094182 -0.7894969 -0.3423268 -57.168107 -20.018702
4995.5	82/ 1/26/ 0	311.3007369	390	0.5836956 -0.7449571 -0.3230143 -51.920262 -18.845316
5000.5	82/ 1/31/ 0	316.3007369	395	0.6533003 -0.6946124 -0.3011847 -46.755505 -17.528777
5005.5	82/ 2/ 5/ 0	321.3007369	400	0.7176877 -0.6388912 -0.2770239 -41.675724 -16.082665
5010.5	82/ 2/10/ 0	326.3007369	405	0.7763635 -0.5782654 -0.2507365 -36.680157 -14.521100
5015.5	82/ 2/15/ 0	331.3007369	410	0.8288872 -0.5132449 -0.2225435 -31.765689 -12.858472
5020.5	82/ 2/20/ 0	336.3007369	415	0.8748758 -0.4443720 -0.1926902 -26.927193 -11.109239
5025.5	82/ 2/25/ 0	341.3007369	420	0.9140064 -0.3722156 -0.1613930 -22.157883 -9.297763
5030.5	82/ 3/ 2/ 0	346.3007369	425	0.9460176 -0.2973645 -0.1289375 -17.449650 -7.408200
5035.5	82/ 3/ 7/ 0	351.3007369	430	0.9707107 -0.2204221 -0.0955752 -12.793379 -5.484429
5040.5	82/ 3/12/ 0	356.3007369	435	0.9879498 -0.1420002 -0.0615714 -8.179231 -3.530015
5045.5	82/ 3/17/ 0	361.3007369	440	0.9976610 -0.0627131 -0.0271924 -3.596888 -1.558205
5050.5	82/ 3/22/ 0	366.3007369	445	0.9998317 0.0168276 0.0072964 0.964222 0.418060

[a]Respectively (top line).
[b]In degrees (bottom line).

TABLE 8.- AVAILABLE SUN ELEVATION ANGLE AS A FUNCTION OF LATITUDE FOR THE WINTER AND SUMMER SOLSTICES AND THE EQUINOXES

Season	λ, deg	Sun elevation angle, ξ, deg, at local time relative to high noon, sidereal hours, of -						
		0	2	4	6	8	10	12
Winter solstice	0	66.6	52.6	27.3	0.0	-27.3	-52.6	-66.6
	10	56.6	45.5	22.5	-4.0	-31.4	-58.4	-76.6
	20	46.6	37.6	17.2	-7.8	-34.6	-62.0	-86.6
	30	36.6	29.3	11.4	-11.5	-36.6	-62.5	-83.5
	40	26.6	20.7	5.5	-14.8	-37.4	-59.8	-73.5
	50	16.6	11.9	-0.6	-17.7	-36.8	-54.6	-63.5
	60	6.6	3.0	-6.6	-20.2	-35.0	-47.9	-53.5
	70	-3.5	-5.9	-12.5	-22.0	-32.1	-40.2	-43.4
	80	-13.5	-14.7	-18.2	-23.1	-28.1	-32.0	-33.5
	90	-23.4	-23.4	-23.4	-23.4	-23.4	-23.4	-23.4
Vernal or autumnal equinox	0	90.0	60.0	30.0	0.0	-30.0	-60.0	-90.0
	10	80.0	58.5	29.5	0.0	-29.5	-58.5	-80.0
	20	70.0	54.5	28.0	0.0	-28.0	-54.5	-70.0
	30	60.0	48.6	25.7	0.0	-25.7	-48.6	-60.0
	40	50.0	41.6	22.5	0.0	-22.5	-41.6	-50.0
	50	40.0	33.8	18.7	0.0	-18.7	-33.8	-40.0
	60	30.0	25.7	14.5	0.0	-14.5	-25.7	-30.0
	70	20.0	17.2	9.8	0.0	-9.8	-17.2	-20.0
	80	10.0	8.6	5.0	0.0	-5.0	-8.6	-10.0
	90	0.0	0.0	0.0	0.0	0.0	0.0	0.0
Summer solstice	0	66.6	52.6	27.3	0.0	-27.3	-52.6	-66.6
	10	76.6	58.4	31.4	4.0	-22.5	-45.5	-56.6
	20	86.6	62.0	34.6	7.8	-17.2	-37.6	-46.6
	30	83.5	62.5	36.6	11.5	-11.4	-29.3	-36.6
	40	73.5	59.8	37.4	14.8	-5.5	-20.7	-26.6
	50	63.5	54.6	36.8	17.7	0.6	-11.9	-16.6
	60	53.5	47.9	35.0	20.2	6.6	-3.0	-6.6
	70	43.4	40.2	32.1	22.0	12.5	5.9	3.5
	80	33.5	32.0	28.1	23.1	18.2	14.7	13.5
	90	23.4	23.4	23.4	23.4	23.4	23.4	23.4
Hour angle, β, deg		0	30	60	90	120	150	180

TABLE 9.- ORBIT PARAMETERS FOR A CIRCULAR ORBIT WHICH PASSES OVER THE SAME SITES ON THE EAST COAST ONCE PER DAY, WITH NORFOLK, VIRGINIA, AS INITIAL CONDITION

Inclination, deg	63.0
Eccentricity	0.0
Semimajor axis, km	6887.371
Anomalistic period, sec	5689.92
Nodal period, sec	5689.80
Mean motion:	
deg/day	5446.5085
Anomalistic revolutions per day	15.184746
Perigee precession rate:	
deg/orbit	0.007654
deg/day	0.116232
Nodal precession rate:	
deg/orbit	-0.227599
deg/day	-3.456029
Repetition factor, Q	15.0

Initial conditions to pass over Norfolk, Virginia ($L = -76.289^{\circ}$, $\lambda = 36.853^{\circ}$) at 12:00 noon EST on Jan 1, 1981:
Longitude of ascending node: $-98^{\circ}.741$
J.D. = 244 4605.2083333
$\omega = 42^{\circ}.309$

TABLE 10.- RELATIVE LOCAL SOLAR TIME (HOUR ANGLE) NADIR COVERAGE OF THE EARTH (NUMBER OF MEASUREMENTS)

IN 36 LATITUDE BANDS OVER 30 DAYS (30 000 POINTS IN 5° STEPS)

(a) 50° orbit at 800 km

Latitude range, deg		Number of measurements at relative local solar time (hour angle, β) of -																						
		1	2	3	4	5	6	7	8	9	10	11	12	13	14	15	16	17	18	19	20	21	22	23	24
90	85	0	0	0	0	0	0	0	0	0	0	0	0	0	0	0	0	0	0	0	0	0	0	0	0
85	80	0	0	0	0	0	0	0	0	0	0	0	0	0	0	0	0	0	0	0	0	0	0	0	0
80	75	0	0	0	0	0	0	0	0	0	0	0	0	0	0	0	0	0	0	0	0	0	0	0	0
75	70	0	0	0	0	0	0	0	0	0	0	0	0	0	0	0	0	0	0	0	0	0	0	0	0
70	65	0	0	0	0	0	0	0	0	0	0	0	0	0	0	0	0	0	0	0	0	0	0	0	0
65	60	0	0	0	0	0	0	0	0	0	0	0	0	0	0	0	0	0	0	0	0	0	0	0	0
60	55	0	0	0	0	0	0	0	0	0	0	0	0	0	0	0	0	0	0	0	0	0	0	0	0
55	50	0	0	0	0	0	0	0	0	0	0	0	0	0	0	0	0	0	0	0	0	0	0	0	0
50	45	0	0	0	0	0	21	102	184	265	346	368	368	368	368	368	393	265	201	136	20	0	0	0	0
45	40	0	0	0	0	24	84	84	84	84	84	155	171	172	174	161	100	91	84	84	75	12	0	0	0
40	35	0	0	0	0	51	72	73	72	73	73	90	143	141	141	79	69	69	70	69	72	64	1	0	0
35	30	0	0	0	27	65	64	65	64	63	63	64	105	129	113	65	66	66	65	65	63	63	17	0	0
30	25	0	0	0	45	60	59	59	61	61	61	61	74	120	73	60	61	61	61	62	62	61	48	0	0
25	20	0	0	7	58	59	58	59	58	59	59	58	60	101	58	57	57	56	57	57	56	57	59	12	0
20	15	0	0	30	56	57	56	56	57	55	56	55	55	63	58	57	57	57	57	56	57	56	55	22	0
15	10	0	0	44	54	54	54	55	54	56	56	55	57	24	55	55	57	55	56	56	56	56	55	45	0
10	5	0	3	53	56	55	55	56	55	54	56	55	50	2	50	53	53	54	54	55	56	55	55	55	5
5	0	0	21	55	55	54	54	55	54	55	54	54	35	0	37	54	54	54	54	53	53	53	53	54	20
0	-5	0	36	55	55	55	55	53	53	54	53	53	20	0	21	55	55	55	55	55	55	55	55	55	34
-5	-10	2	49	53	54	53	53	56	55	54	56	55	5	0	4	54	54	55	56	54	56	55	54	56	50
-10	-15	23	55	57	55	55	57	55	56	56	56	43	0	0	0	45	54	54	54	54	56	56	56	56	55
-15	-20	62	56	57	56	58	56	58	57	57	55	22	0	0	0	30	58	57	57	57	57	55	54	55	55
-20	-25	100	59	56	57	56	57	56	57	57	58	12	0	0	0	7	59	58	59	58	58	59	58	59	60
-25	-30	121	74	62	60	62	61	61	60	61	47	0	0	0	0	0	46	58	59	59	61	61	62	62	74
-30	-35	128	109	66	65	65	65	66	63	63	17	0	0	0	0	0	27	66	65	65	63	63	63	62	106
-35	-40	143	143	78	70	70	70	70	72	64	0	0	0	0	0	0	0	52	73	73	74	73	73	92	143
-40	-45	173	172	162	99	91	84	84	74	12	0	0	0	0	0	0	0	24	84	84	84	84	84	154	172
-45	-50	367	367	368	392	262	201	136	18	0	0	0	0	0	0	0	0	0	22	103	184	266	347	368	368
-50	-55	0	0	0	0	0	0	0	0	0	0	0	0	0	0	0	0	0	0	0	0	0	0	0	0
-55	-60	0	0	0	0	0	0	0	0	0	0	0	0	0	0	0	0	0	0	0	0	0	0	0	0
-60	-65	0	0	0	0	0	0	0	0	0	0	0	0	0	0	0	0	0	0	0	0	0	0	0	0
-65	-70	0	0	0	0	0	0	0	0	0	0	0	0	0	0	0	0	0	0	0	0	0	0	0	0
-70	-75	0	0	0	0	0	0	0	0	0	0	0	0	0	0	0	0	0	0	0	0	0	0	0	0
-75	-80	0	0	0	0	0	0	0	0	0	0	0	0	0	0	0	0	0	0	0	0	0	0	0	0
-80	-85	0	0	0	0	0	0	0	0	0	0	0	0	0	0	0	0	0	0	0	0	0	0	0	0
-85	-90	0	0	0	0	0	0	0	0	0	0	0	0	0	0	0	0	0	0	0	0	0	0	0	0

TABLE 10.- Continued

(b) 80° orbit at 800 km

Latitude range, deg		Number of measurements at relative local solar time (hour angle, β) of -																							
		1	2	3	4	5	6	7	8	9	10	11	12	13	14	15	16	17	18	19	20	21	22	23	24
90	85	0	0	0	0	0	0	0	0	0	0	0	0	0	0	0	0	0	0	0	0	0	0	0	0
85	80	0	0	0	0	0	0	0	0	0	0	0	0	0	0	0	0	0	0	0	0	0	0	0	0
80	75	0	0	0	0	0	0	0	0	0	0	32	117	177	237	256	244	260	235	179	115	31	0	0	0
75	70	0	0	0	0	0	0	0	0	0	31	125	128	128	99	4	0	3	100	127	130	124	29	0	0
70	65	0	0	0	0	0	0	0	0	0	94	116	117	117	21	0	0	0	23	115	116	116	95	0	0
65	60	0	0	0	0	0	0	0	0	20	111	112	112	94	0	0	0	0	0	94	112	113	112	19	0
60	55	0	0	0	0	0	0	0	0	48	110	110	111	62	0	0	0	0	0	65	110	110	110	47	0
55	50	0	0	0	0	0	0	0	0	67	108	108	109	41	0	0	0	0	0	43	107	108	109	67	0
50	45	0	0	0	0	0	0	0	0	82	107	107	109	28	0	0	0	0	0	27	108	108	109	82	0
45	40	0	0	0	0	0	0	0	0	96	108	110	107	12	0	0	0	0	0	16	107	107	108	96	0
40	35	0	0	0	0	0	0	0	0	104	106	105	106	4	0	0	0	0	0	2	106	108	106	104	0
35	30	0	0	0	0	0	0	0	7	106	107	107	98	0	0	0	0	0	0	0	99	105	106	106	9
30	25	0	0	0	0	0	0	0	18	105	106	105	91	0	0	0	0	0	0	0	93	105	106	106	16
25	20	0	0	0	0	0	0	0	25	105	105	106	84	0	0	0	0	0	0	0	82	106	106	107	21
20	15	0	0	0	0	0	0	0	29	105	108	106	75	0	0	0	0	0	0	0	75	106	105	106	33
15	10	0	0	0	0	0	0	0	39	107	105	106	68	0	0	0	0	0	0	0	69	106	105	106	38
10	5	0	0	0	0	0	0	0	45	106	105	106	63	0	0	0	0	0	0	0	64	107	105	106	43
5	0	0	0	0	0	0	0	0	49	103	104	104	58	0	0	0	0	0	0	0	54	107	106	108	49
0	-5	0	0	0	0	0	0	0	55	106	108	108	47	0	0	0	0	0	0	0	49	103	104	103	57
-5	-10	0	0	0	0	0	0	0	65	105	106	105	43	0	0	0	0	0	0	0	45	105	106	105	63
-10	-15	0	0	0	0	0	0	0	71	105	106	105	38	0	0	0	0	0	0	0	39	106	106	105	68
-15	-20	0	0	0	0	0	0	0	75	105	106	107	31	0	0	0	0	0	0	0	30	105	107	107	75
-20	-25	0	0	0	0	0	0	0	83	106	108	106	22	0	0	0	0	0	0	0	23	105	106	106	84
-25	-30	0	0	0	0	0	0	0	92	106	105	106	15	0	0	0	0	0	0	0	19	105	105	106	89
-30	-35	0	0	0	0	0	0	0	98	106	105	106	10	0	0	0	0	0	0	0	6	106	107	107	98
-35	-40	4	0	0	0	0	0	2	106	106	108	102	0	0	0	0	0	0	0	0	0	104	105	106	105
-40	-45	11	0	0	0	0	0	15	107	108	107	96	0	0	0	0	0	0	0	0	0	97	108	108	108
-45	-50	27	0	0	0	0	0	26	108	109	109	81	0	0	0	0	0	0	0	0	0	81	108	107	109
-50	-55	41	0	0	0	0	0	43	107	107	108	68	0	0	0	0	0	0	0	0	0	65	108	110	108
-55	-60	63	0	0	0	0	0	65	110	110	109	48	0	0	0	0	0	0	0	0	0	47	110	110	110
-60	-65	93	0	0	0	0	0	91	113	113	113	18	0	0	0	0	0	0	0	0	0	20	111	112	112
-65	-70	116	22	0	0	0	21	116	116	117	94	0	0	0	0	0	0	0	0	0	0	0	94	116	116
-70	-75	128	99	4	0	2	99	130	126	126	29	0	0	0	0	0	0	0	0	0	0	0	31	123	129
-75	-80	175	240	256	242	260	234	180	112	32	0	0	0	0	0	0	0	0	0	0	0	0	0	32	115
-80	-85	0	0	0	0	0	0	0	0	0	0	0	0	0	0	0	0	0	0	0	0	0	0	0	0
-85	-90	0	0	0	0	0	0	0	0	0	0	0	0	0	0	0	0	0	0	0	0	0	0	0	0

TABLE 10.- Concluded

(c) Sun-synchronous orbit at 800 km

Latitude range, deg		Number of measurements at relative local solar time (hour angle, β) of -																							
		1	2	3	4	5	6	7	8	9	10	11	12	13	14	15	16	17	18	19	20	21	22	23	24
90	85	0	0	0	0	0	0	0	0	0	0	0	0	0	0	0	0	0	0	0	0	0	0	0	0
85	80	0	0	0	118	201	190	198	146	0	0	0	0	0	0	0	0	0	0	0	0	0	0	0	0
80	75	0	71	390	141	0	0	0	102	361	141	0	0	0	0	0	0	0	0	0	0	0	0	0	0
75	70	0	482	0	0	0	0	0	0	0	483	0	0	0	0	0	0	0	0	0	0	0	0	0	0
70	65	220	234	0	0	0	0	0	0	0	65	386	0	0	0	0	0	0	0	0	0	0	0	0	0
65	60	441	0	0	0	0	0	0	0	0	0	441	0	0	0	0	0	0	0	0	0	0	0	0	0
60	55	434	0	0	0	0	0	0	0	0	0	435	0	0	0	0	0	0	0	0	0	0	0	0	0
55	50	431	0	0	0	0	0	0	0	0	0	430	0	0	0	0	0	0	0	0	0	0	0	0	0
50	45	428	0	0	0	0	0	0	0	0	0	375	53	0	0	0	0	0	0	0	0	0	0	0	0
45	40	421	0	0	0	0	0	0	0	0	0	98	326	0	0	0	0	0	0	0	0	0	0	0	4
40	35	264	0	0	0	0	0	0	0	0	0	0	425	0	0	0	0	0	0	0	0	0	0	0	162
35	30	47	0	0	0	0	0	0	0	0	0	0	424	0	0	0	0	0	0	0	0	0	0	0	378
30	25	0	0	0	0	0	0	0	0	0	0	0	423	0	0	0	0	0	0	0	0	0	0	0	422
25	20	0	0	0	0	0	0	0	0	0	0	0	423	0	0	0	0	0	0	0	0	0	0	0	422
20	15	0	0	0	0	0	0	0	0	0	0	0	422	0	0	0	0	0	0	0	0	0	0	0	422
15	10	0	0	0	0	0	0	0	0	0	0	0	422	0	0	0	0	0	0	0	0	0	0	0	421
10	5	0	0	0	0	0	0	0	0	0	0	0	423	0	0	0	0	0	0	0	0	0	0	0	422
5	0	0	0	0	0	0	0	0	0	0	0	0	423	0	0	0	0	0	0	0	0	0	0	0	421
0	-5	0	0	0	0	0	0	0	0	0	0	0	420	0	0	0	0	0	0	0	0	0	0	0	421
-5	-10	0	0	0	0	0	0	0	0	0	0	0	422	0	0	0	0	0	0	0	0	0	0	0	420
-10	-15	0	0	0	0	0	0	0	0	0	0	0	421	0	0	0	0	0	0	0	0	0	0	0	422
-15	-20	0	0	0	0	0	0	0	0	0	0	0	422	0	0	0	0	0	0	0	0	0	0	0	422
-20	-25	0	0	0	0	0	0	0	0	0	0	0	422	0	0	0	0	0	0	0	0	0	0	0	421
-25	-30	0	0	0	0	0	0	0	0	0	0	0	423	0	0	0	0	0	0	0	0	0	0	0	423
-30	-35	0	0	0	0	0	0	0	0	0	0	0	376	47	0	0	0	0	0	0	0	0	0	0	423
-35	-40	0	0	0	0	0	0	0	0	0	0	0	157	266	0	0	0	0	0	0	0	0	0	0	423
-40	-45	0	0	0	0	0	0	0	0	0	0	0	5	421	0	0	0	0	0	0	0	0	0	98	328
-45	-50	0	0	0	0	0	0	0	0	0	0	0	0	426	0	0	0	0	0	0	0	0	0	372	54
-50	-55	0	0	0	0	0	0	0	0	0	0	0	0	430	0	0	0	0	0	0	0	0	0	430	0
-55	-60	0	0	0	0	0	0	0	0	0	0	0	0	433	0	0	0	0	0	0	0	0	0	433	0
-60	-65	0	0	0	0	0	0	0	0	0	0	0	0	441	0	0	0	0	0	0	0	0	0	440	0
-65	-70	0	0	0	0	0	0	0	0	0	0	0	0	213	235	0	0	0	0	0	0	0	66	387	0
-70	-75	0	0	0	0	0	0	0	0	0	0	0	0	0	482	0	0	0	0	0	0	0	482	0	0
-75	-80	0	0	0	0	0	0	0	0	0	0	0	0	0	70	388	142	0	0	0	101	361	140	0	0
-80	-85	0	0	0	0	0	0	0	0	0	0	0	0	0	0	0	115	202	190	198	145	0	0	0	0
-85	-90	0	0	0	0	0	0	0	0	0	0	0	0	0	0	0	0	0	0	0	0	0	0	0	0

TABLE 11.- SOLAR ZENITH ANGLE NADIR COVERAGE OF THE EARTH (NUMBER OF MEASUREMENTS)
IN 36 LATITUDE BANDS OVER 30 DAYS (30 000 POINTS IN 5° STEPS)

(a) 50° orbit at 800 km

Latitude range, deg		Number of measurements at solar zenith angle, deg, of -																						
		7.5	15	22.5	30	37.5	45	52.5	60	67.5	75	82.5	90	97.5	105	112.5	120	127.5	135	142.5	150	157.5	165	172.5	180
85	90	0	0	0	0	0	0	0	0	0	0	0	0	0	0	0	0	0	0	0	0	0	0	0	0
80	85	0	0	0	0	0	0	0	0	0	0	0	0	0	0	0	0	0	0	0	0	0	0	0	0
75	80	0	0	0	0	0	0	0	0	0	0	0	0	0	0	0	0	0	0	0	0	0	0	0	0
70	75	0	0	0	0	0	0	0	0	0	0	0	0	0	0	0	0	0	0	0	0	0	0	0	0
65	70	0	0	0	0	0	0	0	0	0	0	0	0	0	0	0	0	0	0	0	0	0	0	0	0
60	65	0	0	0	0	0	0	0	0	0	0	0	0	0	0	0	0	0	0	0	0	0	0	0	0
55	60	0	0	0	0	0	0	0	0	0	0	0	0	0	0	0	0	0	0	0	0	0	0	0	0
50	55	0	0	0	0	0	0	0	0	0	0	0	0	0	0	0	0	0	0	0	0	0	0	0	0
45	50	0	0	0	0	36	964	824	506	509	409	154	205	72	83	11	0	0	0	0	0	0	0	0	0
40	45	0	0	0	0	223	371	235	201	120	143	109	106	49	79	42	45	0	0	0	0	0	0	0	0
35	40	0	0	0	98	227	184	169	100	134	76	83	110	83	51	35	69	27	6	0	0	0	0	0	0
30	35	0	0	25	114	214	140	85	80	75	84	79	62	71	92	54	37	31	49	0	0	0	0	0	0
25	30	0	0	48	162	137	79	68	72	70	62	72	76	78	60	58	46	36	53	27	6	0	0	0	0
20	25	0	2	98	136	80	65	66	62	63	63	61	60	60	67	80	63	37	28	28	43	0	0	0	0
15	20	0	6	141	73	64	60	58	60	60	62	59	61	61	56	56	54	62	36	34	43	21	1	0	0
10	15	0	60	67	60	58	60	57	56	56	55	56	56	59	60	60	64	65	44	27	27	27	35	0	0
5	10	19	55	31	51	56	54	55	56	54	56	57	57	55	54	56	55	54	58	53	26	31	36	14	0
0	5	35	27	27	33	56	57	55	55	54	55	54	54	54	55	54	55	58	56	54	37	26	27	27	20
-5	0	20	26	27	27	36	54	57	56	57	56	54	55	55	54	56	55	56	57	55	57	34	27	27	34
-10	-5	0	14	37	29	30	55	56	55	54	54	55	54	57	57	54	56	55	54	56	55	51	32	55	18
-15	-10	0	0	34	27	27	27	45	64	64	62	58	59	56	55	56	55	56	59	57	59	61	66	59	0
-20	-15	0	0	1	21	42	36	37	62	56	54	59	62	59	62	61	60	60	57	60	63	71	141	5	0
-25	-20	0	0	0	0	42	26	29	37	63	79	66	60	59	61	63	63	61	66	66	77	137	98	3	0
-30	-25	0	0	0	0	6	26	52	36	45	60	96	76	75	69	65	67	74	66	81	138	165	48	0	0
-35	-30	0	0	0	0	0	0	48	32	37	54	93	71	64	77	85	75	79	85	136	213	114	24	0	0
-40	-35	0	0	0	0	0	0	6	26	69	35	51	36	107	87	75	106	100	170	186	232	97	0	0	0
-45	-40	0	0	0	0	0	0	0	0	44	42	79	49	106	110	142	121	198	236	371	222	1	0	0	0
-50	-45	0	0	0	0	0	0	0	0	0	10	82	71	205	153	409	508	509	820	966	36	0	0	0	0
-55	-50	0	0	0	0	0	0	0	0	0	0	0	0	0	0	0	0	0	0	0	0	0	0	0	0
-60	-55	0	0	0	0	0	0	0	0	0	0	0	0	0	0	0	0	0	0	0	0	0	0	0	0
-65	-60	0	0	0	0	0	0	0	0	0	0	0	0	0	0	0	0	0	0	0	0	0	0	0	0
-70	-65	0	0	0	0	0	0	0	0	0	0	0	0	0	0	0	0	0	0	0	0	0	0	0	0
-75	-70	0	0	0	0	0	0	0	0	0	0	0	0	0	0	0	0	0	0	0	0	0	0	0	0
-80	-75	0	0	0	0	0	0	0	0	0	0	0	0	0	0	0	0	0	0	0	0	0	0	0	0
-85	-80	0	0	0	0	0	0	0	0	0	0	0	0	0	0	0	0	0	0	0	0	0	0	0	0
-90	-85	0	0	0	0	0	0	0	0	0	0	0	0	0	0	0	0	0	0	0	0	0	0	0	0

TABLE 11.- Continued

(b) 80° orbit at 800 km

Latitude range, deg		Number of measurements at solar zenith angle, deg, of -																						
		7.5	15	22.5	30	37.5	45	52.5	60	67.5	75	82.5	90	97.5	105	112.5	120	127.5	135	142.5	150	157.5	165	172.5	180
85	90	0	0	0	0	0	0	0	0	0	0	0	0	0	0	0	0	0	0	0	0	0	0	0	0
80	85	0	0	0	0	0	0	0	0	0	0	0	0	0	0	0	0	0	0	0	0	0	0	0	0
75	80	0	0	0	0	0	0	0	0	75	218	641	419	204	26	0	0	0	0	0	0	0	0	0	0
70	75	0	0	0	0	0	0	0	0	279	211	104	134	147	146	8	0	0	0	0	0	0	0	0	0
65	70	0	0	0	0	0	0	0	60	352	93	17	106	115	125	102	0	0	0	0	0	0	0	0	0
60	65	0	0	0	0	0	0	0	341	106	0	0	61	96	105	120	61	0	0	0	0	0	0	0	0
55	60	0	0	0	0	0	0	61	377	3	0	0	25	64	91	100	120	22	0	0	0	0	0	0	0
50	55	0	0	0	0	0	0	327	106	0	0	0	2	64	81	86	96	99	4	0	0	0	0	0	0
45	50	0	0	0	0	0	115	277	41	0	0	0	0	32	75	77	83	99	66	0	0	0	0	0	0
40	45	0	0	0	0	0	305	110	15	0	0	0	0	6	65	70	76	84	104	29	0	0	0	0	0
35	40	0	0	0	0	176	196	61	12	0	0	0	0	0	41	55	65	73	52	91	8	0	0	0	0
30	35	0	0	0	36	221	79	79	11	0	0	0	0	0	16	66	63	66	70	73	67	0	0	0	0
25	30	0	0	0	180	95	70	66	13	0	0	0	0	0	0	52	54	60	65	70	57	33	0	0	0
20	25	0	0	86	126	75	63	60	15	0	0	0	0	0	0	28	37	57	54	63	70	30	10	0	0
15	20	0	7	146	84	62	60	57	22	0	0	0	0	0	0	4	56	55	56	58	60	69	62	0	0
10	15	0	101	85	56	55	59	56	29	0	0	0	0	0	0	0	45	53	53	56	57	57	73	30	0
5	10	26	84	98	55	53	53	54	42	0	0	0	0	0	0	0	26	54	52	54	55	53	57	64	10
0	5	55	55	52	52	51	52	52	49	0	0	0	0	0	0	13	52	54	52	52	54	52	54	41	
-5	0	41	53	53	52	52	54	52	54	13	0	0	0	0	0	0	0	44	52	51	52	51	52	56	53
-10	-5	10	62	57	55	54	53	54	53	26	0	0	0	0	0	0	0	42	53	53	54	54	59	63	26
-15	-10	0	30	72	54	57	55	53	53	46	0	0	0	0	0	0	0	27	57	59	55	60	66	100	0
-20	-15	0	0	60	70	61	58	55	56	55	9	0	0	0	0	0	0	22	56	60	60	70	147	7	0
-25	-20	0	0	9	81	70	61	61	58	56	29	0	0	0	0	0	0	17	60	63	78	125	81	0	0
-30	-25	0	0	0	31	54	65	66	60	60	50	0	0	0	0	0	0	13	67	69	96	179	0	0	0
-35	-30	0	0	0	0	67	63	64	67	62	60	17	0	0	0	0	0	11	76	78	222	35	0	0	0
-40	-35	0	0	0	0	8	90	84	70	67	65	40	0	0	0	0	0	12	80	153	174	0	0	0	0
-45	-40	0	0	0	0	0	30	103	84	75	70	65	6	0	0	0	0	17	111	304	0	0	0	0	0
-50	-45	0	0	0	0	0	0	67	94	84	77	73	33	0	0	0	0	40	286	112	0	0	0	0	0
-55	-50	0	0	0	0	0	0	5	98	98	85	81	65	1	0	0	0	105	327	0	0	0	0	0	0
-60	-55	0	0	0	0	0	0	0	23	118	100	91	85	29	0	0	3	374	83	0	0	0	0	0	0
-65	-60	0	0	0	0	0	0	0	0	62	119	105	97	65	0	0	109	339	0	0	0	0	0	0	0
-70	-65	0	0	0	0	0	0	0	0	0	100	126	114	107	15	53	352	59	0	0	0	0	0	0	0
-75	-70	0	0	0	0	0	0	0	0	0	9	138	147	139	105	210	276	0	0	0	0	0	0	0	0
-80	-75	0	0	0	0	0	0	0	0	0	0	27	202	415	636	519	76	0	0	0	0	0	0	0	0
-85	-80	0	0	0	0	0	0	0	0	0	0	0	0	0	0	0	0	0	0	0	0	0	0	0	0
-90	-85	0	0	0	0	0	0	0	0	0	0	0	0	0	0	0	0	0	0	0	0	0	0	0	0

TABLE 11.- Concluded

(c) Sun-synchronous orbit at 800 km

Latitude range, deg		Number of measurements at solar zenith angle, deg, of -																						
		7.5	15	22.5	30	37.5	45	52.5	60	67.5	75	82.5	90	97.5	105	112.5	120	127.5	135	142.5	150	157.5	165	172.5	180
85	90	0	0	0	0	0	0	0	0	0	0	0	0	0	0	0	0	0	0	0	0	0	0	0	0
80	85	0	0	0	0	0	0	0	0	0	9	291	459	94	0	0	0	0	0	0	0	0	0	0	0
75	80	0	0	0	0	0	0	0	0	3	269	310	169	372	83	0	0	0	0	0	0	0	0	0	0
70	75	0	0	0	0	0	0	0	0	178	282	23	0	156	294	32	0	0	0	0	0	0	0	0	0
65	70	0	0	0	0	0	0	0	69	296	69	0	0	1	224	225	4	0	0	0	0	0	0	0	0
60	65	0	0	0	0	0	0	28	270	149	0	0	0	0	28	271	142	0	0	0	0	0	0	0	0
55	60	0	0	0	0	0	0	207	229	3	0	0	0	0	0	94	254	56	0	0	0	0	0	0	0
50	55	0	0	0	0	0	116	271	43	0	0	0	0	0	0	0	143	236	12	0	0	0	0	0	0
45	50	0	0	0	0	37	271	126	0	0	0	0	0	0	0	0	16	251	154	0	0	0	0	0	0
40	45	0	0	0	2	219	205	0	0	0	0	0	0	0	0	0	0	77	279	64	0	0	0	0	0
35	40	0	0	8	129	268	35	0	0	0	0	0	0	0	0	0	0	0	167	242	17	0	0	0	0
30	35	0	0	44	273	107	0	0	0	0	0	0	0	0	0	0	0	0	14	242	169	0	0	0	0
25	30	0	0	226	193	0	0	0	0	0	0	0	0	0	0	0	0	0	0	67	277	74	0	0	0
20	25	0	136	256	31	0	0	0	0	0	0	0	0	0	0	0	0	0	0	0	157	244	21	0	0
15	20	50	274	95	0	0	0	0	0	0	0	0	0	0	0	0	0	0	0	0	16	237	175	0	0
10	15	235	167	0	0	0	0	0	0	0	0	0	0	0	0	0	0	0	0	0	0	60	277	84	0
5	10	391	28	0	0	0	0	0	0	0	0	0	0	0	0	0	0	0	0	0	0	0	150	247	25
0	5	367	56	0	0	0	0	0	0	0	0	0	0	0	0	0	0	0	0	0	0	0	8	233	160
-5	0	179	233	8	0	0	0	0	0	0	0	0	0	0	0	0	0	0	0	0	0	0	0	56	365
-10	-5	24	241	150	0	0	0	0	0	0	0	0	0	0	0	0	0	0	0	0	0	0	0	27	393
-15	-10	0	65	274	62	0	0	0	0	0	0	0	0	0	0	0	0	0	0	0	0	0	0	187	235
-20	-15	0	0	175	236	11	0	0	0	0	0	0	0	0	0	0	0	0	0	0	0	0	48	273	51
-25	-20	0	0	21	244	157	0	0	0	0	0	0	0	0	0	0	0	0	0	0	0	30	256	135	0
-30	-25	0	0	0	76	276	54	0	0	0	0	0	0	0	0	0	0	0	0	0	0	195	223	5	0
-35	-30	0	0	0	0	164	245	14	0	0	0	0	0	0	0	0	0	0	0	0	106	273	44	0	0
-40	-35	0	0	0	0	16	241	166	0	0	0	0	0	0	0	0	0	0	0	34	263	126	0	0	0
-45	-40	0	0	0	0	0	70	274	77	0	0	0	0	0	0	0	0	0	0	206	217	3	0	0	0
-50	-45	0	0	0	0	0	0	157	251	18	0	0	0	0	0	0	0	0	114	270	37	0	0	0	0
-55	-50	0	0	0	0	0	0	12	236	183	0	0	0	0	0	0	0	43	273	114	0	0	0	0	0
-60	-55	0	0	0	0	0	0	0	57	294	42	0	0	0	0	0	2	224	206	1	0	0	0	0	0
-65	-60	0	0	0	0	0	0	0	0	141	270	30	0	0	0	0	149	269	26	0	0	0	0	0	0
-70	-65	0	0	0	0	0	0	0	0	4	225	223	1	0	0	66	296	89	0	0	0	0	0	0	0
-75	-70	0	0	0	0	0	0	0	0	0	32	244	156	0	23	262	177	0	0	0	0	0	0	0	0
-80	-75	0	0	0	0	0	0	0	0	0	0	82	371	170	308	286	3	0	0	0	0	0	0	0	0
-85	-80	0	0	0	0	0	0	0	0	0	0	0	92	458	291	9	0	0	0	0	0	0	0	0	0
-90	-85	0	0	0	0	0	0	0	0	0	0	0	0	0	0	0	0	0	0	0	0	0	0	0	0

1. Report No.	2. Government Accession No.	3. Recipient's Catalog No.
NASA RP-1009		

4. Title and Subtitle	5. Report Date
AN INTRODUCTION TO ORBIT DYNAMICS AND ITS APPLICATION TO SATELLITE-BASED EARTH MONITORING MISSIONS	November 1977
	6. Performing Organization Code

7. Author(s)	8. Performing Organization Report No.
David R. Brooks	L-11710
	10. Work Unit No. 683-75-33-02
9. Performing Organization Name and Address NASA Langley Research Center Hampton, VA 23665	11. Contract or Grant No.
	13. Type of Report and Period Covered Reference Publication
12. Sponsoring Agency Name and Address National Aeronautics and Space Administration Washington, DC 20546	14. Sponsoring Agency Code

15. Supplementary Notes

16. Abstract

A self-contained tutorial treatment is given to the long-term behavior of satellites at a level of complexity suitable for the initial planning phases of Earth monitoring missions. First-order perturbation theory is used to describe in detail the basic orbit dynamics of satellite motion around the Earth and relative to the Sun. Surface coverage capabilities of satellite orbits are examined. Several examples of simulated observation and monitoring missions are given to illustrate representative applications of the theory. The examples stress the need for devising ways of maximizing total mission output in order to make the best possible use of the resultant data base as input to those large-scale, long-term Earth monitoring activities which can best justify the use of satellite systems.

17. Key Words (Suggested by Author(s))	18. Distribution Statement
Orbit dynamics Remote sensing Satellite monitoring	Unclassified - Unlimited Subject Category 13

19. Security Classif. (of this report)	20. Security Classif. (of this page)	21. No. of Pages	22. Price*
Unclassified	Unclassified	84	$5.00

* For sale by the National Technical Information Service, Springfield, Virginia 22161

NASA-Langley, 1977